



REGOLITH CHARACTERISATION AND GEOCHEMISTRY AS AN AID TO MINERAL EXPLORATION IN THE HARRIS GREENSTONE BELT, CENTRAL GAWLER CRATON, SOUTH AUSTRALIA.

Volume I

M.J. Sheard and I.D.M. Robertson

CRC LEME OPEN FILE REPORT 155

May 2004

CRCLEME

(PIRSA-Minerals and Energy Resources Group,
South Australia, Report Book, 2003/10
CSIRO Exploration and Mining, Report 1165F)



REGOLITH CHARACTERISATION AND GEOCHEMISTRY AS AN AID TO MINERAL EXPLORATION IN THE HARRIS GREENSTONE BELT, CENTRAL GAWLER CRATON, SOUTH AUSTRALIA.

Volume 1

M.J. Sheard and I.D.M. Robertson

CRC LEME Open File Report 155

May 2004

(PIRSA-Minerals and Energy Resources Group,
South Australia, Report Book, 2003/10
CSIRO Exploration and Mining, Report 1165F)

© CRC LEME 2004

CRC LEME is an unincorporated joint venture between CSIRO-Exploration & Mining, and Land & Water, The Australian National University, Curtin University of Technology, University of Adelaide, Geoscience Australia, Primary Industries and Resources SA, NSW Department of Mineral Resources and Minerals Council of Australia.

Headquarters: CRC LEME c/o CSIRO-Exploration and Mining, PO Box 1130, BENTLEY WA 6102, Australia.

© CRC LEME 2004

This report presents outcomes of a collaborative CRC LEME research project between the Department of Primary Industries, Adelaide, South Australia (PIRSA) and CSIRO Exploration and Mining, Perth, Western Australia, that commenced in mid 2001 and continued until late 2003. There were no confidentiality agreements entered into regarding any aspects of this collaborative research project nor covering any primary data—images or derived data—images collected during the execution of this project. All contents, data and samples associated with this report are open file items. All reference materials (regolith samples, drill cores, impregnated core blocks, thin sections, polished sections & polished block mounts) have been retained by PIRSA at their Core Store Facility, 23 Conyngham St, Glenside, South Australia, 5065. Those materials can be viewed without restriction by prior arrangements with the Core Store Facility Manager [ph: (08) 8379 9574 ; Fax: (08) 8338 1925].

Copies of this publication can be obtained from:

The Publications Officer, CRC LEME c/o CSIRO-Exploration and Mining, PO Box 1130, BENTLEY WA 6102, Australia. Information on other publications in this series may be obtained from the above or from <http://crcleme.org.au>

Cataloguing-in-Publication:

Sheard, M.J. and Robertson, I.D.M.

Regolith Characterisation and Geochemistry as an Aid to Mineral Exploration in the Harris Greenstone Belt, Central Gawler Craton, South Australia.

ISBN: v1: 0 643 06855 4 v2: 0 643 06856 2 set: 0 643 06857 0

1. Regolith – South Australia. 2. Greenstones – South Australia. 3. Geochemistry – South Australia. 4. Landforms – South Australia. 5. Nickel – South Australia.. 6. Gold – South Australia.

I. Sheard, M.J. II. Title.

CRC LEME Open File Report 155.

ISSN: 1329-4768

Addresses and Affiliations of the Authors:

M.J. Sheard

Cooperative Research Centre for Landscape
Environments and Mineral Exploration
C/- PIRSA, Mineral Resources Group
Geological Survey Branch
GPO Box 1671
ADELAIDE SA 5001
Australia

I.D.M. Robertson

Cooperative Research Centre for Landscape
Environments and Mineral Exploration
C/- CSIRO Exploration and Mining
PO Box 1130
BENTLEY WA 6102
Australia

PREFACE AND EXECUTIVE SUMMARY

The Harris Greenstone Belt, southeast of Tarcoola in the Central Gawler Craton, is a newly outlined greenstone province that has been the focus of recent drilling investigation to determine its extent and potential to host mineralisation, in particular nickel and gold. Over 95% of the greenstone, inferred from geophysical interpretation, is under regolith cover.

Investigations detailed in this report focus on the regolith units and compliment the bedrock drilling programs reported elsewhere.

The objectives were to:

- evaluate the use of components of the transported cover and *in situ* weathered bedrock to identify the presence of underlying fresh mafic and ultramafic rocks of the greenstone package.
- evaluate the use of surface and shallow soil geochemistry as a means of outlining subsurface greenstone and to locate areas of anomalous metal concentration in bedrock sources.

The approach adopted was:

- characterisation of the regolith at 3 key sites using drill cuttings augmented by purpose-drilled, fully-cored reference holes through the regolith and including petrography and geochemistry of those drill cores.
- regolith mapping at one key site, Lake Harris, together with characterisation of surface regolith samples and shallow soil and surface sample geochemistry over a portion of the mapped area.
- review of landscape evolution based on previous work and placing each key site in context with regard to this review.

The results show that:

- greenstone packages are commonly more deeply weathered than adjacent felsic rocks and in places are preferentially eroded and filled by up to 80m of younger channel fill sediments.
- shallow transported cover (<5m) over buried greenstone usually contains components of the underlying bedrock that can be used to identify it by geochemistry of appropriate sample media. These areas are expected to also show element anomaly related to shallow bedrock mineralisation. Regolith mapping that incorporates cover thickness is an important aid for interpretation of any geochemical data.
- recognition of the unconformity boundary between transported cover and *in situ* weathered bedrock proved difficult at one site due to the presence of a debris flow deposit of similar mineralogy and weathering to underlying *in situ* bedrock. The availability of core samples was critical to recognition of this unit. Zircon contents may be helpful in defining the transported/*in situ* boundary on weathered greenstone.
- pedolith zone on greenstone is typically thinly developed or poorly preserved (commonly <5m). The usually thicker saprolite zone (up to 90m) is readily identified as formed from greenstone protolith by mineralogy (smectite), chemistry (elevated Cr, Ni, Cu, Mg, etc) and petrography (spinifex textures preserved in metakomatiites).

M.J. Sheard and I.D.M. Robertson,
May 2004

Contents	Page #
Figure Listing	iv
Table Listing	v
Photo Listing	v
Abstract	1
Key Recommendations	1
Acknowledgements	1
Introduction	2
Background	2
Work Program	2
Location and Topography	3
Access and climate	3
Methods	3
Drilling	3
Surface sampling	10
Logging	10
Limitations	10
Sample contamination	11
Mapping	11
Sample treatment and analysis	12
Size fraction	12
Heavy liquid mineral separation	12
Microscopy and photography	12
Geochemical analysis	12
XRD	13
PIMA	13
Petrography	14
Regolith in Profile	14
Selected aircore drill lines	14
Lake Harris	15
<i>In situ</i> Basement	15
Transported Cover	15
Hopeful Hill	18
<i>In situ</i> Basement	18
Transported Cover	19
Mullina Well	22
<i>In situ</i> Basement	22
Transported Cover	25
Cored drillholes	26
Lake Harris KLHRDD-1	26
<i>In situ</i> Greenstone	26
Transported Cover	28
Hopeful Hill THHRDD-1	29
<i>In situ</i> Greenstone	29
Transported Cover	32
Mullina Well TMWRDD-1	34
<i>In situ</i> Greenstone	34
Transported Cover	37
Petrography	42
Drillhole KLHRDD-1	42
Drillhole THHRDD-1	43
Drillhole TMWRDD-1	45
Mineralogy	57
Results	57
Geochemistry	57
Drillhole KLHRDD-1	57
Drillhole THHRDD-1	59
Drillhole TMWRDD-1	59
Distinguishing cover from basement	59
Basalt classification and prospectivity	62

Continued

Contents continued	Page #
Key regolith zonal components	63
<i>In Situ</i> – Protolith	63
– Saprock	63
– Saprolite	63
– Pedolith (plasmic)	64
Transported Cover	64
Description of surficial materials at Lake Harris site	65
Sand Cover	65
Red dune sand	65
Yellow dune sand and gypsum crust	68
Lag	68
Lag on Gawler Range Volcanics	68
Lag on granite	73
Lag on ultramafic rocks	73
Gypsum	73
Creek Sediments	80
Calcrete	80
Silcrete	83
On granite	83
On ultramafic rocks	84
Silcrete chemistry	84
Gravelly Detritus	85
Saprolite and Saprock	85
On granite	85
On ultramafic rocks	86
Chemistry	86
Soil Geochemistry	86
Regolith Landform Map and Explanatory Notes	90
Landscape Evolution	94
Regional landscape evolution	94
Palaeozoic and Mesozoic	94
Early—Middle Cainozoic	94
Late Cainozoic	95
Localised landscape evolution, Lake Harris	95
Localised landscape evolution, Hopeful Hill	97
Localised landscape evolution, Mullina Well	98
Geochemistry Interpretation	99
Conclusions	100
Recommendations	101
Project Products	101
References	102

Appendices Listing, Volume 2

Appendix 1: Drillhole logs, photos – chip samples and core.

Appendix 2: Assay data, down hole plots & surface geochemistry plans.

Appendix 3: XRD data.

Appendix 4: PIMA spectral data.

Appendix 5: Petrography and Airborne Electro-Magnetic profiling.

Appendix 6: Lake Harris Regolith Landform Map (1:10,000 scale, folded,

Appendix 7: CD-ROM, Data, Report pdfs. Regolith Map: pdf and ArcReader version.

—oo0oo—

Figure Listing	Page #
1: Harris Greenstone Domain bedrock and regolith drilling. Bedrock Drilling Locations. Modified after Davies (2002b). _____	5
2: Harris Greenstone Domain bedrock and regolith drilling. Drillhole Localities over 1 st Vertical Derivative. Modified after Davies (2002b). _____	6
3: Harris Greenstone Domain bedrock and regolith drilling. Lake Harris drilling. Modified after Davies (2002b). _____	7
4: Harris Greenstone Domain bedrock and regolith drilling. Hopeful Hill drillholes. Modified after Davies (2002b). _____	8
5: Harris Greenstone Domain bedrock and regolith drilling. Mullina Well drillholes, eastern end. Modified after Davies (2002b). _____	9
6: Lake Harris drilled section regolith zones. [fold out sheet] _____	16
7: Hopeful Hill drilled section regolith zones. [fold out sheet] _____	21
8: Mullina Well drilled section regolith zones. [fold out sheet] _____	23
9: Regolith drill core from Lake Harris (KLHRDD-1) and Hopeful Hill (THHRDD-1). _____	31
10: Regolith drill core from Hopeful Hill (THHRDD-1) and Mullina Well (TMWRDD-1). _____	36
11: Regolith drill core from Mullina Well (TMWRDD-1). _____	41
12: Petrography of samples from cored drillholes KLHRDD-1 and THHRDD-1. _____	48
13: Petrography of samples from cored drillhole KLHRDD-1. _____	50
14: Petrography of samples from cored drillholes THHRDD-1 and TMWRDD-1. _____	52
15: Petrography of samples from cored drillhole THHRDD-1. _____	54
16: Petrography of samples from cored drillhole TMWRDD-1. _____	56
17: Ternary plots of major elements (Si, Al, Fe) for (A) the Lake Harris drillhole, (B) the Hopeful Hill drillhole and (C) the Mullina Well drillhole showing weathering trends in the weathered basement rocks and sedimentary and weathering trends in the overlying sediments. _____	57
18: Log and geochemistry of Drillhole KLHRDD-1 at Lake Harris. _____	58
19: Log and geochemistry of Drillhole THHRDD-1 at Hopeful Hill. _____	60
20: Log and geochemistry of Drillhole TMWRDD-1 at Mullina Well. _____	61
21: Bivariate plots (A-C) and a trivariate plot (D) illustrating how basement rocks may be largely distinguished geochemically from the covering sediments. _____	62
22: Bivariate ratio plots of minimally mobile elements to illustrate classification of mafic basement rocks at the two sites (after Barnes pers. com., 2003). _____	62
23: Surface regolith – Dune Sand, and petrography. _____	67
24: Surface regolith – Silcretes + GRV lag, and petrography. _____	70
25: Surface regolith – GRV lag, Silcrete lag, Ultramafic lags, and petrography. _____	72
26: Surface regolith – Lags, Calcrete, Ultramafic saprolite, and petrography. _____	75
27: Surface regolith – Granite saprolite, Colluvium, Hardpan, Gypsum, and petrography. _____	77
28: Surface regolith – Gypsum, Stream sediments, Silcrete, and petrography. _____	79
29: Surface regolith – Calcrete, Granite saprolite, Ultramafic amphibolites, and petrography. _____	82
30: Ternary Si-Al-Fe diagram showing the silcretes and the weathered granites from which some of them developed. The silcrete with chalcedony fragments (silcrete UM), lying on an ultramafic saprolite, is similar. A ferruginous silcrete is similarly Al depleted but has a higher Si:Al ratio. _____	85
31: A log-log plot of ranges against means of anomalous elements (As, Fe, Mg, Cr, Ni, V and Co) indicate exposed komatiitic lithologies elsewhere covered by transported overburden with a largely granitic provenance. _____	87
32: Chromium content of soil samples at Lake Harris showing both the upper (20-150 mm) and lower (200-250 mm) media in relation to major geomorphic units. _____	88
33: Lead content of soil samples at Lake Harris showing both the upper (20-150 mm) and lower (200-250 mm) media in relation to major geomorphic units. _____	89
34: The Kingoonya Palaeochannel valley in relation to the Harris Greenstone Belt. _____	96
35: Landscapes of the Lake Harris area. _____	97

—oo0oo—

Table Listing	Page #
1: Analytical Methods used for Regolith Characterization. _____	13
2: Analytical Methods used for Drilling and Surface Samples. _____	13
3: Generalized <i>in situ</i> regolith components from drill cuttings at Lake Harris, in S-N sequence and from freshest to most weathered rock. _____	17
4: Generalized transported cover components from surface regolith mapping and drill cuttings at Lake Harris; oldest to youngest units. _____	18
5: Generalised <i>in situ</i> regolith components from drill cuttings at Hopeful Hill. _____	19
6: Generalized transported cover components from drill cuttings at Hopeful Hill; oldest to youngest units. _____	22
7: Generalized <i>in situ</i> regolith components from drill cuttings at Mullina Well. _____	24
8: Generalized transported regolith components from drill cuttings at Mullina Well; oldest to youngest units. _____	26
9: Cored diamond drillhole locations, coordinates and final depths. _____	26
10: Summary log of Lake Harris cored drillhole KLHRDD-1 (not to scale). _____	29
11: Summary log to Hopeful Hill cored drillhole THHRDD-1 (not to scale). _____	34
12: Summary log to Mullina Well cored drillhole TMWRDD-1 (not to scale). _____	39
13: Thresholds for Distinguishing Greenstones from Sediments. _____	63
14: Energy dispersive spectroscopy analysis of micro-coprolite ferruginising cement. _____	68
15: Stream sediment size distributions. _____	83
16: Regolith Landform Map unit symbol notation. _____	91
17: Modified RED scheme units symbols as used on the Lake Harris Regolith Landform Map. _____	92

—oo0oo—

Photo Listing	Page #
1: Lake Harris greenstone outcrop and thin surficial cover. _____	4
2: Top-drive rotary aircore and diamond capacity drill rig drilling HQ core, Hopeful Hill, June 2002. _____	4
3: Silcrete block (polished), Lake Harris greenstone outcrop, with ultramafic derived clasts. _____	65

Appendix 1 Photos

A1P1-4: Lake Harris chiptray profiles to 22 aircore drillholes (on 4 panels). _____	Vol. 2
A1P5-6: Hopeful Hill chiptray profiles to 12 aircore drillholes (on 2 panels). _____	Vol. 2
A1P7-10: Mullina Well chiptray profiles to 21 aircore drillholes (on 4 panels). _____	Vol. 2
A1P11-20: Lake Harris HQ drillhole cores KLHRDD-1 (10 trays). _____	Vol. 2
A1P21-28: Hopeful Hill HQ drillhole cores THHRDD-1 (8 trays). _____	Vol. 2
A1P29-35: Mullina Well HQ drillhole cores TMWRDD-1 (7 trays). _____	Vol. 2

—oo0oo—

Regolith Characterisation and Geochemistry as an Aid to Exploration in the Harris Greenstone Belt, Central Gawler Craton, South Australia.

M.J. Sheard¹ and I.D.M. Robertson²

1. South Australian Geological Survey, Mineral Resources Group, PIRSA, Adelaide, S. Aust. & CRC LEME
2. CSIRO Exploration & Mining, Perth, W. Aust. & CRC LEME

ABSTRACT

Komatiitic greenstones were first recognised in South Australia from drillcore at Lake Harris on the Gawler Craton by Mines and Energy SA personnel in 1991. Subsequent petrography and detailed aeromagnetic data interpretation led to targeted drilling by PIRSA Geological Survey in 2001 and 2002. That drilling aimed to confirm the greenstone strike continuity, establish stratigraphy and contact relationships, elucidate details of the lava flows, establish the depth of cover, regolith assemblages, geochemistry and landscape evolution of the targeted areas. Over 130 aircore holes were drilled into regolith, unweathered greenstone and quartzo-feldspathic basement. Eleven had additional diamond core tails and significant diamond core into fresh basement was retrieved from another eight holes. This regolith study was run in parallel with the 2001-2002 basement drilling programs and used a selection of the available aircore samples, augmented by an additional three fully cored regolith profiles drilled in mid 2002. These provided control on the earlier aircore chip logging and more detail of weathering and related geochemical dispersion. Together, these projects have provided significant new information for key sections of the Harris Greenstone Belt.

Aircore drill cuttings provided a good orientation sample set within weathered greenstone terrain. Drill cuttings and core required revisiting and reinterpretation when assay, petrographic and other results became available. As the drillcore dried out, some subtle regolith features became more apparent. Erosion of the deeply weathered greenstones has produced, in at least one area, a mass wasting or landslide of a surface to form a debris flow deposit (>5 m thick) with remarkably similar properties to its source. Ferruginous cappings on the Harris Greenstone Belt are very thin (<1 m) or have been removed by erosion. Greenstone spinifex textures in the serpentinised komatiite are preserved in saprolite at Lake Harris to within 17 m of the surface and to within about 2.5 m of the main unconformity (transported on *in situ*). Bioturbation of greenstone-derived ferruginous resistate materials may provide a supplementary exploration sample medium and may make it possible to 'see through' 5-10 m of transported cover. Soil sampling revealed komatiite indicator elements (Mg, Cr, Ni, As, Co, Fe, Mn and V) are elevated over exposed weathered greenstones or where that lithology is mantled by very thin cover. Mineralization-related elements (Au, Bi, Cu, Pb and W) are elevated there too, indicating prospective ground for base metals. Detailed regolith mapping at prospect or 1:10 000 scale can provide an 'outcrop *versus* transported cover' framework to better target surficial geochemical sampling. It can also lead to landscape evolution models that may provide vectors to dispersed mineral signatures or from those towards mineralization.

Key Recommendation

Difficulties encountered in accurately identifying the major unconformity between *in situ* and transported regolith in covered terrain, using aircore drill cuttings, are reduced markedly when compared with full regolith profile drillcore. Access to at least one targeted drillcore per mineral prospect, passing through the regolith profile, would aid regolith modelling, geochemical sampling and/or interpretation, and in more cost effective siting of further drilling.

Acknowledgements

The authors wish to acknowledge the assistance received from the following: South Australian Government – Targeted Exploration Initiative (TEiSA) for significant funding over two years; M. Kessel, Manager of North Well Sheep Station for site access, water supply access and accommodation at Yerda Out Station; P. Ailiffe, Manager of Wilgena Sheep Station for site access and water supply access; A. Vartesi and C. Steel for drafting the cross-sections and some of the photograph annotation and layouts; M. Davies for locality plan compilations and E. Appelbee for formal drafting of locality plans; S.J. Barnes advised on interpretation of komatiite geochemistry; P. Trethaway and J.B. Ragless for compiling the digital Regolith Landform Map, its pdf and ArcReader versions; Ultratrace Analytical Laboratories completed the XRF and ICP analyses; the samples were prepared for analysis by P. Thornley; B. Singh and J. Keeling for providing valuable peer review comment on the final draft of this report; and J. Campbell for assisting with final document production. All this is acknowledged with appreciation.

Introduction

Background

The metakomatiites of the Harris Greenstone Belt were discovered in 1991 at the NW corner of Lake Harris (Daly and van der Stelt, 1992; Figures 1-3). Previous mapping in the 1970s had found limited outcrop of a deeply weathered crystalline basement with bright green clays. These contain resistant bands or pods of dark green to black altered amphibolite (GAIRDNER 1:250 000 and Kokatha 1:100 000 map sheets; Blissett, 1977; 1985; Photo 1).

Diamond drilling by the South Australian Department of Mines and Energy – Geological Survey in 1991 investigated the fresher subsurface basement rocks beneath the known small mapped outcrop (Daly and van der Stelt, 1992). Diamond drilling at Lake Harris (DDH-1 and DDH-2) below the weathered zone, intersected fine-grained subvertical grey to greyish black metakomatiite, composed predominantly of serpentine with less chlorite, tremolite, magnetite and chromite. The serpentine replaces abundant, predominantly metamorphic olivine, although some original igneous olivine is still preserved. Magnesia content varies from 27 to 41% (volatile free) and very fine spinifex fabrics are preserved in the upper part of the N-facing flow or flows. Metal contents for the serpentine-rich metakomatiite range up to 2500 ppm Ni, 1820 ppm Cr, 100 ppm Co, 10 ppb Au and 6 ppb Pt. Some ferruginized surface samples contain up to 6500 ppm Ni (Daly and Fanning, 1993).

Interpretation of imaged aeromagnetic data outlined a sub-surface metamorphosed mafic sequence with an ENE strike of at least 25 km, a width of 1.2-2.0 km and a depth extent of at least 600 m. Similar greenstone occurrences at Hopeful Hill and Mullina Well have been confirmed by surface mapping and exploration drilling. An overall strike length of at least 120 km was initially proposed for what came to be called the Harris Greenstone Belt (HGB). More recently, detailed interpretation of the geophysical data suggests a minimum strike of 300 km. This consists of three or possibly four distinct belts that may represent spatially separate belts or one that has been tightly folded (Hoatson *et al.*, 2002) (Figure 2). These belts contain not only Archaean komatiite but also high-Mg basalts and metasediments that form a complex layered sequence. However, there are only sporadic and limited outcrops of the basalts and metasediments (Schwarz *et al.*, 2002).

In mid 2001, the Gawler Craton Team of the PIRSA Office of Minerals and Energy Resources (OMER) – Geological Survey Branch began further investigative drilling in the Harris Greenstone Belt (HGB). This was to confirm overall strike length, establish stratigraphy, contact relationships, and elucidate details of the lava flows in selected areas. During this first phase, 131 aircore holes were drilled through the regolith and into the unweathered basement. Eleven had additional diamond core tails and significant diamond core into fresh basement was obtained from eight of those (Davies, 2002a).

Work Program

This project formed part of broader regolith studies, namely a) CRC LEME Program 2: ‘Mineral exploration in areas of cover’ and b) the PIRSA Mineral Resources Group – Geological Survey Branch, Gawler Craton Team’s, ‘Regolith and Landscape Evolution Project’. Their common aim – to develop technically efficient procedures for mineral exploration through a comprehensive understanding of regolith and landscape evolution and their influence on the surface expression of concealed mineralization.

Transported cover and deeply weathered crystalline basement together form a major exploration impediment over much of the Gawler Craton and especially over the HGB greenstones. Therefore finding ways to make exploration more efficient would further encourage exploration investment. The PIRSA-sponsored Harris Greenstone Belt drilling program of 2001 sparked interest in the ubiquitous transported cover and deeply weathered materials that, together, conceal much of the ultramafic metavolcanic-metasedimentary greenstone package. Funding from the Targeted Exploration Initiative of SA (TEISA) was provided for 18 months to involve PIRSA Minerals Resources Group and CRC LEME in a study of the HGB regolith. This funding commenced in July of 2001 and was continued into 2003. Additional CRC LEME staff were assigned in November 2001. PIRSA-Mineral Resources Group and CSIRO

Exploration and Mining, operating within the Cooperative Research Centre for Landscape Environment and Mineral Exploration (CRC LEME) provided the relevant staff and regolith laboratory facilities.

Preliminary work began in July 2001 and was fully underway by September, it sought to establish the depth of cover, regolith assemblages, regolith components and geochemistry. A second drilling phase took place in mid 2002, designed to more fully test earlier sparsely drilled areas and explore untested sites beyond. During this new phase, 61 aircore holes were drilled, of which nine had additional diamond core tails into unweathered basement (Davies, 2002b). Three cored holes (yielding 130 m of HQ diameter core) were drilled from surface, through the weathered zone to fresh rock and formed the regolith component of the drilling. Sites were selected to complement and provide regolith zone control for the earlier aircore drilling of 2001 which only generated drill cuttings through the transported cover and weathered zones, making assignment of some critical regolith boundaries either difficult or inconclusive.

The regional work program included studies on the weathered HGB, adjoining rocks and associated transported cover. Follow-up work on a selected area at Lake Harris included: regolith-landform mapping, surface sampling with geochemical and petrographic investigation. Landscape evolution and interpretation of geochemical dispersion were the focus of more detailed studies. There has been no similar previous study over greenstones in South Australia.

Location and Topography

This study covered three parts of the central Gawler Craton, at Lake Harris, Hopeful Hill and Mullina Well. Approximate centroids for each locality¹ are i) Lake Harris (0511800 E, 6567600 N), ii) Hopeful Hill (0492100 E, 6575800 N) and iii) Mullina Well (0461100 E, 6592400 N). All three are within the Harris Domain of the central Gawler Craton, to the E and ESE of Tarcoola, and S of the Transcontinental Railway between Adelaide and Perth. Within each, a drilled transect was selected to represent the greenstone belt, weathered basement and transported cover (Figures 1-5).

The Harris Domain (a crustal tectonic structural domain) is of low relief where elevations range from about 120 m ASL in the large ephemeral lakes, through plains at about 150-165 m, to local highs like Hopeful Hill (185 m), Tarcoola ridge (171 m), Kychering Hill (192 m), Bulpara Hill (244 m), and to the highest point at Mt Fink (369 m). Most high points rise abruptly from a surrounding plain, providing excellent observation points, most with survey trig beacons. Overall, drainage is subdued, gradients are very low and ephemeral creeks tend to terminate in salt lakes and clay pans. Sand dunes cover large areas.

Access and Climate

All three localities are accessed from the Glendambo - Kingoonya - Tarcoola unsealed road and along well-established tracks on North Well and Wilgena Pastoral Stations. Access by vehicle to the islands in Lake Harris was inadvisable, due to soft clay-rich lake-sediments underlying the thin halite crust, so both islands were reached on foot. Drilling was limited to track or road easements and avoided areas that may be subject to Native Title.

This region is arid, with an average annual rainfall of about 200 mm and an annual evaporation rate of >3000 mm, however some years have little or no rainfall. Summers are generally hot and dry, winters are cool and rainfall occurs mostly in early spring (September) or autumn (March-April) (Griffin and McCaskill, 1986).

Methods

Standard regolith methods were used as below. The regolith terminology mostly follows that of Eggleton (2001) and draws upon the work of Robertson *et al.*, (1996b) and Robertson and Butt (1997). Variations to defined terminology and standard methods are indicated below where first mentioned.

Drilling

Most of the PIRSA-sponsored 2001 and 2002 drilling programs used top drive rotary aircore drill rigs (Photo 2) with moderate pressure compressed air and polymer mud-foam as necessary to maintain drillhole

¹ All coordinates used herein are UTM, using the WGS 84 datum and fall within Zone 53J.

stability. These yielded cuttings, fines and minor short weathered rock cores (<300 mm long). The returning air from the drill stem, with suspended cuttings, was discharged into a cyclonic sample separator-collector. Sample depth uncertainty is about 2 m. The drillholes were uncased, unless absolutely necessary (generally only needed for near-surface loose sand) so there has been some down-hole sample contamination by over-cutting, partial collapse and drill stem abrasion. Drillhole-to-hole sample hygiene was not ideal for regolith investigations, as some fresh bottom-of-drillhole rock chips were transferred to the next drillhole top (2-4 samples) due to poor cleaning of the drill rods, top-drive, hose and cyclone.

Sampling was at 2 m intervals. Samples included i) 20 litre bags, ii) about 425 g in reference sample bottles and iii) about 25 g of cuttings (per interval) placed in 20-chamber chiptrays. All reference samples (cores, cuttings, chiptrays, surface hand specimens, thin-sections and polished mounts) have been lodged with the PIRSA Core Store Facility at 23 Conyngham St, Glenside, South Australia. The primary 20 litre bag samples (2001 drilling) were retained on site at three bag farms to allow additional reference and sub-sampling during the orientation phases. Those samples were disposed of in June-July 2002.

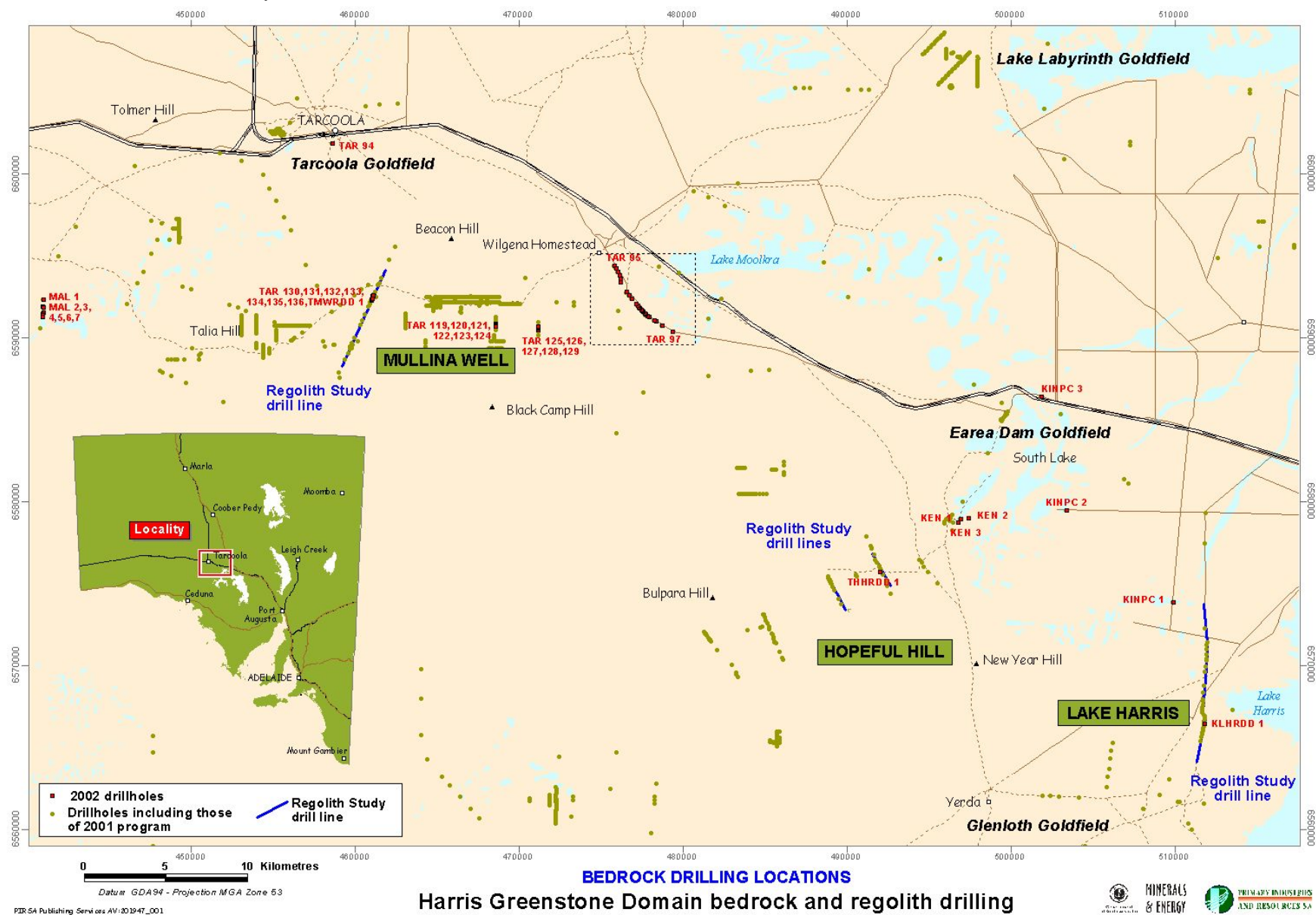
The regolith was cored in 2002 with HQ size diamond bits through the transported cover, *in situ* pedolith and top of the upper saprolite. This bit type was unsuitable for the remaining regolith due to the drilling process producing a very greasy clay-talc-serpentine paste that prevented further drill penetration. A toothed tungsten carbide bit was used to successfully core the remaining section into relatively unweathered serpentinite. Standard triple-barrel core-tubes with inner splits were used for core collection and core barrel recovery was by wire-line retrieval. A suspension of polymer mud in water formed the cuttings return fluid. High solute contents of the circulating drill mud (NaCl, MgSO₄, MgOH), contributed by the local ground water and the regolith, significantly altered the drilling fluid viscosity, rheological properties and pH. This required constant monitoring to maintain optimum drilling rate, core plus cuttings recovery and to prevent rod jams.

Photo 1: Part of the recently exhumed Lake Harris deeply weathered Archaean greenstones (foreground) intruded by Palaeoproterozoic felsic dykes and quartz veins. Pallid cliffs (background) are saprolite of the Glenloth Granite overlain by thin, orange colluvium.

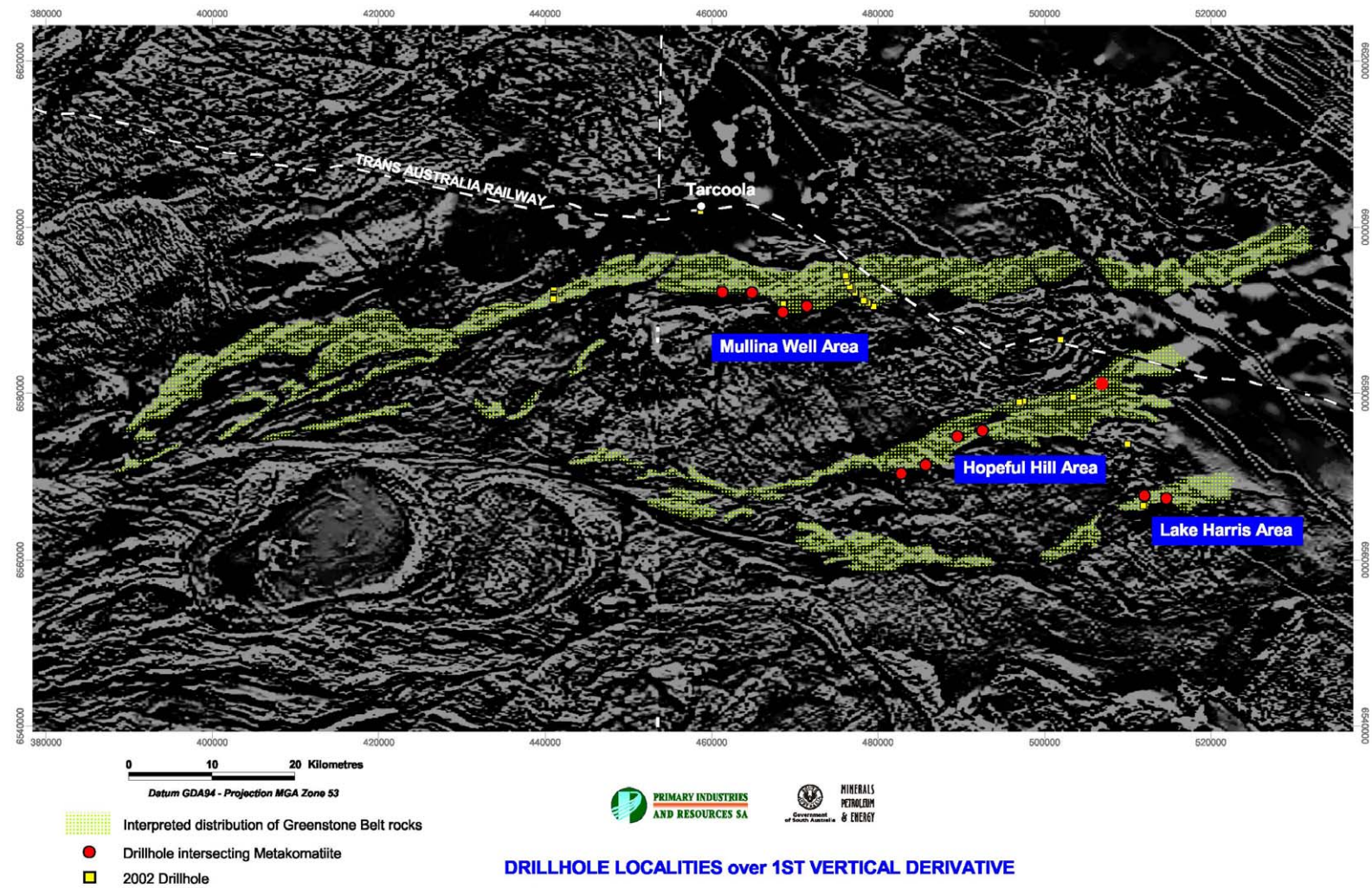


Photo 2: Top-drive rotary aircore and diamond coring drill rig taking HQ core, using triple barrel, with wireline recovery at Hopeful Hill (June 2002).





BEDROCK DRILLING LOCATIONS
Harris Greenstone Domain bedrock and regolith drilling
Figure 1: Modified after Davies (2002b).



PIRSA Publishing Services AV/201755_002

Figure 2: Modified after Davies (2002b).

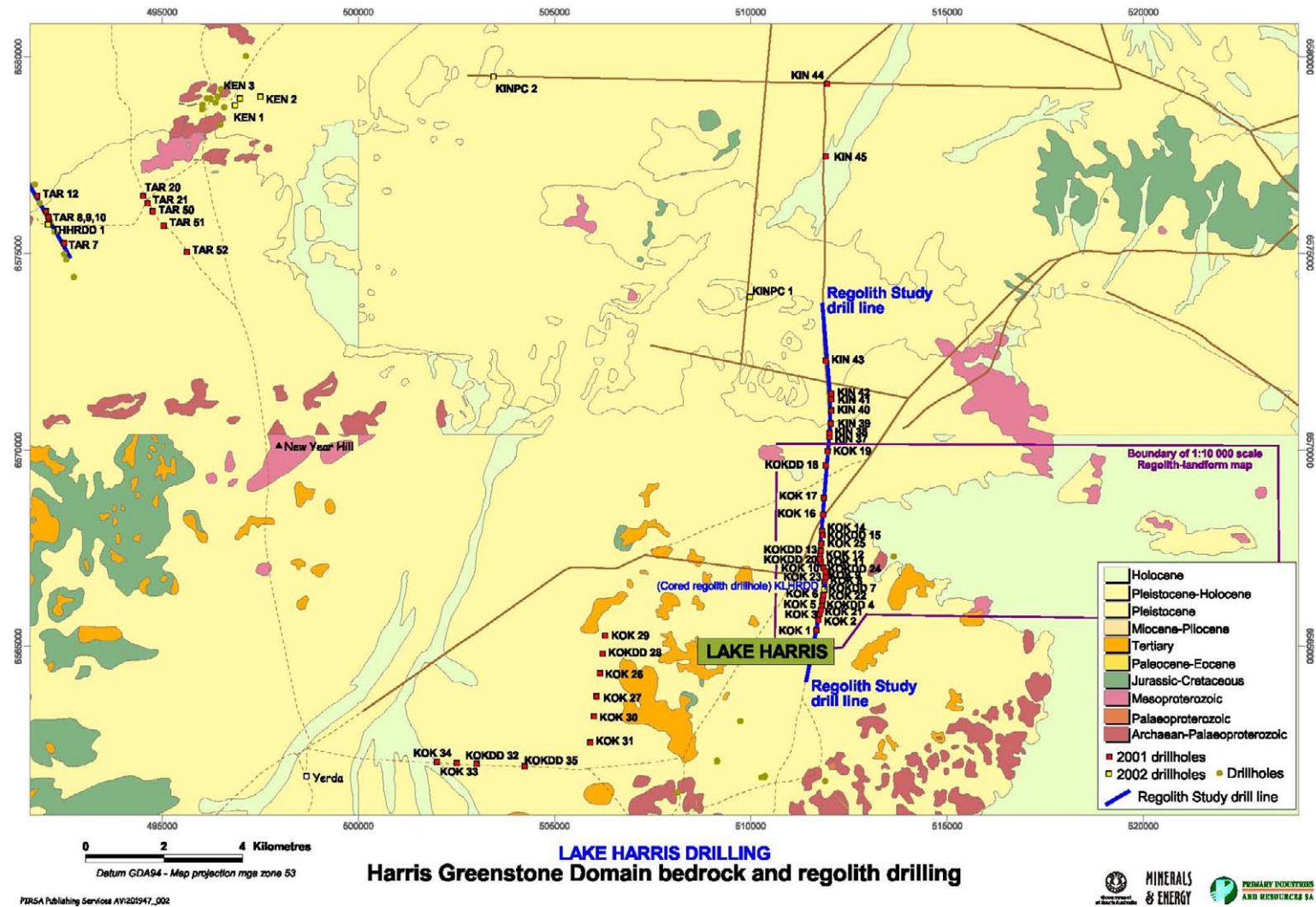


Figure 3: Modified after Davies (2002b).

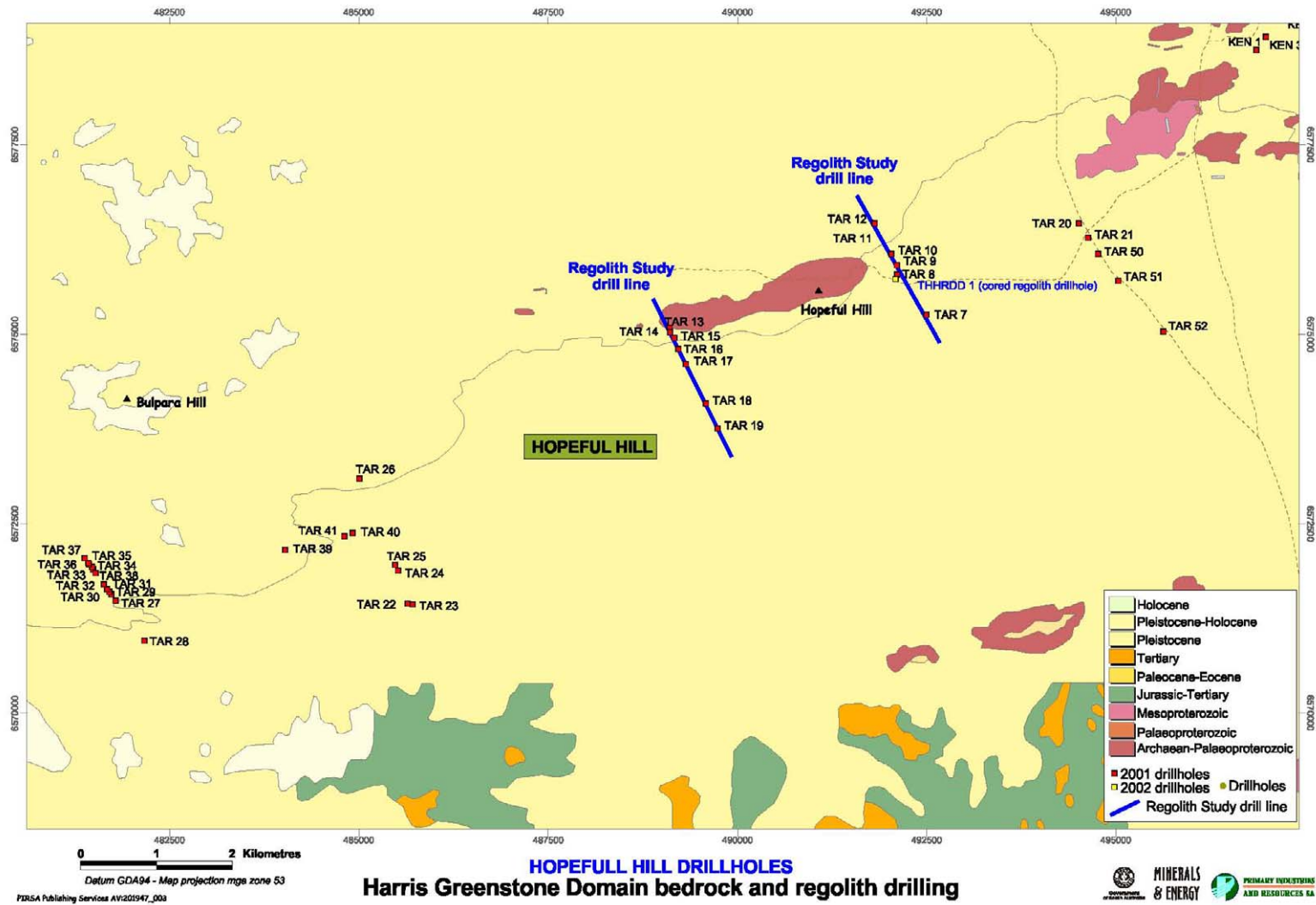


Figure 4: Modified after Davies (2002b).

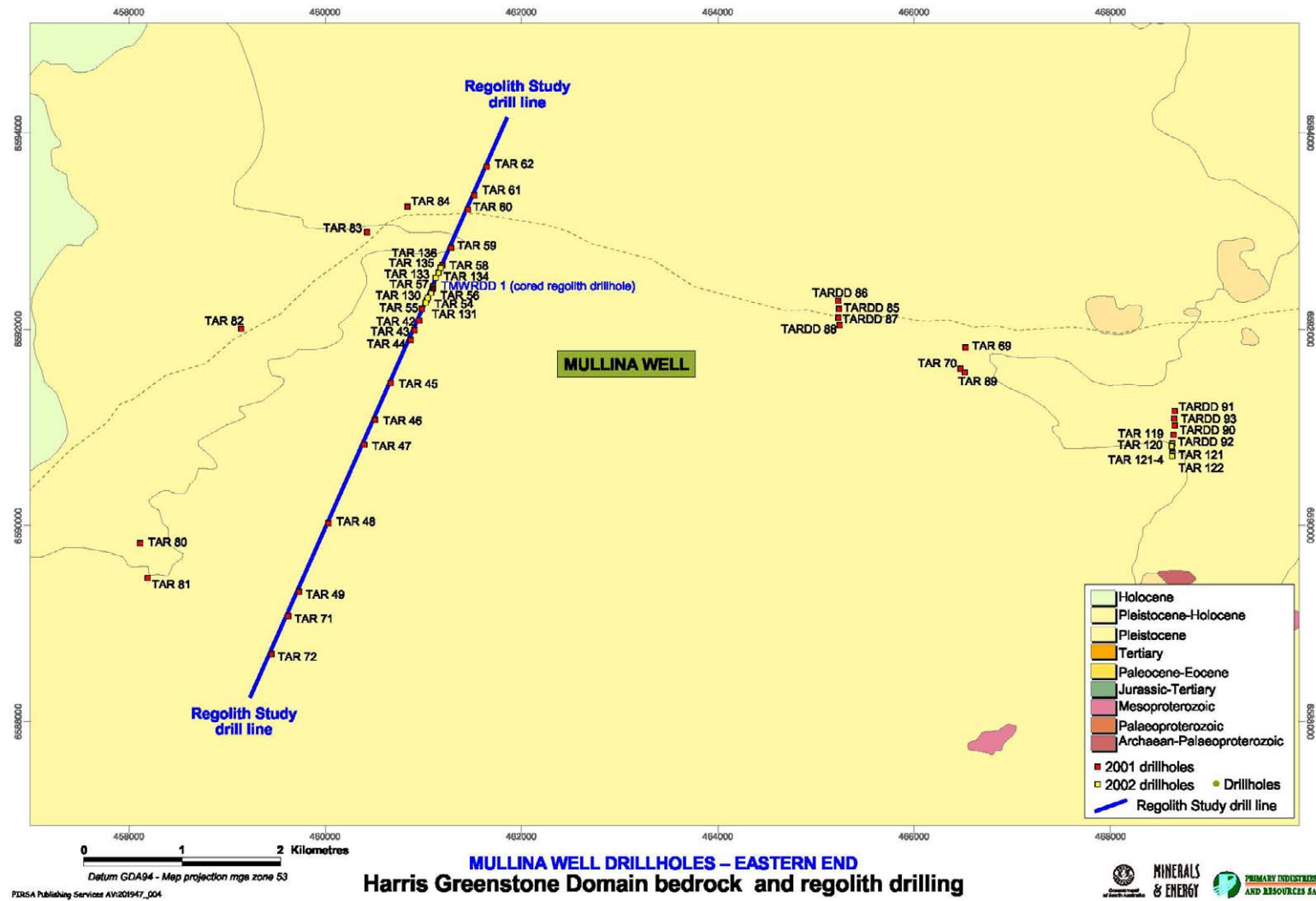


Figure 5: Modified after Davies (2002b).

Surface sampling

In the Lake Harris area four suites of surface samples were collected; firstly, a range of exposed regolith materials comprise the weathered surface rock set, discussed in “Description of surficial materials at Lake Harris” and “Soil Geochemistry” sections). Those samples aided the regolith mapping and materials characterisation aspects. Secondly, a suite of soil samples was collected on the N-S drilled traverse along the Kingoonya-Glenloth Mine track, at intervals varying from 120-400 m. One sample lies N of the mapped area. Those samples were selected to test near surface geochemical dispersion in transported cover that may have geochemical signatures derived from underlying basement. They were also assayed to reveal any geochemical differences within the 0-0.25 m soil profiles. Soil samples from that traverse augmented the bulked 0-2 m cuttings from each drill site. Two more traverses (3rd and 4th) were sampled at closer intervals (50-120 m). One started from the DME 1457 benchmark, extending N across the exposed basement rocks towards the NW end of Lake Harris. The other, began 550 m further E and nearer Lake Harris, converging with the previous traverse to the NW. Soil samples (from 20-150 mm depth) were collected at each site, and at many, an additional deeper sample was also taken between 200-250 mm depth. Traverses 3 and 4 cross ground where cover is generally relatively thin or even absent and so permitted testing of cover thickness versus geochemical signal strength. The drill line parallel traverse is where cover units are generally quite thick (10-20 m). Many of the deeper samples were cemented by calcrete or hardpan. Details of the materials encountered and the resultant analyses (Table A2.1) with site location plans are given in Appendix 2, while the three soil traverse lines are also displayed on the Lake Harris Regolith Landform Map of Appendix 6. Soil sampling sites are displayed with elemental geochemistry in the figures associated with section entitled “Soil Geochemistry”.

A small suite of stream sediment samples was collected from the N-flowing drainage that lies mostly to the W of the Kingoonya-Glenloth Mine track wherever the stream bed was sufficiently well defined. Sample locations and geochemistry are shown in Table A2.1, Appendix 2.

Logging

All aircore drill cuttings were logged by supervising geologists in the field. Later, the regolith of 55 selected drillholes was logged in detail, using the chiptray and 425 gm bottle samples at the PIRSA Core Store Facility in Adelaide. Logging of cuttings involved both visual and binocular microscopic examination of minerals and grain/clast morphologies. Initially assigned regolith zone boundaries were adjusted using down hole geochemical plots of elements and selective element ratios (Appendix 2). Colour standards from Munsell (1975) plus Kelly and Judd (1976) provided useful references and guidance for sample descriptions. All aircore sample logs are given in Appendix 1 and the CD-ROM (Appendix 7). These are set out in a spread sheet where five levels of description are provided for each 2 m interval as follows:

- Level 1, provenance (transported or *in situ*),
- Level 2, colour,
- Level 3, regolith zones and modifiers (cements, staining, mottles, etc),
- Level 4, graphic log in colour: weathering zones and modifiers, bulk basal rock type and assay sample intervals,
- Level 5, sample description: details of materials, fabrics, grains, cements, reaction with acid (carbonate).

The three fully cored drillholes were logged on-site by the supervising geologist after cleaning off some of the adhering drilling mud. Later, the core was logged in detail, after the remaining mud had been removed, photographed and sampled at the PIRSA Core Store Facility. Logs of the cores are provided as a table with a colour graphic column indicating regolith zones, cementation, staining, mottling, other indicative features, core tray numbers and relevant photographs (Appendix 1). Logs and geochemistry are given graphically in Appendix 2 as pdf files.

Limitations

When logging aircore, RAB and RC drill cuttings, it is difficult to determine regolith zones and locate boundaries. Much important detail such as colour, mottles, fabric and banding are homogenised by the

drilling. Drill cuttings provide, at best, only about 20% of the information possible from drillcore. Thus, cuttings should be logged keeping in view the limitations, and over-interpretation should be avoided.

Some regolith profiles are complex. The pedolith may retain some key residual metal geochemistry from the deeper, less weathered basement, although much of the upper (generally leached) saprolite can be metal depleted. Zones can be missing, through erosion or inadequate recovery, so expecting these possibilities is crucial to interpreting the drilling and resultant surface geochemical anomalies. Determining if pedolith is present (in whole or in part) is crucial to accurate logging.

Sample Contamination

Down-drillhole and drillhole-to-drillhole sample contamination was evident in many drilled intervals. Generally, contamination was obvious, *i.e.* near surface derived calcrete nodules and silcrete fragments occurred in intervals many metres below their source, or fresh basement fragments from the previous drillhole had contaminated the topmost highly weathered intervals of a new drillhole. However, there were also less obvious contaminants at similar depths, including well-rounded quartz clasts (3-10 mm diam.) within clay-rich materials with a definite basement character. To resolve this in a few difficult cases, the fines were washed from the bulk cuttings. These were examined with a microscope for *in situ* materials (including relict resistate minerals with delicate shapes such as multi-grained lithic fragments, quartz micro-vein fragments or minerals not likely to have been transported by fluvial or aeolian processes). Fresh basement fragments within a transported unit indicated contamination between drillholes.

Once visual logging is complete, the unconformity between *in situ* weathered basement and transported material must be located. At several drill sites, this was difficult. Petrography, geochemistry and mineral analysis have provided useful adjuncts to logging and locating the unconformity (see later descriptions). Allowances have to be made for down-drillhole contamination and the fairly broad 2 m sampling interval.

Mapping

Regolith materials boundaries were mapped in the field directly onto 1:10 000 scale air photograph hard copy enlargements derived from digital colour air photography (Survey 3005, 1:87 200 scale, 20/10/1983). The air photograph and Regolith Landform Map of cover part of the GAIRDNER 1:250 000 map sheet and the Kokatha (5935) 1:100 000 map sheet. The air photograph portions involved are reproduced on the Regolith Landform Map lower edge (Appendix 6 in rear pocket).

Mapping and gathering of surface information was from traverses on foot and by vehicle; locations were obtained by hand-held GPS. Surface sampling, excavation of soil profiles by shovel, use of drill logging, surface photography and air photograph interpretation augmented this work. Colour standards of Munsell (1975) plus Kelly and Judd (1976) provided useful references and guidance for sample descriptions in the laboratory context. Geological mapping principles were used within a regolith landform context. Regolith polygons, sample points and notes were marked on enlarged air photographs in the field. The area mapped (about 5 x 12 km) covers a selection of the regolith materials, including weathered greenstones, adjoining granitoids and volcanics and transported cover. Depth information has been added from drillhole data, soil pits and gully exposures. A detailed explanation of the map is given below under **Map Explanatory Notes**. The final map was compiled in Adelaide with cartography by the Spatial Information Branch at PIRSA (Appendix 6 & 7).

Specific height data in the Lake Harris area were taken from two Mines and Energy Survey benchmarks (DME 1456 and 1457) and the public domain 1:250 000 scale GAIRDNER topographic map covering this area (R.A.S.C., 1983). Additional local elevations for geochemical traverses were by digital altimeter, using short, closed traverses, tied to the DME Survey benchmarks. This provided relative profile height precision to, at best, 1.0 m and, in a relative sense, gave good profile topographic control in areas of low relief.

Sample treatment and analysis

Size fractionation

Stream sediments and dune sands were separated into >2000, 1000-2000, 710-1000, 500-710, 250-500, 180-250, 75-180 and <75 µm fractions by shaking on nylon sieves using a Ro-tap sieve-shaker for 20-30 minutes. Size fractions were weighed and examined by binocular microscope.

Heavy liquid mineral separation

A heavy liquid, LST (Li polytungstate liquid with a SG of 2.85), was used to separate heavy minerals in the 1000-2000 µm fraction in a separating funnel. The heavy liquid was removed by washing with hot, deionized water. This particular size fraction tended to clog the funnel outlet; the 500-1000 µm fraction would have been more amenable.

Microscopy and photography

Thin and polished sections were examined in transmitted and reflected light on a petrographic microscope and photographed as the examination proceeded. Polished blocks and sieved size fractions were examined on a binocular microscope and similarly photographed.

Where required, mineral grains and aggregates were removed with fine forceps. They were placed on an adhesive layer on an Al mount for further investigation by scanning electron microscope (Phillips XL40 controlled pressure SEM with an EDAX energy dispersive X-ray spectrometer). This allowed the surface appearance of the grains to be examined and photographed and some semi-quantitative chemical analysis for mineral identification. Polished blocks were similarly examined as required.

Geochemical analysis

Two analytical streams were used.

- i) The relatively small number of surface samples that required regolith characterisation were prepared in a clean environment and milled in a K1045 low-contamination ring mill at CSIRO that has well-established contamination characteristics (Robertson *et al.*, 1996a). The mill was cleaned with a quartz wash and ethanol-wipe of mill components between each sample. Analysis of major elements and some trace elements was by well-established and reproducible XRF analysis after fusion of the sample in Li tetraborate at CSIRO and later by Ultra Trace Pty Ltd. Trace elements that could not be analysed to a sufficient sensitivity by this means were analysed by ICP-MS after a four-acid digest by Ultra Trace Pty Ltd in Perth (see Table 1.). The results are given in Table A2.3, Appendix 2.
- ii) The much larger number of drilled samples was analysed in as near an exploration environment as was compatible with best practice. Ultra Trace (Perth) prepared the samples by pulverising a 100 g aliquot in a carbon-steel mill with quartz washes between samples. Analysis was by ICP and ICP/MS after either a 4-acid digest or fusion with sodium peroxide. Care was taken in the design of the analytical scheme to ensure as complete a sample digestion as possible (see Table 2). Certain refractory minerals remain insoluble despite the 4-acid attack (Hall, 1999) including cassiterite (Sn), rutile (Ti), monazite (Ce, REE, P), ilmenite (Ti), garnet, wolframite (W), spinels (Cr, Zn), sphene (Ti), beryl (Be), zircon (Zr) and tourmaline. This scheme provided a compromise between quality and cost. Results are given in Table A2.4, Appendix 2.

Throughout, camouflaged in-house standards were inserted into the analytical stream to monitor analytical quality. Although the geochemical data are given in digital format as four Excel tables on the CD of the Appendix 7, they are also provided in archival form (ASCII format, tab delimited, one record per sample, with header records) for posterity.

Table 1: Analytical Methods used for Regolith Characterization

Elements	Dissolution	Method	Notes
Si, Al, Fe, Mn, Mg, Ca, Na, K, Ti, P, Ba, Ce, Cl, Cr, Co, Cu, Ga, La, Ni, Nb, Pb, Rb, S, Sr, V, Y, Zn, Zr.	Li-tetraborate fusion	XRF	Accurate and precise, well established method of total analysis
Ag, As, Sb, W, Mo, Cd, Bi, Tl, Sn, Te.	HF/HClO ₄ /HNO ₃ /HCl	ICP-MS	Low concentrations – significant concentrations of W and Sn unlikely

Table 2: Analytical Methods used for Drilling and Surface Samples

Elements	Dissolution	Method	Notes
Si Al Fe Ti Ca Mg K W Zr Ba Cr.	Na ₂ O ₂ fusion	ICP-OES	Major elements and elements with likely refractory host minerals
Mn V Ca Cu Zn Co.	HF/HClO ₄ /HNO ₃ /HCl	ICP-OES	Abundant and relatively soluble
Ag As Sb W Pb Mo Ni Bi U Cd Tl Rb Sn Te.	HF/HClO ₄ /HNO ₃ /HCl	ICP-MS	Low concentrations but non-refractory minerals
Sn Ce La REE.	Na ₂ O ₂ fusion	ICP-MS	Likely refractory host minerals
Au Ag Cu.	Cyanide leach – mini BLEG	ICP-MS	Very sensitive but dissolution can be incomplete

XRD

Small samples of about 0.1 g each were selected from the drill core and pulverised in agate. The pulp (<75 µm) was smeared onto an aluminium mount in ethanol and allowed to dry. Pulps generated from the regolith outcrop materials were loaded and compressed into aluminium carriers. X-Ray diffraction analysis was performed using a Phillips PW1478 instrument using Cu K α radiation, scanning from 2-65°2 θ at about 1°20/min and data were collected at 0.02° 2 θ intervals. Semi-quantitative interpretation was by XPLLOT (V1.34) software using the ICDD mineral database. The smectites were largely montmorillonite. Where smectite occurs, chlorite and hydromuscovite become difficult to distinguish; goethite and hematite are also difficult to distinguish in the presence of kaolinite. Although maghemite and chromite are difficult to distinguish, their presence in the profile may imply partial alteration of primary Fe-Cr spinel.

PIMA

All of the Lake Harris aircore holes have PIMA spectral data (Appendix 4 & CD-ROM Appendix 7); time and logistics prevented gathering this data from the cored drillholes.

The initial aims in using PIMA infra-red spectra were: i) to establish an approximate weathered mineral inventory and ii) to locate the unconformity (to within ± 2 m) using kaolin crystallinity indices based on graphed spectral absorption line slope ratios. In most circumstances elsewhere, transported kaolin or kaolin developed within transported materials, have less well-developed crystallinity than that developed within *in situ* weathered rocks. Determining a location for the prime unconformity involves plotting down-drillhole stacked PIMA spectra, calculating their relevant kaolinite crystallinity indices (KCI) and plotting those as depth related bar charts (Pontual, *et al.*, 1997, p29). A sharp decrease in the KCI to 1.05 or less often marks the transition from a basement profile weathered *in situ* to transported clay-rich materials. However, there is substantial inter-mineral spectral interference in materials from the Harris Greenstone Belt, leading to very noisy down-hole kaolinite crystallinity index plots. These have generally defied interpretation, both regarding the unconformity position and the relative abundances of kaolinite plus smectite. It is also possible that in many cases a low kaolinite abundance within smectite-rich intervals are problematic to interpret. Therefore, KCI's are not a useful tool in this domain, unlike other areas with a more felsic basement (Pontual, *et al.*, 1997; Linton *et al.*, 2002, 2004). Hydromuscovite and montmorillonite crystallinity indices were also tried but with no improvement. Raw PIMA spectra are available from the attached CD-ROM (Appendices 7) for reference and analysis by the reader. Further

identification of individual mineral signatures and provenance for the HGB may now form another interpretive PIMA project for late 2004-2005.

Petrography

Thin sections were cut from selected field and drill core specimens. Although some materials were very sturdy to slightly friable, others were highly friable to weakly bound or contained a high percentage of low strength clays unsuited to normal thin sectioning. Normal thin sectioning at CSIRO Exploration and Mining (Perth) sufficed for the sturdy materials, although most required drying and embedding in epoxy resin prior to sectioning. The very friable materials and moist clays required a water replacement procedure involving a very low viscosity epoxy resin that was introduced to each sample through a lengthy immersion; this stabilised the clays. This part of the pre-sectioning sample preparation was by CSIRO Land and Water in Canberra. Once fully resin impregnated (about 8 weeks), exposing the resin-setting catalyst to UV light solidified the sample. Large thin sections (50 x 75 mm) of these blocks were cut by Pontifex and Associates in Adelaide. Epoxy-stabilised blocks were polished on oiled carborundum paper and photographed to illustrate the fabrics.

Regolith in profile

Selected aircore drill-lines

A subset of 55 drillholes was selected from 131 aircore holes drilled for PIRSA in 2001. These were used to construct regolith profiles along four drill lines. The Lake Harris line consists of 22 drillholes, the Hopeful Hill lines include 12 drillholes, and the Mullina Well line 21 drillholes (Figures 3-8). Two short line sections selected from the Hopeful Hill drilling have been combined to form a single section. It was not possible to examine all 131 drillholes, however the 55 drillholes examined provided a satisfactory representative set for each area.

Logging attempted to distinguish transported from *in situ* materials and the degree of weathering. However, limitations imposed by using drill cuttings, a 2 m sample interval and variable down-hole and between hole contamination have made this difficult. A number of intervals appear gradational or hint at features not clearly preserved in the chips (mottle type and their internal fabric, mottle patterns and spacing, mineral veining, banding thinner than the sample interval, broad secondary mineral partitioning like mottles and staining patterns, etc). The regolith includes transported cover, pedolith, saprolite, saprock and protolith. Where possible, protolith and saprock have been indicated broadly or specifically. Splitting the saprolite into upper and lower parts is based mainly on colour and competence; this subdivision has recently been used successfully at several Gawler Craton regolith research sites (Lintern *et al.*, 2002, 2003). Upper saprolite tends to be lighter coloured, is weakly bound and its stiffness is low to moderate; in comparison, lower saprolite is darker coloured, coherent and firm to stiff. Both parts retain relict primary fabrics and metamorphic foliation.

Pedolith (as described herein from drill cuttings) may also include colluvium derived from both deeply weathered basement and sedimentary terrains. This regolith zone has variably been strongly affected by pedogenic processes (silicification) and yet commonly does not display obvious sedimentary characteristics. Petrography, XRD and geochemical analyses have indicated that the major unconformity occurs somewhere within the visually logged pedolith.

Cuttings did not provide large enough fragments for consistent subdivision of the pedolith into plasmic or arenose zones. However, duricrusts of silica and ferruginous materials were indicated where recognized. It was because of these difficulties that three fully cored regolith profiles were drilled in 2002, one on each line, to provide a reference profile to allow extrapolation into areas where only cuttings were available.

Lake Harris

Locations for this set of drillholes are provided in Figure 3, the associated 22 regolith logs and the chiptray profile photographs are in Appendix 1. A regolith cross-section, from those logs, is given in Figure 6.

In situ Basement

Below the transported cover, weathered *in situ* crystalline basement rocks form a distinct S-N sequence: granitic-ultramafic-mafic-sedimentary-felsic. At the S end of the section is weathered Palaeoproterozoic Glenloth Granite (drillholes KOK 1, 3), followed northwards by greenstones: as weathered Archaean serpentine-altered metakomatiite (KOK 21 to 14), weathered and altered Archaean metakomatiitic basalts (KOK 15 to 19), followed by weathered Archaean metasediments (KIN 37, 39). Near the N end, weathered Mesoproterozoic felsic Gawler Range Volcanics were penetrated (KIN 40 to 43).

In general, the felsic rocks are less deeply weathered than the metamorphosed mafic to ultramafic basement but the ultramafic rocks are the most deeply and variably weathered. The weathering front is irregular, even within the same rock type, and may reflect structurally controlled permeability variations due to cleavage, fracturing, joints and shearing. Mapping by Daly and van der Stelt (1992) has established that the Glenloth Granite intrudes the greenstones but, at the small outcrop east of the drill line, the contact is sheared. Mapping for this study has confirmed this local relationship. A summary of the weathered *in situ* basement rock types from drilled chip samples is given in Table 3.

Transported Cover

Transported cover (blue on the section) ranged from <1 to ~18 m in thickness and includes, soil, calcrete, Pleistocene aeolian sand, Tertiary to Modern fluvial sediments, Tertiary silcrete bands and possibly Mesozoic to Tertiary age colluvium. Aeolian sand plains and dunes mantle most of the area. They are not recovered very well by the drilling methods used. Sediments below the soil-sand layer are dominantly fluvial and range from silty clays to sand and gravel or mixtures of these. There are some pebbles exceeding 30 mm. These are cemented by calcrete, are incipiently silicified and pass into silcrete. Broad layering can be observed from sample to sample but finer layering can only be inferred from limited evidence in the cuttings. A modern ephemeral creek runs west of and parallel to the drill line; it crosses just north of drillhole KOK 15. A palaeochannel intersects Lake Harris NW corner and contains Tertiary sediments, the Lake Harris line crosses it between drillholes KOK 16 and KIN 40 and is presently partially delineated by a chain of ephemeral salt pans trending NW-WNW from the lake's northwestern corner inlet. A summary of the transported cover units from drilled chip samples is set out in Table 4.

An electromagnetic survey was flown for PIRSA over the Lake Harris and Hopeful Hill drilled areas by Fugro Airborne Surveys, using the TEMPEST AEM system. Geoscience Australia provided data processing, analysis and interpretation (Lane, 2001a). A conductivity data slice from that survey, matching the Lake Harris drill line (Lane, 2001b) is provided in Appendix 5. The zone of highest conductivity along the section coincides with a combination of transported cover and the pedolith to saprock zones within the regolith profile. Although this conductance anomaly mostly lies within the Archaean greenstone belt, the anomaly also coincides with highly saline groundwaters associated with Lake Harris and the Tertiary palaeochannel at the northern end of the section. However at Lake Harris, it is impossible to separate the transported cover from the weathered basement by this geophysical technique. The Hopeful Hill data are less amenable to the same treatment, possibly due to a much thinner zone of weathering and transported cover; the groundwater is either less saline or no groundwater occurs within the regolith.

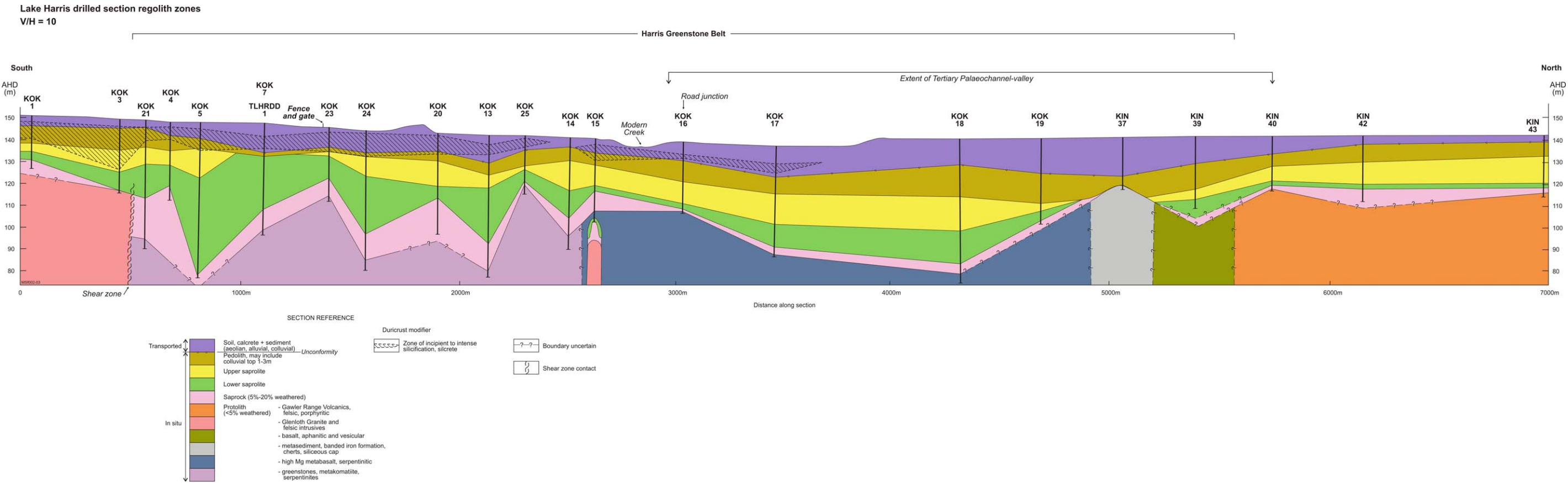


Figure 6:
Lake Harris drilled section regolith zones
[fold out sheet]

Table 3: Generalized *in situ* regolith components from drill cuttings at Lake Harris, in S-N sequence and from freshest to most weathered rock.

Glenloth Granite	Characteristic features	Diagnostic points
Protolith	Medium- to coarse-grained, brown, partly weathered granite, weakly foliated; quartz, fresh K-feldspar, Na-plagioclase and mica.	Typical granite, igneous fabric with weak metamorphic foliation.
Saprock	Pink to reddish, partly weathered granite; clay, quartz and feldspar with Fe-staining on fractures.	Relict granite fragments; mica, K-feldspar and quartz.
Lower saprolite	Weathered rock, brown clay, quartz and relict feldspars; Fe-staining.	Clay and quartz, relict metamorphic foliation and igneous fabric.
Upper saprolite	Highly weathered rock, cream to grey or brown; kaolinite and quartz, some Fe-staining.	Kaolinite and quartz, relict structure and igneous fabric.
Pedolith	Extremely weathered rock, white to pale grey; quartz grit or kaolinite dominant; weak Fe-staining, may have silicified at top.	Kaolinite and quartz, no relict primary fabric.
Meta-komatiite	Characteristic features	Diagnostic points
Protolith	Aphanitic dark green-grey to dark grey serpentinite with some clay lining on fractures, metamorphic foliation and relict fabric.	Dark serpentinite, relict igneous fabric, metamorphic foliation. Relatively soft.
Saprock	Partly weathered rock, brown-grey to dark green-grey, serpentinite, Fe-staining of fractures, metamorphic foliation and relict fabric.	Serpentine with smectite on fractures, Fe-stained, relict igneous fabric, metamorphic foliation. Relatively soft.
Lower saprolite	Weathered rock, green to blue and brown smectitic clays, relict grey serpentinite and talc, Fe-staining.	Sticky clays, darker than upper saprolite, relict veining and metamorphic foliation.
Upper saprolite	Highly weathered rock, cream to yellow or pale green, smectite-rich, talcose, may be Fe-stained.	Clay-rich, pale coloured with relict chalcedony veins and relict metamorphic foliation.
Pedolith	Extremely weathered rock, brown, grey or yellow, clay-rich weak rock; Fe-mottled, may have silicified top.	Clay-rich, dark coloured, relict chalcedony veins.
Metabasalt	Characteristic features	Diagnostic points
Protolith	Dark-grey to dark-brown aphanitic metabasalt, massive to amygdaloidal (voids filled with epidote).	Dark coloured metabasalt, epidote.
Saprock	Partly weathered rock, dark grey, various shades of green and brown clay with relict mafic rock, relict metamorphic fabric, quartz veins.	Dark relict mafic rock with clay; relict metamorphic foliation.
Lower saprolite	Weathered rock, green and brown clay with relict mafic rock, Fe-staining.	Clay-rich, strong colours, relict mafic rock, plastic clays, moderately stiff.
Upper saprolite	Highly weathered rock, pale brown, cream, yellow-brown, clay-rich, massive.	Clay-rich, pale coloured, relict metamorphic foliation, friable sub-plastic to plastic clays.
Pedolith	Extremely weathered rock, red-brown to cream, clay-rich, Fe-stained and mottled, may be in part silicified.	Clay-rich, strong colours, weak and friable to cemented, no relict primary structure.
Metasediments	Characteristic features	Diagnostic points
Protolith	Metasediments; Banded Iron Formation (BIF), gneiss or schist.	Quartz and fresh lithic fragments of BIF and gneiss.
Saprock	Partly weathered metasediments, BIF, gneiss or schist; Fe-staining on fractures.	Relict lithic fragments; mica, feldspar and quartz.
Lower saprolite	Weathered rock, brownish clays with gritty quartz.	Clays and quartz, relict metamorphic foliation.
Upper saprolite	Highly weathered rock, pale greyish clays with gritty quartz.	Kaolinite and quartz; relict metamorphic foliation.
Pedolith	Extremely weathered rock, greyish clays with or without mottles.	Kaolinite and quartz, no relict primary structure.

Table Cont.

Felsic volcanics	Characteristic features	Diagnostic points
Protolith	Pink, red-brown, purple-grey, felsic, fine-grained + or – recognizable igneous porphyritic fabrics.	Typical felsic volcanic, igneous fabric, non foliated.
Saprock	Partly weathered rock, brown to grey, fine-grained, in places with a recognizable porphyritic felsic volcanic fabric.	Relict volcanic rock fragments and clays.
Lower saprolite	Weathered rock, pale brownish to brownish grey; clays and gritty quartz.	Clays and quartz; relict primary igneous fabric.
Upper saprolite	Highly weathered rock, cream to pale brownish clay-rich, relict primary fabric.	Kaolinite and quartz; relict igneous fabric.
Pedolith	Extremely weathered rock, brown to pale brown clay-rich, no relict primary structures.	Kaolinite and quartz; no relict primary structure, mottled.

Table 4: Generalized transported cover components from surface regolith mapping and drill cuttings at Lake Harris; oldest to youngest units.

Unit, age	Characteristic features	Diagnostic points
Colluvium, ?Mesozoic-Cainozoic	Greyish to cream to pale and strong browns, clay + sand, grit & larger clasts, reworked weathered rock, mixed lithotypes, poorly sorted, angular to subrounded, matrix to clast supported (latter only seen in core or outcrop) readily forms lag.	Generally polymictic, angular to subrounded clasts, poorly sorted, fragments of contained ferruginous pisoliths.
Fluvial sediments, Cainozoic	Red-brown to grey, clay to cobbles, clast supported (latter only seen in core or outcrop); clays and quartz, loose to cemented.	Well rounded clasts amongst drill fragments of the same, <1 to >8 m thick.
Silcrete, Tertiary	Duricrust , grey to pale yellow, silica cementation of alluvium, colluvium or weathered basement, partial to full cementation, poor in clay-silt fines, may contain major unconformity - (latter only seen in core or outcrop).	Cryptocrystalline semi-translucent cream to pink cement, hard to very hard drilling, clasts cemented so firmly as to force any breakage through rather than around them, thickness <0.5 to about 2 m, may occur in several horizons.
Calcrete, Quaternary	Duricrust , white to pale yellow to pale pink or orange, massive competent and/or nodular, pedogenic carbonate.	Noticeable pallid soil horizon, effervescent reaction with acid, may host geochemical signature.
Aeolian sands, Pleistocene	Mantles much of the landscape, orange, siliceous, dunes and sand plains, can contain nodular calcrete and platy gypsum. Sand forms a sample dilutant to any locally derived mineral-lithic grains.	Mostly loose, uniformly sorted, frosted quartz grains in fine-medium sand size, <1 to >8 m thick.

Hopeful Hill

Locations for these drillholes are given in Figure 4, the associated 12 regolith logs and the chiptray profile photographs are in Appendix 1. A regolith zone cross-section, from those logs, is provided in Figure 7. This is a composite of two short drill lines projected onto the same section.

In situ Basement

Below the transported cover, a series of weathered crystalline basement rocks forms a broadly banded sequence: felsic-mafic-granitic-ultramafic-mafic-metasedimentary-felsic. Here, the weathered profile on the basement is much thinner than at Lake Harris. At the S end, weathered felsic porphyry and Mesoproterozoic granite were intersected (TAR 19-16) but in TAR 18 this is overlain by a highly weathered medium- to coarse-grained mafic gneiss of possible gabbroic origin. The weatherability differential between the mafic gneiss and underlying felsic basement (34-44 m) has given rise to the complex regolith zone repetition depicted in Figure 7. Further N, greenstones were intersected. These comprised weathered, Archaean, serpentine-altered, metamorphosed, ultramafic rocks and their schistose

equivalents (TAR 15, 13, 7-10), followed northwards by weathered and altered, felsic, medium- to coarse-grained gneiss (TAR 11). At the N end of the section, TAR 12 intersected a weathered, highly strained (mylonitic) felsic rock. In general, the felsic rocks are more deeply weathered than the ultramafic rocks, the reverse of the situation at Lake Harris. The deepest weathering (28m) in an ultramafic rock is around TAR 8. As at Lake Harris, the weathering front is irregular, even within the same rock type, and may reflect water permeation along cleavages, fractures, joints and shears. A summary of the weathered *in situ* basement rocks, from drilled chip samples, is given in Table 5.

Transported Cover

Transported cover, shown as blue on the section, ranges from about 1-15 m in thickness and includes, soil, calcrete, Pleistocene aeolian sand, Tertiary fluvial sediment, discontinuous Tertiary silcrete bands and some presumed Mesozoic to Tertiary age colluvium. Aeolian sand plains and sand dunes mantle much of this area and are poorly recovered by the drilling method used. Sediments below the soil-sand layer are predominantly fluvial and range from silty clays to sand and gravel or mixtures of these. Some gravel clasts exceed 30 mm. Cements include calcrete, incipient silicification and recognizable silcrete. Broad layering may occur from sample to sample, as indicated by colour and/or textural changes, but finer layering can only be inferred from specific sample fragment evidence.

At Hopeful Hill, a prominent basement inlier rises to about 30 m above its surroundings; it is a likely source for much of the transported colluvium-alluvium intersected by the 2001-2002 drilling. Transported cover is generally thickest in drillholes TAR 16–19, 7 and 8; there is probably no transported cover intersected by drillhole TAR 13, while TAR 12 intersected only thin cover. A summary of transported cover units from drilled chip samples is given in Table 6.

Table 5: Generalised *in situ* regolith components from drill cuttings at Hopeful Hill.

Granite	Characteristics	Diagnostic points
Protolith	Medium- to coarse-grained brown granite.	Typical granite with igneous fabric.
Saprock	Partly weathered rock, grey to dark-brown relict granite; clay, mica, quartz and feldspar.	Relict granite fragments; mica, feldspar and quartz.
Lower saprolite	Weathered rock, mid-grey clay, quartz and relict feldspar.	Clays and quartz; relict igneous fabric and foliation.
Upper saprolite	Highly weathered rock, pink-cream to grey or white; kaolinite and quartz.	Kaolinite and quartz; relict structure and foliation.
Pedolith	Extremely weathered rock, pink to cream, brown and red Fe-stained, silicified top; gritty quartz or kaolinite dominant.	Kaolinite and quartz, no relict primary fabric.
Meta-ultramafic rock	Characteristics	Diagnostic points
Protolith	Aphanitic, mid green-grey, mid grey or black serpentinite; brown clay on fractures, foliation, chalcedony veins.	Dark serpentinite; metamorphic foliation and relict igneous fabric.
Saprock	Partly weathered rock, mid-grey to green-grey serpentinite; Fe-staining of fractures, foliation.	Serpentinite with smectite in fractures.
Lower saprolite	Weathered rock, pale green-grey, yellow and brown; smectite, relict grey serpentine and talc.	Greasy to sticky clays; pale to moderate colours, relict serpentine and metamorphic foliation.
Upper saprolite	Highly weathered rock, pale green to cream, white and pale brown, remnant foliation; smectite-rich with talc.	Clay-rich, pale, relict chalcedony veins, greasy (smectite), slight metamorphic foliation preserved.
Pedolith	Extremely weathered rock, red-brown, brown and black, clay-rich, with or without Fe-duricrust, Fe-mottled, may have silicified horizon(s).	Clay-rich, indurated, strong colours, relict chalcedony veins.

Table Cont.

Meta-mafic rock	Characteristics	Diagnostic points
Protolith	Not intersected.	—
Saprock	Partly weathered rock, mid- to light-grey clay with relict metamorphic foliation.	Dark, relict mafic rock with clay, relict metamorphic foliation.
Lower saprolite	Weathered rock, yellow-brown to grey clay with relict metamorphic foliation.	Clay-rich, moderate colours, relict metamorphic foliation.
Upper saprolite	Highly weathered rock, cream to pale tan, brown, clay-rich with quartz grit, massive.	Clay-rich, pale to strong colours, relict foliation, friable clays.
Pedolith	Extremely weathered rock, pale-pink, red to cream, clay-rich, Fe-mottled, may be partially silicified, no remaining primary fabric or foliation.	Clay-rich, moderate strength colours, materials are weak and friable to cemented.
Felsic gneiss	Characteristics	Diagnostic points
Protolith	Gneiss, possibly a metasediment.	Fresh lithic fragments; metamorphic foliation.
Saprock	Partly weathered rock, greyish felsic gneiss.	Relict lithic fragments; mica, feldspar and quartz, foliation.
Lower saprolite	Weathered rock, greyish yellow-brown clays with gritty quartz and remnant feldspars.	Clays and quartz; relict metamorphic foliation.
Upper saprolite	Highly weathered rock, pale grey-brown to cream clays with gritty quartz.	Pallid kaolinite with quartz; relict structure and some with relict foliation.
Pedolith	Extremely weathered rock, dark brown, red-brown to creamy clays with mottles.	Kaolinite and quartz; no relict primary structure.
Felsic porphyry	Characteristics	Diagnostic points
Protolith	Dark grey to brown rock, fine-grained with or without porphyritic feldspar and quartz, with or without green fracture infill.	Typical felsic porphyry, volcanic fabric.
Saprock	Partly weathered rock, red, brown or grey, fine-grained, with or without recognizable felsic porphyry.	Relict volcanic porphyry fragments.
Lower saprolite	Weathered rock, pale grey to reddish clays with gritty quartz.	Clay and quartz; relict metamorphic foliation.
Upper saprolite	Highly weathered rock, pale grey, clay-rich, relict primary fabrics.	Kaolinite and quartz, relict metamorphic foliation.
Pedolith	Extremely weathered rock, dark red-brown to pale brown or grey, clay-rich, no relict primary fabric; Fe-rich duricrust may occur, with or without mottling.	Kaolinite and quartz; no relict primary fabric, with or without Fe- or Si-duricrust.

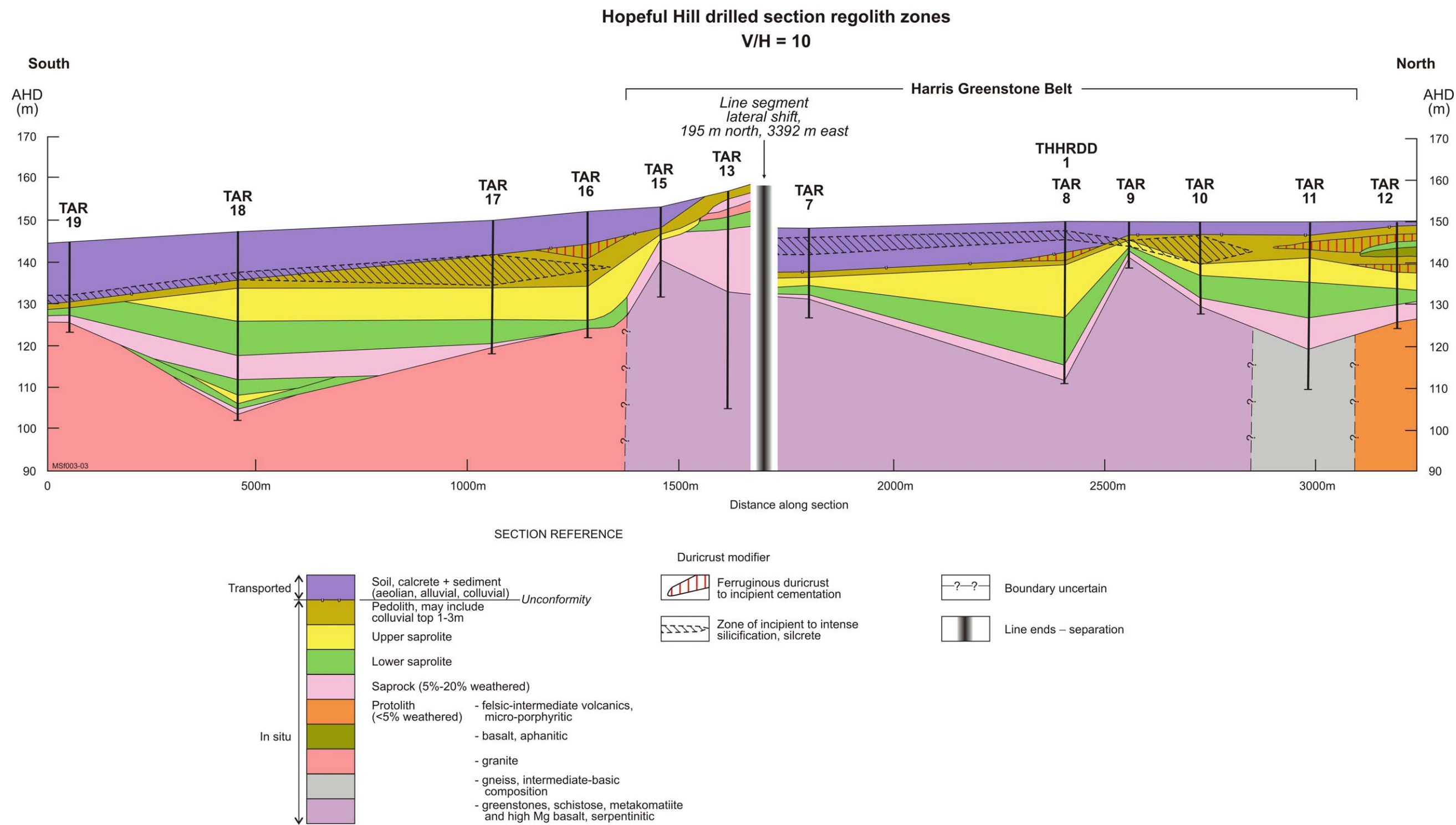


Figure 7:
Hopeful Hill drilled section regolith zones
[fold out sheet]

Table 6: Generalized transported cover components from drill cuttings at Hopeful Hill; oldest to youngest units.

Unit, age	Characteristics	Diagnostic points
Colluvium, ?Mesozoic-Tertiary	Cream to brown sediment of clay with sand, grit and cobbles, of mixed rock types, poorly sorted, angular to subrounded clasts, matrix to clast supported – (latter only seen in core); reworked weathered rock and readily forms a lag.	Generally polymictic, angular to subrounded clasts, poorly sorted, with fragmentary Fe-pisoliths and clay to silt matrix.
Fluvial sediments, Cainozoic	Red-brown to grey, clay to cobbles, loose to cemented, clast supported - (latter only seen in core); clay and quartz.	Well-rounded clasts among drill fragments of the same, <1 - >10 m thick.
Silcrete, Tertiary	Duricrust , grey to pale yellow, silica partial to full cementation of alluvium, colluvium or weathered basement, may contain major unconformity - (latter only seen in core); clay-silt, poor in fines.	Cryptocrystalline semi-translucent cement, hard to very hard drilling, clasts bound so firmly as to force any breakage through rather than around clasts; thickness <0.5 - >2 m, may be in several horizons.
Calcrete, Quaternary	Duricrust , white to pale tan, nodular aggregates to massive, fragmentary to competent; pedogenic.	Noticeable pallid soil horizon, effervescent reaction to HCl, may host geochemical metal signature.
Aeolian sands, Pleistocene	Mantles much of the landscape, orange, siliceous, can contain nodular to massive calcrete; dunes and sand plains. Sand forms a sample dilutant to any locally derived mineral-lithic grains.	Mostly loose, uniformly sorted, frosted quartz grains in fine-medium sand size; <1 - >5 m thick.

Mullina Well

Locations for this set of drillholes are given in Figure 5, the associated 21 regolith logs and the chiptray profile photographs are in Appendix 1. A regolith cross-section from those logs is given in Figure 8.

In situ Basement

Below the transported cover, the rocks of the weathered crystalline basement form a broad sequence: felsic volcanic-granitic-metasedimentary-mafic-ultramafic-felsic volcanic-granitic. At the S end of the section, a mixture of variably weathered granites and felsic porphyry (?Mesoproterozoic) were intersected (TAR72, TAR71 and TAR49-45). TAR 44 intersected weathered and unweathered Archaean metasediments. Further N, weathered and altered Archaean metakomatiitic basalts were intersected (TAR42 and TAR43). Drillholes TAR54-57 intersected greenstones. These are weathered, highly to moderately strained Archaean meta-ultramafics, where serpentine alteration is pervasive, and schistose equivalents were encountered in drillholes TAR54-55. Weathered and altered metasediments as medium- to coarse-grained paragneisses were intersected by the next three drillholes (TAR58-60). These ranged from felsic to intermediate, one being amphibole rich. Further N, TAR 61-62 and TAR73-74 penetrated various granitic rocks (granite to granodiorite). The weathering front is highly irregular along this drill line but no rock type is consistently more weathered than any other. This contrasts with the other two drill lines of this study. The deepest weathering of an ultramafic rock is around TAR55, where it reaches 68 m and possibly reflects the low competency and high permeability of this significantly strained protolith. A summary of the weathered *in situ* basement rocks from drilled chip samples is given in Table 7.

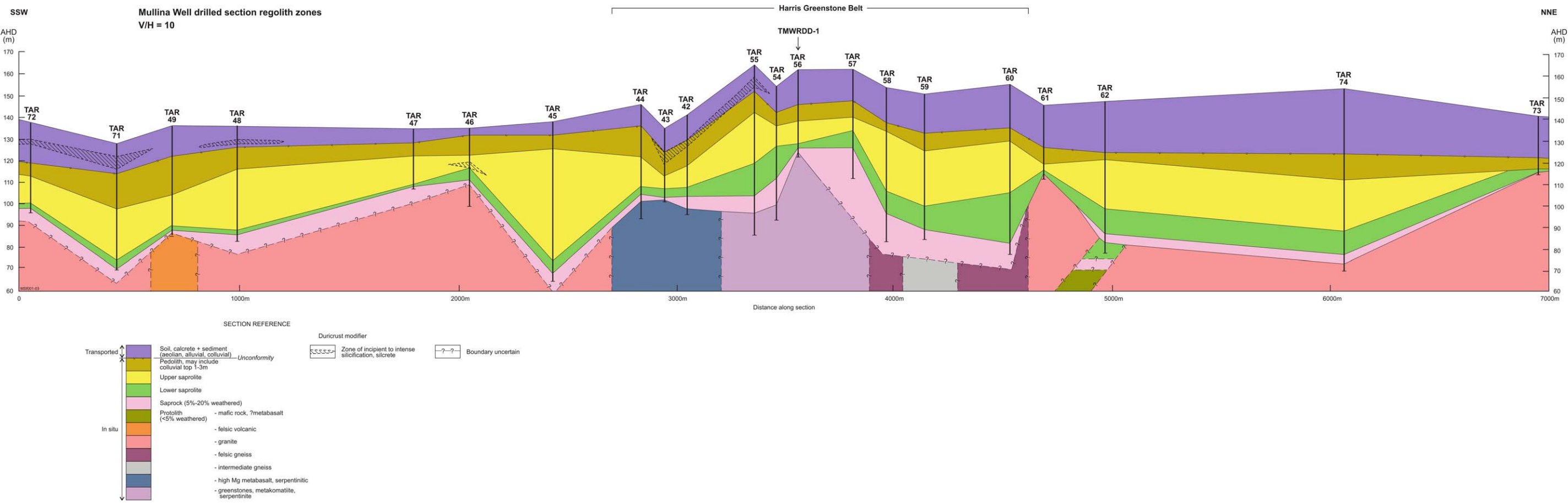


Figure 8:
Mullina Well drilled section regolith zones
[fold out sheet]

Table 7: Generalized *in situ* regolith components from drill cuttings at Mullina Well.

Southern granite	Characteristics	Diagnostic points
Protolith	Medium- to coarse-grained pink to brown granite.	Typical foliated granite.
Saprock	Partly weathered, grey to brown relict granite; clay, mica, quartz and feldspar.	Relict granite fragments; mica, K-feldspar and quartz.
Lower saprolite	Weathered, khaki to mid-grey to brown-grey; clay, quartz and relict feldspar.	Clays and quartz; relict metamorphic foliation.
Upper saprolite	Highly weathered, greyish to pink, reddish and yellow to white, clay – weakly plastic; kaolinite and quartz.	Kaolinite and quartz; relict igneous fabric and metamorphic foliation.
Pedolith	Extremely weathered, tan to brown and white, reddish to maroon, brown or red, Fe-mottled; silicified top; quartz grit or kaolinite dominant.	Kaolinite and quartz; strong colours, no relict primary fabric or foliation.
Metasediments	Characteristics	Diagnostic points
Protolith	Grey-black and brown, aphanitic metasediment.	Fresh lithic fragments.
Saprock	Partly weathered, very fine-grained metasediment, dark grey and brown, Fe-staining on fractures.	Relict aphanitic lithic fragments.
Lower saprolite	Weathered, grey to yellow-brown clays with a greenish tint.	Clay, generally indurated.
Upper saprolite	Highly weathered, pale yellowish grey clays; weak Fe-staining.	Kaolinite and quartz; sub-plastic clay.
Pedolith	Extremely weathered, medium grey to dark red-brown clays with Fe-mottles and maroon staining.	Clay; plastic, strong colours, no relict primary structures.
Meta-ultramafic	Characteristics	Diagnostic points
Protolith	Ultramafic schist, grey to black with yellow-brown clay on fractures.	Dark meta-ultramafic rock; metamorphic foliation and relict igneous fabric.
Saprock	Partly weathered, grey to black, serpentine and amphibole, quartz, chlorite, feldspar, opaque spinels; schistose, Fe-stained fractures.	Schistose ultramafic with smectite on fractures, relict metamorphic foliation.
Lower saprolite	Weathered, pale yellow-brown, grey to greenish; smectite, relict grey serpentine with talc, chlorite and amphibole with or without Mn-staining.	Dark, greasy to sticky plastic clays; relict metamorphic foliation.
Upper saprolite	Highly weathered, white, pale grey to pale greenish blue or maroon, possibly weakly banded with remnant foliation, with or without Mn-staining; smectite-rich with talc.	Clay-rich, pallid to moderately coloured, greasy feel, hint of relict metamorphic foliation.
Pedolith	Extremely weathered, red-brown to yellow, cream, maroon and dark pink, clay-rich, Fe-mottled, may have silicified horizon(s) with or without Mn-staining and flecking.	Clay-rich, strongly coloured.
Meta-mafic	Characteristics	Diagnostic points
Protolith	Dark grey to black, fine-grained meta-mafic igneous rock with green and yellow clays in fractures.	Dark, fine-grained meta-mafic igneous rock.
Saprock	Partly weathered, dark yellow-brown to dark grey; clay and lithic fragments with relict primary fabric and relict metamorphic foliation.	Dark relict mafic rock with clay, relict metamorphic foliation.
Lower saprolite	Weathered, dark yellow-brown to greenish grey clay with relict metamorphic foliation.	Clay-rich, moderately coloured, relict metamorphic foliation, partly competent.
Upper saprolite	Highly weathered, medium grey to yellow-brown, massive; clay dominant with gritty quartz.	Pale, sub-plastic clay-rich; relict foliation.
Pedolith	Extremely weathered, cream, brown, greenish, reddish, Fe-mottled and stained or cemented, may be partly silicified, plastic; clay-dominant with gritty quartz.	Clay-rich with gritty quartz; medium to strongly coloured, plastic to cemented, no primary structure or fabric.

Table Cont.

Felsic gneiss	Characteristics	Diagnostic points
Protolith	Possibly a metasediment, brown, felsic, medium- to coarse-grained; amphibole, quartz, feldspar, white and black micas, sericite.	Typical gneissic rock.
Saprock	Partly weathered, yellow-brown to dark brown to greyish; felsic gneiss weakly recognizable.	Relict lithic fragments; mica, feldspar and quartz.
Lower saprolite	Weathered, greyish yellow and brown, strong remnant foliation; clay, gritty quartz.	Moderately coloured clays and quartz; relict foliation.
Upper saprolite	Highly weathered, pale grey to yellow and maroon, weak foliation; clays, gritty quartz, vein quartz.	Pallid kaolinite and quartz; relict structure and some metamorphic foliation.
Pedolith	Extremely weathered, red-brown and maroon to grey and yellow; clays with Fe-mottles.	Kaolinite and gritty quartz, strongly coloured, no relict primary structure.
Northern granite	Characteristics	Diagnostic points
Protolith	Medium- to coarse-grained pink to yellowish grey and brown medium-grained granite, massive to foliated.	Typical granite, igneous fabric and may have metamorphic foliation.
Saprock	Partly weathered, pinkish to multicoloured, relict granite; clay, mica, quartz and feldspar.	Relict granite fragments, micas, K-feldspar and quartz.
Lower saprolite	Weathered, dark pink clay; quartz and relict feldspar.	Clay and quartz; relict metamorphic foliation.
Upper saprolite	Highly weathered, khaki, greenish grey, orange, yellow and white; kaolinite and quartz.	Kaolinite and quartz; moderate strength colours, relict metamorphic foliation.
Pedolith	Extremely weathered, reds to brown, white and purple, brown or red Fe-mottled, silicified top; gritty quartz or kaolinite dominant.	Kaolinite and quartz; strong colours, no relict primary structure.

Transported Cover

Transported cover, blue on the section, ranged from about 2-30 m in thickness and includes, soil, calcrete, Pleistocene aeolian sand, Cainozoic fluvial sediment and some presumed Mesozoic-Tertiary colluvium, and laterally discontinuous Tertiary silcrete bands were intersected. Aeolian sand plains and sand dunes mantle much of this area but are not recovered well by the drilling method used. Sediments below the soil-sand layer are predominantly fluvial and range from silty clays to sand and gravel, or are mixtures of these and have gravel plus a few pebble clasts up to 20 mm. Cements include calcrete, incipient silicification and silcrete. Over the length of the section, silcrete is limited to two areas, between drillholes TAR 72, TAR 71 and TAR 48 and the five drillholes TAR 42-44, TAR 55 and TAR 56. There can be broad layering inferred from sample to sample but finer layering can only be inferred from cuttings evidence. There is a significant palaeochannel occupying the northern third of the cross-section (drillholes TAR 60-73) where some or all of the pedolith may have been eroded by fluvial activity. At drillhole TAR 74 within the sample interval 40-42 m, material logged as remnant pedolith may be a weakly Fe-stained top to the upper saprolite. A summary of weathered *in situ* basement rocks from drilled chip samples is given in Table 8.

Table 8: Generalized transported regolith components from drill cuttings at Mullina Well; oldest to youngest units.

Unit, age	Characteristics	Diagnostic points
Colluvium, ?Mesozoic-Tertiary	Brown clay with fine sand and grit, difficult to distinguish from fluvial clay if sample is drill cuttings.	Any clasts are generally polymictic angular to subrounded and poorly sorted, fragments of Fe-pisoliths.
Fluvial sediments, Cainozoic	Red-brown to brown, clay and sand to minor gravel, loose to cemented, matrix supported – (latter only seen in core); clay and quartz.	Clay-rich to sandy with well rounded clasts among drill fragments of the same, <1 to >34 m thick.
Silcrete, Tertiary	Duricrust , grey to pale yellow, silica cementation of alluvium, colluvium and weathered basement, partial to full cementation, may contain major unconformity (latter only seen in core); poor in clay and silt fraction.	Cryptocrystalline semi-translucent cement, hard to very hard drilling, clasts bound so firmly as to force any breakage through rather than around clasts, thickness <0.5 to >2 m, may occur as several horizons.
Calcrete, Quaternary	Duricrust , white to pale reddish brown as nodules or aggregates, fragmentary to competent, pedogenic.	Noticeable pallid soil horizon, effervescent reaction to HCl; may host geochemical metal signature.
Aeolian sand, Pleistocene	Mantles much of the landscape, orange, siliceous, dunes and sand plains; can contain nodular to massive calcrete. Sand forms a sample dilutant to any locally derived mineral-lithic grains.	Mostly loose, uniformly sorted, frosted quartz grains in fine-medium sand size, <1 to about 8 m thick.

Cored drillholes

Three fully cored 120 mm diameter diamond drillholes (Table 9) for this study yielded 60 mm diameter HQ-cores that have been used as reference profiles to facilitate correlation with the adjacent aircore drilling. Refer to Methods section for drilling techniques. Locations of these reference drillholes are shown in (Figures 3-5).

Table 9: Cored diamond drillhole locations, coordinates and final depths.

Diamond Drillhole	Location	Coordinates	Final depth (m)
KLHRDD-1	Lake Harris line (near KOK 07)	0511863 E, 6566452 N	51.25
THHRDD-1	Hopeful Hill eastern line (near TAR 08)	0492082 E, 6575794 N	39.25
TMWRDD-1	Mullina Well line (near TAR 56)	0461096 E, 6592412 N	40.00

Lake Harris diamond core KLHRDD-1

A site about 6 m S of the air core drillhole KOK 07 (W side of Glenloth Mines track) and was selected as being representative of the regolith profile over weathered greenstone with a reasonable drilling depth to unweathered serpentinized metakomatiite. Drilling was vertical into a subvertical greenstone; the drilled profile most likely only intersects one or two narrow subvertical bands within the weathered and folded metakomatiite. A summary of that profile is provided in Table 10 with comprehensive log and core photographs in Appendix 1; geochemical, mineralogical and petrological data are in Appendices 2-5 & 7.

In situ Greenstone

Protolith (<5% weathered minerals) forms only a very minor component of this diamond core as small enclaves within the saprock below about 49.6 m. The drillhole did not terminate in true protolith. The protolith enclaves are dark grey to dark blue-green-grey with minor yellow-brown and lime-green clays along fractures. Relict primary fabric and metamorphic foliation occur within the serpentinitic greenstone. Cuttings from the nearby aircore drilling (KOK 07) imply that the protolith should have been intersected at

or near 48 m, well above the actual weathering front in the diamond core (>51.25 m). It is concluded that i) cuttings alone are not the best medium for regolith boundary identification and ii) the depth of the weathering front varies significantly, even over short lateral distances.

Saprock (49.15–49.6 m) has 5–20% of weatherable minerals weathered, mostly to clay filling fractures and as patchy, incipient alteration of the dominant serpentinite. The saprock is dark blue-green to green-grey with minor bright green and brown clay seams. Yellow Fe-oxides have stained the joint surfaces. Relict primary fabric and metamorphic foliation are preserved in less weathered greenstone. Talc is also present and makes these materials feel very greasy; originally formed by hydrothermal-metamorphic processes but it easily survives weathering and is probably left in the clay matrix as the only remnant of the original rock.

The **lower saprolite** sub-zone (41.6–49.15 m) of weathered greenstone has several patches of both clay saprolite and greenstone saprock enclosed within it (each >2 m thick). The lower saprolite is generally darker than the upper saprolite, is more competent, the clay is stiffer and serpentine is obvious. It is blue-green-grey to dark green-grey. Bright yellow-green and brown ferruginous clay fills fractures and forms stains around fractures in some of the more highly weathered intervals. Regular conjugate joint sets lie at 45°, 60° and 80° to the core axis and are variably slickensided.

A thick and complex, highly weathered **upper saprolite** sub-zone occurs between 14.75–41.6 m. It is predominantly light to bright green with minor blue-green, yellow-green to blue-grey. This includes patches of more and less weathered greenstone; some of these patches are >2 m in size. The upper saprolite is dominated by clay and is variably soft to stiff, with the clay being sticky and plastic due to abundant smectite. Towards the top, a weathering-induced breccia occurs that has jig-saw-fit clay-rich blocks without fracture infill. Talc- and vermiculite-like minerals give many intervals in this sub-zone a distinctive greasy feel. There is also a weak relict metamorphic foliation and regular conjugate sets of slickensided joints at 30°, 45° and 60° to the core axis. These joints indicate compression induced movement, possibly related to volume changes caused by mineral weathering and hydration. In spite of the deformation and weathering, there are relict primary structures preserved such as spinifex quench fabrics (at about 17 m, see petrography section). Red, ferruginous megamottles and bright yellow to brown Fe-oxide staining are common in this sub-zone (Figure 9A). Differential weathering has yielded pseudo-breccias with differentially coloured rims on geometric or irregular shaped greenstone blocks at scales of 5–100 mm (Figure 9B). White to pale grey chalcedony veins (about 2–35 mm thick) occur throughout. Black Mn-oxide flecks and dendrites occur in some intervals (14.75–16.5, 23.4–25.9 m). Dark red-brown to brown, strongly ferruginous intervals, where Mn-oxide is also abundant, occur at 37.45 m and at 38.5 m (both 300–350 mm thick). The upper saprolite is mostly composed of smectite-hydromuscovite clays with talc, chlorite and relict serpentine.

XRD analysis shows that the deeper saprolites and bedrock (>27 m) contain major proportions of clinocllore, tremolite and a ferruginous ortho-amphibole. Above this, smectites and interstratified smectite-chlorites dominate, with palygorskite developed above about 20 m. Palygorskite is probably related to the saline alkaline environment with abundant Mg in solution (Taylor and Eggleton, 2001; J. Keeling, PIRSA, pers. comm. 2004). Petrography (see below) indicates remnants of a pyroxene spinifex fabric and possibly some olivine spinifex textures as well.

The top of this extremely weathered *in situ* greenstone was intersected at 14.52 m where a relict pedolith forming a truncated **plasmic zone** 0.23 m thick occurs, the upper surface of which forms an angular unconformity (about 45°) to the overlying transported cover (colluvium). The unconformity is only visible on the dry core; its true location was not visible when the core was first logged damp and required petrography to refine a likely interval to examine in more detail (Figure 9C). This zone consists of pale grey-green smectite- to hydromuscovite-rich material with bluish intervals, yellow stains and streaks. It has a jig-saw fit smectitic clay-rich breccia fabric (similar to the upper saprolite below) but here the darker pale grey-green clay fragmental blocks are cemented together or have their surrounding fractures infilled by a slightly paler bluish grey-green less smectitic clay. There is no ferruginous capping although remnants of this can be seen at the nearby recently exhumed greenstone outcrop area and evidence for it once having been here is in the overlying colluvium (see below). Pedogenesis has destroyed any primary foliation or fabric; the brecciation appears to be related to weathering and pedogenic processes.

Transported Cover

Transported cover here is 14.52 m thick Table 10, consisting of >4 m of clay-rich colluvium resting on the unconformity, overlain by 5.4 m of alluvium, overlain in turn by 4.6 m of red-brown hardpanized colluvium-alluvium, and the whole then covered by <1.0 m of aeolian sand.

A pale, mottled **colluvial unit** forms the basal 4.02 m of the cover sequence. It consists of pale grey-green or pale blue-grey clays grading upwards into yellow to pale brown clay, quartz sand and grit, and broken 3–5 mm ferruginous pisoliths (Figure 9D). There are angular to subrounded rip-up clasts of pedolith and saprolith clays floating within the unstructured clay-rich colluvium between 14.40–14.52 m. Widespread red to brown Fe-oxide staining and megamottles imply this unit has been affected by pedogenesis. Much is locally reworked pedolith derived from weathered greenstone and adjacent granitic terrain. The ferruginous pisoliths all have broken or missing cutans, having been dislodged from an eroding surface and transported a short distance. They seem to be the only remaining and indirect evidence of a pre-existing, probably thin ferruginous cap, once developed on the greenstones but now mostly eroded. There is an angular unconformity (about 45°) at the base of this multicoloured colluvial interval. Later silicification has partially indurated the interval 10.5 to ~13.5 m.

Overlying the colluvium, a mostly brown coloured unnamed **alluvium** (5.10–10.50 m) that consists of clast-supported channel sand to cobbles in which well-rounded to subangular quartz-rich clasts predominate. Some pebble to gravel sized clasts, consisting of reworked, silicified, weathered granite are conspicuous components (Figure 9E, F). Interlayered with those coarse-grained layers are overbank clays with rhythmic cycles 300–500 mm thick. Some of the more porous intervals of the alluvium have been silicified to silcrete. This duricrust is pedogenic and probably marks an early or middle Tertiary silicification episode.


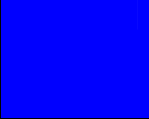
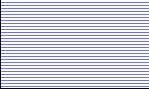

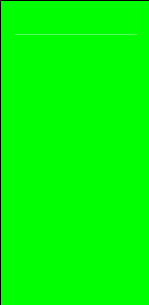

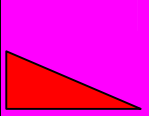
Red-brown hardpan (as used herein) refers to a dominantly colluvial-fluvial material (0.7–5.1 m). It is a strongly reddish brown clayey to sandy material containing abundant matrix-supported polymictic gravel. The hardpan is variably cemented by carbonate and hyaline silica, thereby making this unit variably competent. The hardpanization is presumed to be Pliocene to Pleistocene in age.

Pedogenic **calcrete** forms an earthy to moderately compact but low-density, white to creamy layer within the soil-sand profile. Exposures of aggregated calcrete nodules that laterally become laminated or massive sheets in the nearby drill sump demonstrated the variability of this soil B_{Ca} horizon. There are additional but less obvious carbonate cementing materials to a depth of 5.1 m (reacts with 10% HCl).

Thin **aeolian sand** covers the drill site and was not cored well. It is red-brown to orange, less than a metre thick, uniformly sorted and hosts later formed calcrete (see above).

NOTE: The significant discrepancy of nearly 10 m between the position of the *in situ*—transported unconformity in adjacent diamond cored and air-cored drilling, about 6 m apart, demands explanation. Logging of aircore drillhole KOK 07, that had bulked 2 m interval cuttings, determined the major unconformity at about 4 m; but diamond core from KLHRDD-1 determined it at 14.52 m. The majority of this difference is due to drill sampling methods – 2 m bulked regolith cuttings are inferior to continuous core. Cuttings of colluvial clay-rich materials strongly resemble deeply weathered *in situ* materials, making the major unconformity position uncertain. It required the assistance of petrography, XRD mineralogy and geochemistry to locate properly. Here the pedolith commonly has an upper portion of mixed provenance, allowing the major unconformity in KOK 07 to be altered to about 7 m depth. Local variations in a steep palaeotopography between two adjacent sites may also contribute to the difference. This example demonstrates very well the efficacy of regolith drill core over cuttings when working with transported materials on weathered basement.

Table 10: Summary log of Lake Harris cored drillhole KLHRDD-1 (not to scale)

Depth Range (m)	Graphic Log (vert. not to scale)	Regolith Zone	Description
0.00-0.70		soil-sand	soil in loose red-brown aeolian sand with ~300 mm of calcrete.
0.70-10.50		sediment	alluvial clay + sand + gravel + cobbles, weakly bound to silicified. Upper 1~5 m is red-brown hardpan colluvium-alluvium, the remainder is an older fluvial channel to overbank deposit with silcrete bands.
10.50-14.52		colluvium	pale clays plus rip-up pedolith clasts, quartz sand and grit with fragmentary Fe-pisoliths, locally deriving from eroded pedolith of both felsic and ultramafic terrains, red Fe-megamottled.
14.52-14.75		<i>in situ</i> Pedolith (plasmic)	extremely weathered greenstone; pedogenic clay-rich breccia, pale green to bluish and greyish, Fe-stained, top eroded, NO ferricrete cap.
14.75-41.60		upper saprolite	Highly weathered greenstone; upper ~1 m displays weathering brecciation. Mostly a complex sub-zone with several enclaves of less + more highly weathered material. Clay-rich, soft to stiff and sticky-plastic clay (smectitic) light to bright greens + blue-greens + yellow-greens + blue-greys. Relict foliation and conjugate joint sets, red Fe-mega-mottling and yellow to brown Fe-staining, white to pale grey chalcedony veins, black MnOx flecks and dendrites. Some intervals have a distinctly greasy feel (talc). Sub-zone is smectite (dominant above 29 m), chlorite, talc + relict serpentine.
41.60-49.15		lower saprolite	Weathered greenstone; complex sub-zone, has several enclaves of less or more highly weathered rock. Sub-zone is generally darker hued and more competent than the one above (less altered). Blue-green-grey weathered serpentinite + bright green and brown clay seams + talc and yellow Fe-staining, well jointed, relict fabric-foliation.
49.15-51.25		saprock – protolith	Partially weathered greenstone; serpentinite, dark green-grey, some clay fracture infill, progressively more competent with depth but still retains enclaves of more weathered material. Weathering Front probably just below end of drillhole.

Hopeful Hill diamond core THHRDD-1

A site about 6 m south of TAR 08 (Photo 2) was selected to represent the regolith profile on a substantial thickness of weathered metakomatiite. As the drillhole was vertical and was drilled into a subvertical greenstone, the recovered core most likely only intersected one or two narrow bands within the weathered metakomatiite. A summary of the profile is in Table 11 with a more comprehensive log and core photographs in Appendix 1, geochemical, mineralogical and petrological data are in Appendices 2-5 & 7.

In situ Greenstone

A continuous **Protolith** was not intersected because significant weathering reaches to the end of the drillhole (39.25 m). However, enclaves of what appears to be remnants of the protolith occur within saprock and lower saprolite. It is dark grey to dark green-grey, with minor brown alteration and thin, pale green clay along fractures. Relict primary fabric and metamorphic foliation are preserved in the serpentinite. Cuttings from the nearby aircore drillhole (TAR 08) suggest protolith occurs at or above 38 m, higher than that indicated by the diamond core (>39.25 m). However, drill cuttings are not the best medium for regolith boundary identification and the depth of the weathering front may vary significantly, even over short distances.

A thin (4.75 m) **Saprock** zone occurs just below 34.5 m. It is a dark green-grey to dark grey, partially weathered serpentinite with minor bands and seams of bright green and brown clay. There is minor brown staining by Fe-oxides, mostly along joints. Relict primary fabric and metamorphic foliation occur in the less weathered serpentinite. Joints angled at 60° to the core axis are variably altered and/or stained. Talc is a minor relict from an earlier metamorphic-hydrothermal alteration process.

Figure 9 explanation: Regolith drill core from Lake Harris (KLHRDD-1) and Hopeful Hill (THHRDD-1).

A. Drillhole KLHRDD-1: 37.5-37.75 m, Fe-mottled upper saprolite (upper core).	B. Drillhole KLHRDD-1: 16.98-17.16 m, upper saprolite displaying a subtle weathering induced pseudo-breccia.
C. Drillhole KLHRDD-1: 14.40-14.72 m, subtle unconformity at 14.52 m (lower core, 2 cm from RH end of blue scale bar). Weakly mottled colluvium in upper core.	D. Drillhole KLHRDD-1: 12.90-13.10 m, lower core, weakly mottled colluvium with small dark brown Fe-pisolith fragments distributed randomly throughout.
E. Drillhole KLHRDD-1: 9.2-9.4 m (upper core) & 10.3-10.5 m (lower core), fluvial sediment containing silcrete cobbles displaying variably altered rims, polymict gravel and cemented by a later silcrete.	F. Drillhole KLHRDD-1: 5.50-5.70 m (upper core) & 6.40-6.60 m (lower core) both displaying partially silicified alluvium with variably clayey matrix. Clasts are of mixed lithotypes and display a wide range in transport history degree of rounding.
G. Drillhole THHRDD-1: 18.98-19.15 m (lower core), saprolite consisting of a weathering pseudo-breccia where fracture-like features are composed of bright yellow-green smectitic clay in contrast to the less altered dark olive-grey centres.	H. Drillhole THHRDD-1: 17.70 m is on centre core at bar scale mid point. Colourful saprolite with alteration veining – some of which is pale blue (LH end centre core; Ni or Cr stained kaolinite). Upper core displays red Fe-staining, lower core includes similar material as displayed in image G.

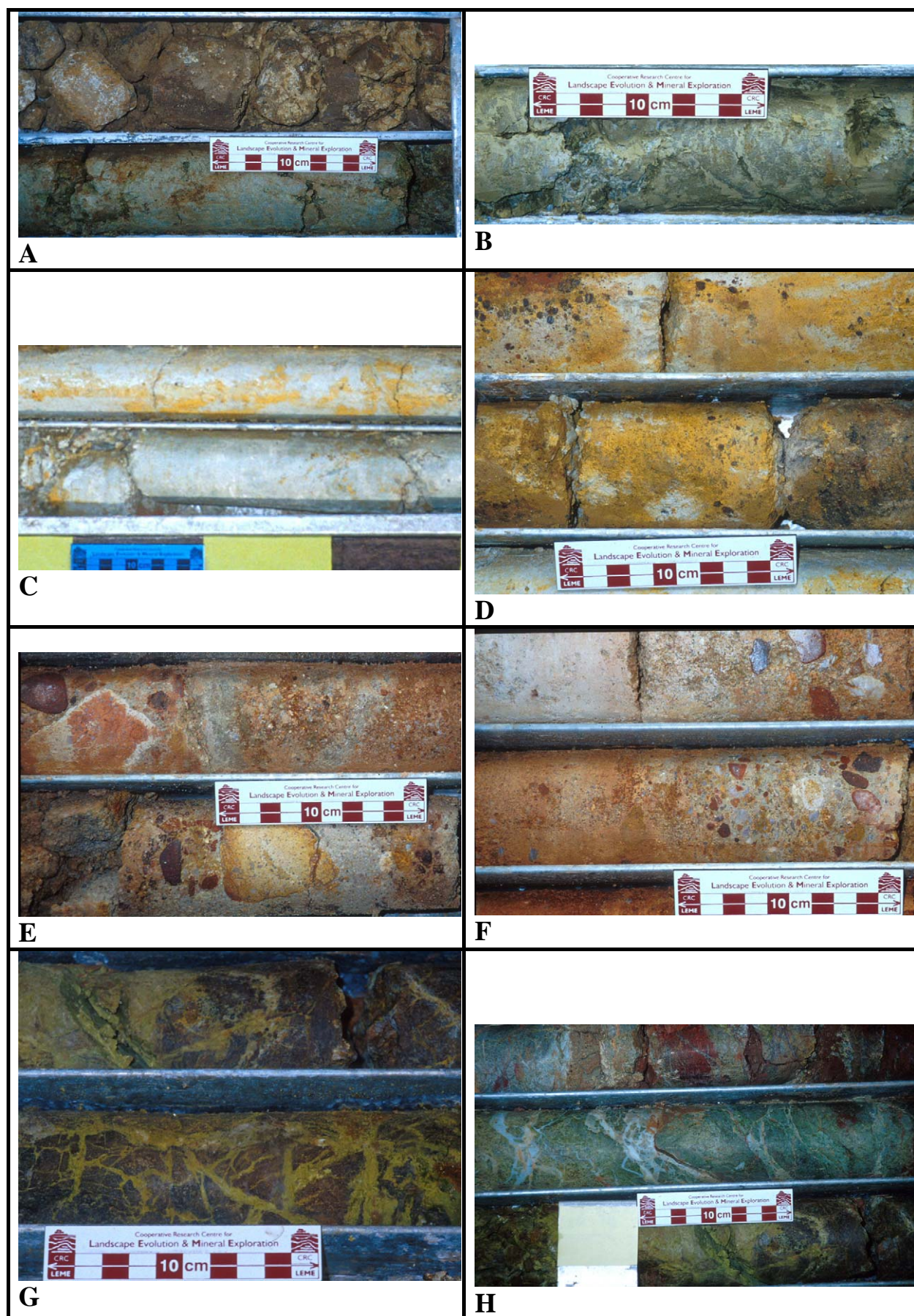


Figure 9: Regolith drill core from Lake Harris (KLHRDD-1) and Hopeful Hill (THHRDD-1).

Above the saprock a more weathered **lower saprolite** sub-zone occurs between 23-34.5 m; it is complex and contains several patches of more or less weathered greenstone. This sub-zone is thicker (11.5 m) than that at Lake Harris (7.55 m). Included clay saprolite and saprock enclaves are <1.5 m in size. The lower saprolite is mostly darker than the upper saprolite, with neutral hues, higher competency, the clay is stiffer and weakly altered serpentinite is abundant. Highly fissile fractured material occurs throughout and was difficult to drill. Typically, this sub-zone is dark grey to dark green-grey with bright yellow-green clay filling fractures. Yellow and brown Fe-oxide staining and more pervasive alteration occurs around fractures and, in places, expands to more broadly weathered intervals. Regular conjugate joint sets occur at 45-60° to the core axis and these are variably slickensided, altered and stained with Fe-oxides.

An **upper saprolite** sub-zone (9.65-23.00 m) occurs above the lower saprolite and is highly weathered, complex and consists mostly of smectite, chlorite, hydromuscovite, talc and relict serpentinite. Here upper saprolite is 13.35 m thick, which is about half that intersected at Lake Harris (27.1 m). This sub-zone is multicoloured with bright greens that contrast sharply with the adjacent dark olive and medium-greens below (Figure 9H). Subordinate colours include blue-green, yellow-green and blue-grey. The upper saprolite includes several patches or enclaves of more or less weathered greenstone; some enclaves are >2 m thick. This sub-zone is dominated by clays and is variably soft, friable to coherent or stiff and, in places, quite competent. The clays are sticky and plastic (smectitic), sub-plastic (illitic) or are intermingled. Talc and vermiculite-like minerals, in places, make this sub-zone variably greasy. Relict metamorphic foliation and regular conjugate joints occur at about 45° and 60° to the core axis. These joints are strongly slickensided, indicating compressive movement, possibly in response to weathering-induced volume changes. Differential weathering has formed pseudo-breccias that appear as paler or more brightly coloured rims to geometric or irregular shaped less altered greenstone blocks on scales of 50 to 100 mm (Figures 9G, H, 10B). Red ferruginous megamottles and blotches of brown Fe-oxide staining occur here (Figures 9H, 10A). Pale grey and turquoise chalcedony veins, 2 to >10 mm in thickness, are scattered throughout. Black Mn-oxide flecks and dendrites occur in some intervals (*i.e.* at 11.35 m and 11.75 m). There is a dark brown, strongly ferruginous interval between 15.20-15.95 m, that contains branching fracture veins of a pale bluish to turquoise translucent clay; similar veining occurs near 17.7 m (<1 to 5 mm, possibly a Ni- or Cr-stained kaolinite; Figure 9H; see also geochemistry Table A2.2, Appendix 2).

Extremely weathered *in situ* greenstone forms a truncated **plasmic zone** 0.6 m thick, the upper surface of which forms an angular unconformity with the overlying transported cover at 9.05 m (Figure 9A). Materials of the plasmic zone consist of a pale green and grey smectite- and hydromuscovite-rich clay with brown, less smectitic, illuviated clay infilling fractures. This interval is variably brecciated but retains a jig-saw-fit relationship to the blocks, has conspicuous red to brown megamottles and is extensively stained. All these attributes are pedogenic. There is no remnant ferruginous cap here but there is evidence in the overlying colluvium for a pre-existing Fe-cap (see next section below). Pedogenic dissolution and precipitation of clays has removed any primary fabric or metamorphic foliation but relict joints persist, imparting a blocky structure to this shallowest *in situ* zone.

Transported Cover

The **sedimentary cover** is 9.05 m thick, consisting of a basal colluvium overlain by alluvium, hardpan and aeolian sands. The lower parts have been partly cemented by Fe-oxides, the middle parts have been partly silicified to silcrete and hardpan, and the upper parts partly cemented to calcrete.

A **colluvial unit**, variably and subtly tinted greyish (gley coloured), is strongly megamottled and forms a basal 0.5 m interval to the cover sequence. It consists of pale yellow-grey to very pale brown clay, quartz sand and grit with broken 3-5 mm ferruginous pisoliths (Figure 10C, D). Widespread red to brown Fe-oxide staining and mega-mottling imply this unit has been affected by pedogenic processes. Much of this interval is locally reworked pedolith from weathered medium-grained felsic rocks and fine-grained greenstones. The ferruginous pisoliths have broken or missing cutans; these seem to have been eroded and transported a short distance. They appear to be the only remaining evidence of a pre-existing, thinly developed ferruginous cap on the greenstones. The base to this multicoloured colluvial interval is an angular unconformity at 9.05 m.

Overlying the colluvium is a variably silicified red-brown unnamed **fluvial unit** (5.15-8.45 m) consisting of clast-supported channel sand to pebbles with predominantly well rounded to subangular quartz-rich clasts. Layer selective silicification of this to a silcrete banded unit probably occurred in the early or middle Tertiary (Figure 10C).


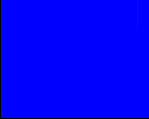

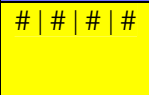
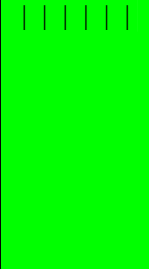

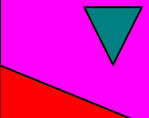
A **red-brown hardpan** occurs between 0.5-5.15 m and is strongly coloured, clayey to sandy. Where polymictic gravel is locally abundant, this is matrix-supported (Figure 10C, E). It is variably cemented by calcrete and hyaline silica, making it relatively competent.

Pedogenic **calcrete** forms an earthy to moderately compact white to creamy layer within the soil-sand profile between 0.2-0.5 m. Aggregated calcrete nodules, that laterally become laminated or massive sheets, are exposed in the drill sump, next to the drillhole. This demonstrates the variability of this soil B_{Ca} horizon. There are additional obvious calcrete and less obvious carbonate cements to a depth of 5.15 m that react with 10% HCl.

Aeolian sand to a depth of about 0.2 m covers the drill site and was only partly recovered by the coring process. It is red-brown to orange, uniformly sorted and hosts later formed calcrete (see above).

NOTE: There is a minor difference in logged position for the major unconformity between adjacent drill sites (about 6 m apart) where dissimilar drilling methods were used. For aircore drillhole TAR 08, bulked 2 m interval cuttings suggest the boundary is between 6-8 m; but in continuous core from drillhole THHRDD-1 it is clearly at 9.05 m (a difference of 1-2 m). Firstly, a major portion of this difference comes directly from uncertainties caused by the sampling and bulking of the aircore drilling – continuous core is preferable. The pedolith zone indicated on the aircore cuttings logs and derived cross-sections commonly has had a mixed provenance within its upper 1-3 m.

Table 11: Summary log to Hopeful Hill cored drillhole THHRDD-1 (not to scale)

Depth Range (m)	Graphic Log (vert. not to scale)	Regolith Zone	Description
0.00-0.50		soil-sand	soil in loose red-brown aeolian sand with 300 mm of calcrete.
0.50-8.45		sediment	alluvial clay + sand + gravel + pebbles, weakly bound to partly silicified. Upper 1~5 m is red-brown hardpan colluvium-alluvium, the remainder is an older fluvial sheet flow deposit with minor channel bed material, irregular silcrete bands.
8.45-9.05		colluvium	gley clay + quartz sand-grit with fragmentary Fe-pisoliths, locally deriving from eroded pedolith, red to brown Fe-megamottled.
9.05-9.65		<i>in situ</i> Pedolith (plasmic)	extremely weathered greenstone; pedogenic, clay-rich, strong red and brown to pale greens, megamottled, pedogenic jig-saw-fit breccia, illuviated clay fracture infill, top eroded, part silicified.
9.65-23.00		upper saprolite	Highly weathered greenstone; complex sub-zone with several enclaves of less + more highly weathered material. Clay-rich, soft to stiff and sticky-plastic clay (smectitic) bright greens + blue-greens + yellow-greens + blue-grey. Relict foliation and conjugate joint sets, red Fe-megamottles + yellow to brown Fe-staining, white to pale turquoise chalcedony veins, black MnOx flecks and dendrites. Some intervals have a distinctly greasy feel (talc). Sub-zone is mostly smectite + talc + relict serpentine. Fe-rich interval between 15.20-15.95 m
23.00-34.50		lower saprolite	Weathered greenstone; complex sub-zone, has several enclaves of less or more highly weathered rock. Generally darker hued and more competent than the sub-zone above. Dark grey or green-grey weathered serpentinite + bright green and brown clay seams + talc, yellow Fe-stains, well jointed, relict foliation, chalcedony veins.
34.50-39.25		saprock – protolith	Partially weathered greenstone; serpentinite, dark green-grey, some clay fracture infill, progressively more competent with depth but still retains enclaves of more weathered material. Weathering Front probably just below end of drillhole.

Mullina Well diamond core TMWRDD-1

A site about 10 m ESE of the aircore drillhole TAR 56 (Figures 5, 7) was selected to represent the regolith profile over weathered greenstone within a practical drilling depth. The vertical drillhole most likely intersected one or two narrow bands within the subvertical weathered meta-mafic-ultramafic greenstones. A summary is given in Table 12 with a more comprehensive log and core photographs in Appendix 1; other data are in Appendices 2-7.

In situ Greenstone

Protolith greenstone was penetrated at 39.12 m but the ~0.9 m of core recovered is very fissile, schistose and the serpentinitic character is masked. The core has a pervasive alteration that is difficult to define as incipient weathering, tectonic shearing or hydrothermal modification. The protolith of serpentinite here is grey to dark green-grey (dominant) with subordinate brownish alteration and thin, pale-green clays along large fractures.

The **saprock** zone is thin (0.62 m) and begins at 38.5 m. It is dark green to grey-green, partly altered serpentinite with a relict primary fabric and metamorphic foliation, and has minor bright green and brown clay seams and minor brown Fe-oxide staining, mostly along joints. Joints at about 75° to the core axis are variably altered and stained.

Figure 10 explanation: Regolith drill core from Hopeful Hill (THHRDD-1) and Mullina Well (TMWRDD-1). **Note** Mullina Well core is reversed to normal and runs right to left.

A. Drillhole THHRDD-1: 13.3-13.6 m, (upper core) 14.25-14.55 m (lower core), upper saprolite displaying a weathering pseudo-breccia in many greens and randomly spaced reddish Fe-staining.	B. Drillhole THHRDD-1: 9.78-9.85 m, a jig-saw-fit breccia developed in upper saprolite, fracture infill matrix is clay weakly stained by Fe.
C. Drillhole THHRDD-1: 5.15-9.85 m. Transported materials: red-brown hardpan + alluvium + colluvium on <i>in situ</i> weathered greenstone. Unconformity is at 9.05 m, (lower core, 2 x 10 cm scale units from LH end).	D. Drillhole THHRDD-1: 8.50-8.75 m, (lower core) colluvium above unconformity, derived from both weathered felsic and ultramafic sources. Red-brown hardpan and alluvium above the paler basal colluvium.
E. Drillhole THHRDD-1: 4.40-4.60 m, (lower core), red-brown hardpan.	F. Drillhole TMWRDD-1: 36.70-36.83 m, pale green clay-rich saprolite with subtle yellow staining.
G. Drillhole TMWRDD-1: 34.45-34.70 m, black Mn-oxides as stains, flecks and dendrites in pale green clay-rich saprolite.	H. Drillhole TMWRDD-1: 32.90-33.15 m, pale green upper saprolite displaying fracturing. yellow staining and pale yellow alteration (?mottling)..

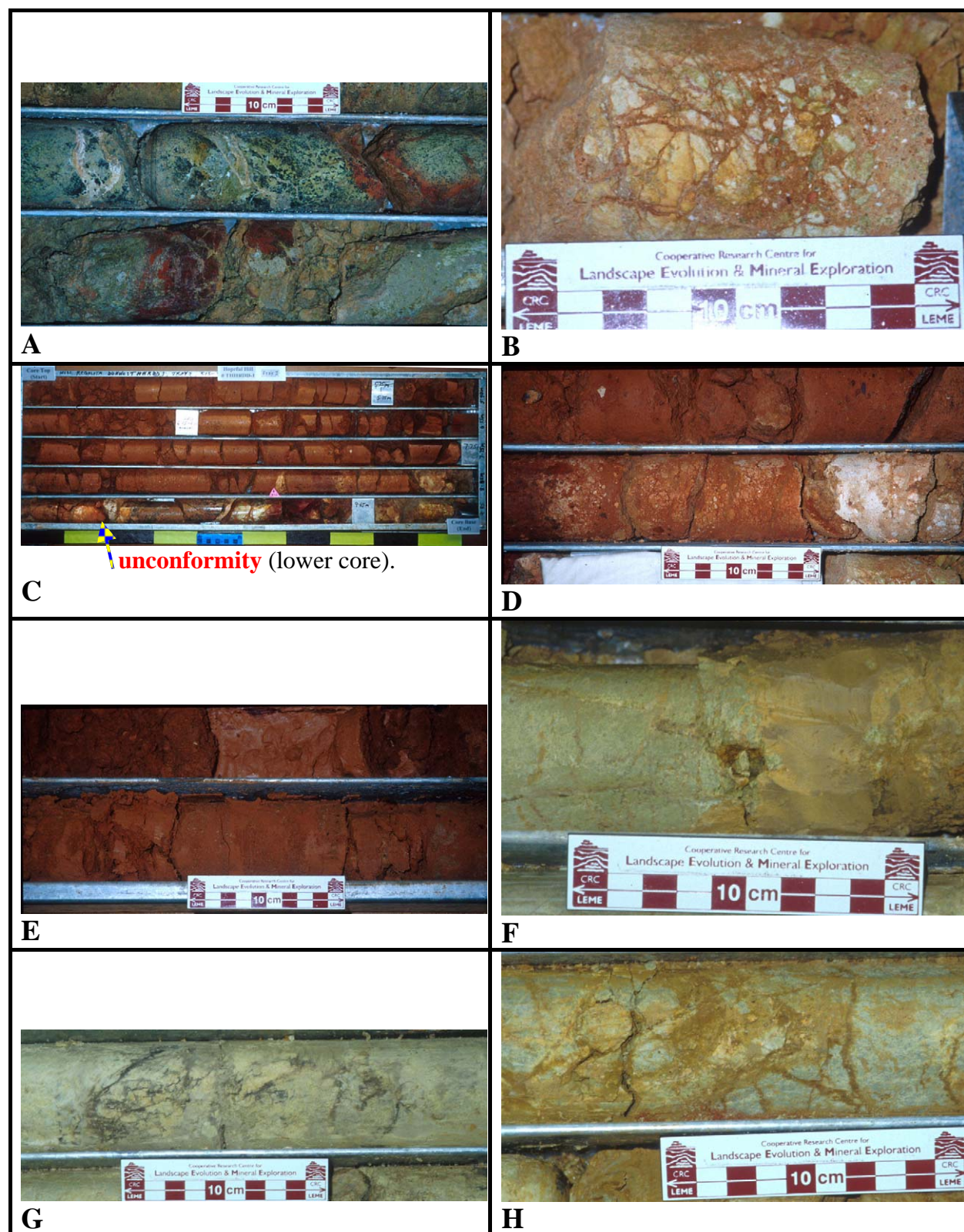


Figure 10: Regolith drill core from Hopeful Hill (THHRDD-1) and Mullina Well (TMWRDD-1).

Note Mullina Well core is reversed to normal and runs right to left.

The **lower saprolite** sub-zone is less complex than the overlying, thick, upper saprolite. It is thin (37.9-38.50 m) compared with the other cored sites and is mostly darker than the upper saprolite. It is also more competent, the clay is stiff, and there is abundant unaltered serpentinite. Typically, it is dark to pale green with some grey, with yellow to brown clay infillings to fracture voids. Fracture surfaces have yellow and brown ferruginous staining which becomes pervasive in places. Regular conjugate joints occur at 45-60° to the core axis and are variably slickensided.

The strongly leached **upper saprolite** is moderately thick (23.3-37.9 m) and is a complex, multicoloured sub-zone where various medium green and variably subtly tinted greyish colours (gleys) are overprinted by red, ferruginous megamottles and black Mn-oxide staining (Figures 10F-H; 11A, B). Subordinate colours include blue-green, blue-grey and bright yellow-greens. The top ~5 m interval is highly leached, mostly pallid (near white to very pale grey) containing dark red-brown megamottles and fracture wall staining (>100 mm wide) in similar red-browns to the megamottles (Figure 11A, B). The upper saprolite includes patches or enclaves of less weathered greenstone; some are >2 m in size and they demonstrate an incomplete or irregular weathering process. Between 25.35 and 27.85 m there was **no** core recovery. Here, the drill rods fell under their own weight through either an open subvertical fracture (>200 mm wide) or through a 2.5 m interval filled with a low-strength hydrous smectite-rich gel at or near its liquid limit (*i.e.* moisture content much greater than 100% by dry weight of clay). The former is more likely. The upper saprolite is clay-rich, variably soft to moderately stiff, and friable to compact. Its clays are sticky and plastic (smectitic) to sub-plastic (illitic). Talc and vermiculite-like minerals give this sub-zone a variably greasy feel in places. There is relict foliation and ghosts of a primary fabric (lizardite) in some parts and not in others. Regular conjugate joints occur at about 45-60° to the core axis; many are strongly slickensided. Black Mn-oxide flecks and dendrites occur in a few intervals of 200-300 mm (at 34.5 and 35.1 m; Figure 10G). Strongly ferruginous dark brown intervals occur at 36.15, 37.7 and 37.9 m, and contain Mn-oxides. The upper saprolite generally consists of smectite-hydromuscovite, kaolin and chlorite with relict serpentinite and talc.

An eroded remnant **pedolith** plasmic zone interval of intensely weathered greenstone was intersected between 22.7 to 23.3 m. Its thin upper portion (22.7-22.9 m) is a competent fine-grained ferricrete, containing pedogenic structures such as wavy parallel dark brown Fe-banding, incipient Fe-nodule development, and brecciation with re-cementation (Figure 11C). There is an eroded upper surface forming an angle of about 15° to the core axis. Below the ferricrete, a pedogenic breccia occurs, comprising a jig-saw-fit set of fragments in pale yellow, pale yellow-grey, and very pale brown clay-rich material, to 100 mm in size. The fracture infill is pale grey clay but this has no associated obvious sedimentary sand- or grit-sized clasts. It is unclear how much of this zone has been eroded, nor is it clear whether that erosion was totally or partially related to the overlying debris flow.

Transported Cover

Sedimentary cover here is 22.7 m thick, consisting of a substantial debris flow deposit, alluvial clays, colluvium, alluvium and a hardpan, with an aeolian sand plain mantling the whole area. Boundaries are indistinct below the hardpan, especially the unconformity, due to similar materials above and below.

A **debris flow** (wet landslide or avalanche deposit) occurs between 17.35 and 22.7 m; it forms the basal unit to the transported cover sequence. Typically it consists of a highly weathered jumbled mix of angular to subrounded clay-rich saprolitic boulders to irregular small clasts (500 to <10 mm), either matrix or clast supported, with an unstructured similarly coloured but less smectitic colluvial clay infill to the inter-clast portions. That infill clay also contains felsic-terrain derived quartz grit to sand with other small lithic rip-up clasts – all showing some degree of abrasion due to transportation. Much of this deposit is pallid (near white to greyish) but some clasts are pale yellow-green or pale yellowish grey. It generally has a randomly occurring red-brown megamottle overprint (Figure 11D, E). The whole interval represents a mass-wasting landslide that has involved some water and has been deposited as a debris flow. Reference to the cross-section derived from aircore drillhole data (Figure 8) reveals that this cored site is on a topographic rise that has persisted for a considerable time, and the site is also adjacent to a palaeo-valley. Undercutting of a water-saturated, deeply weathered creek bank by storm water or the erosional over steepening of a slope of wet saprolite could cause a landslide and result in a mass-flow deposit.

This significant unit was not recognized in the core at first because of its similarity to underlying, highly weathered *in situ* materials. Moreover, the clay-rich boulder to pebble sized subangular clasts are not visible in moist core. Petrography, with assistance from geochemistry and XRD mineralogy, helped define a 4.9 m interval where careful logging of the now dry core was able to locate the main unconformity and recognize the colluvial fabric above it.

A **clay-sand-silt** sediment overlies the debris flow deposit between 11.47 and 17.35 m. An upper metre or so of this unit is sandy with subdominant silt; the remainder is clay-rich. The clay is typical of a fluvial overbank deposit as it is generally structureless and unbedded with pale greys to pale grey-green (gleyed colours, Figure 11F) that become more yellowish grey between 12.6 and 13.5 m. Later pedogenesis has overprinted the bulk clay colours with spaced but conspicuous red megamottles (Figure 11G). Clay stiffness, plasticity, degree of stickiness and, to a lesser degree, the XRD mineralogy all suggest this clay is derived from an eroding deeply weathered ultramafic to mafic terrain rather than a felsic terrain.

A variably silicified **colluvium-alluvium** occurs between 9.9 and 11.47 m. It consists of red-brown plastic clay and minor quartz sand to grit and is unlike units in equivalent positions at Lake Harris or Hopeful Hill. Here it has indistinct widespread dark red to brown Fe-oxide staining and megamottling. Much of this interval was probably derived locally from a weathered mixed lithotype basement terrain.

Overlying the colluvium is a variably silicified red-brown **fluvial clay-silt-sand unit** about 2.0 m thick, consisting of overbank and sheet flow deposited materials. Variable pedogenic silicification within this unit probably occurred during the early or middle Tertiary (Figure 11H).

A strongly coloured **red-brown hardpan** overlies the alluvium and is dominantly a colluvial-alluvial unit of clay, sand and grit, variably cemented with carbonate and hyaline silica, making it relatively competent. This unit is 7.1 m thick.

Pedogenic **calcrete** forms a moderately compact cream coloured layer within the soil-sand profile between 0.3-0.5 m but additional overt and less obvious carbonate cements transported regolith to a depth of about 6.00 m. Exposures of calcrete in the drill sump, next to the cored drillhole, laterally changed from nodules to aggregated nodules to a laminated pan to a massive sheet over a short distance and amply demonstrated the variability of this soil B_{Ca} horizon.

Aeolian sand to a depth of about 0.8 m forms the uppermost transported cover unit. It is red-brown to orange, uniformly sorted and hosts later formed calcrete (see above).

NOTE: The significant discrepancy of nearly 15 m between the position of the unconformity in adjacent diamond cored and air-cored drilling, roughly 10 m apart requires explanation. Logging of aircore drillhole TAR 56, that had bulked 2 m interval cuttings, determined the unconformity to be at about 6-12 m; while logging of the diamond core from TMWRDD-1 determined it to be at 22.7 m. The majority of this difference is due to drill sampling methods – 2 m bulked regolith cuttings are inferior to continuous core. Cuttings of colluvial clay-rich materials strongly resemble deeply weathered *in situ* materials, making the unconformity very cryptic to the human eye. It required the assistance of petrography, XRD mineralogy and geochemistry to locate precisely. The pedolith commonly has an upper portion of mixed provenance (aircore samples) allowing the unconformity in TAR 56 to be changed to about <18 m depth. The debris flow material is impossible to differentiate by eye alone from *in situ* saprolite in drill cuttings. This example demonstrates very well the efficacy of at least **some** strategic regolith drill core (from the surface) to augment the more commonly available drill cuttings when working with transported materials on weathered basement. It is especially so when trying to elucidate landscape evolution, palaeo-surfaces, the subtleties of palaeodrainages and mechanical transport of basement mineralization pathfinders.

Table 12: Summary log to Mullina Well cored drillhole TMWRDD-1 (not to scale)

Depth Range (m)	Graphic Log (vert. not to scale)	Regolith Zone	Description
0.00-0.80		soil-sand	soil in loose red-brown aeolian sand with ~300 mm of calcrete.
0.80-~10.00		sediment	red-brown alluvial clay + sand + gravel, weakly bound to partly cemented. Carbonate to ~6 m. Upper ~6 m is red-brown hardpan colluvium-alluvium, the remainder is an older fluvial overbank to sheet flow + channel deposit, irregularly silicified, silcrete bands.
~10.00-11.47	# # # # # #	colluvium	brown clay, plastic and sticky, + quartz sand-grit, silicified, red to brown Fe-megamottles + MnOx staining.
11.47-17.35	# # # # # # # # # # # #	sediment	sedimentary clays to claystones, silty to sandy at top, mostly structureless & unbedded, yellowish grey grading to greenish grey (gleyed), clays are stiff & plastic, smectitic to kaolinitic. Bright yellow and/or red Fe-megamottles. some Fe-pisoliths within megamottles, MnOx dendrites in a few intervals.
17.35-22.70		debris flow colluvium	Landslide deposit. Unsorted jumble of clay-rich saprolitic blocks to 500 mm, angular to subrounded, clast to matrix supported, matrix clay structureless + polymict quartz & lithic clasts from mixed source, rests unconformably on partly eroded pedolith, unit represents a wet mass wasting event yielding a debris flow.
22.70-23.30	Fe Fe Fe # # # # #	<i>in situ</i> Pedolith (plasmic)	remnant pedolith, extremely weathered greenstone; upper part is ferruginous, brown fines-rich, cemented & partially eroded to an angle of ~15°. Lower 2/3 is pale grey-green or yellowish grey + variable Fe-mottling, has pedogenic breccia & illuvial clay infill
23.30-37.90		upper saprolite	Highly weathered greenstone; complex sub-zone with several enclaves of less + more highly weathered material. Clay-rich, soft to stiff and sticky-plastic clay (smectitic) bright greens + blue-greens + yellow-greens + blue-greys. Relict foliation + lizard skin-like patternation, conjugate joint sets, red Fe-megamottles + yellow to brown Fe-staining throughout, black MnOx flecks and dendrites in sub-zone 34.5-35.3 m. Some intervals have a distinctly greasy feel (talc). Sub-zone is mostly smectite + kaolinite + chlorite + talc + relict serpentine. Dark brown Fe-rich intervals between 36.15-37.90 m
37.90-38.50		lower saprolite	Weathered greenstone; generally darker hued and more competent than the sub-zone above. Dark green-grey weathered serpentinite + bright green and brown clay seams + talc, yellow Fe-stains, well jointed, micro to macro fractured, relict foliation.
38.50-39.12		saprock	Partially weathered serpentinite + clay enclaves, dark green-mid grey, some clay fracture infill, hard to brittle, Fe-staining.
39.12-40.00		protolith	Schistose serpentinite, incipiently weathered, dark green-grey, cross cut by white quartz and chalcedony veins. Weathering Front is near the 40 m level.

Figure 11 explanation: regolith drill core from Mullina Well (TMWRDD-1).

Note: Mullina Well core is reversed to normal and runs right to left.

A. Drillhole TMWRDD-1: 24.6-24.95 m (upper core) [no core between 25.35-27.85 m] & 28.19-28.45 m (lower core). Iron mega mottles in pallid clay saprolite.	B. Drillhole TMWRDD-1: 23.65-23.87 m, pale grey clay saprolite with white clay veins (moist), same interval is white when dry.
C. Drillhole TMWRDD-1: 22.70-22.83 m, a megamottle in the pedolith plasmic zone. Iron oxide is not uniformly distributed within the mottle. Host clay is pallid.	D. Drillhole TMWRDD-1: 18.80-18.94 m, mottled debris flow colluvium.
E. Drillhole TMWRDD-1: 18.50-18.75 m, debris flow colluvium, some clasts are selectively Fe-stained and some random mottling is also present.	F. Drillhole TMWRDD-1: 15.75-15.90 m, alluvial clay, mottled.
G. Drillhole TMWRDD-1: 12.70-12.92 m (upper core) alluvial clay, mottled. 14.15-14.40 m (lower core), complex Fe-staining and mottling in alluvial clay.	H. Drillhole TMWRDD-1: 8.05-8.17 m, weakly cemented (silica & carbonate) alluvial gravel and sand with minor clay.

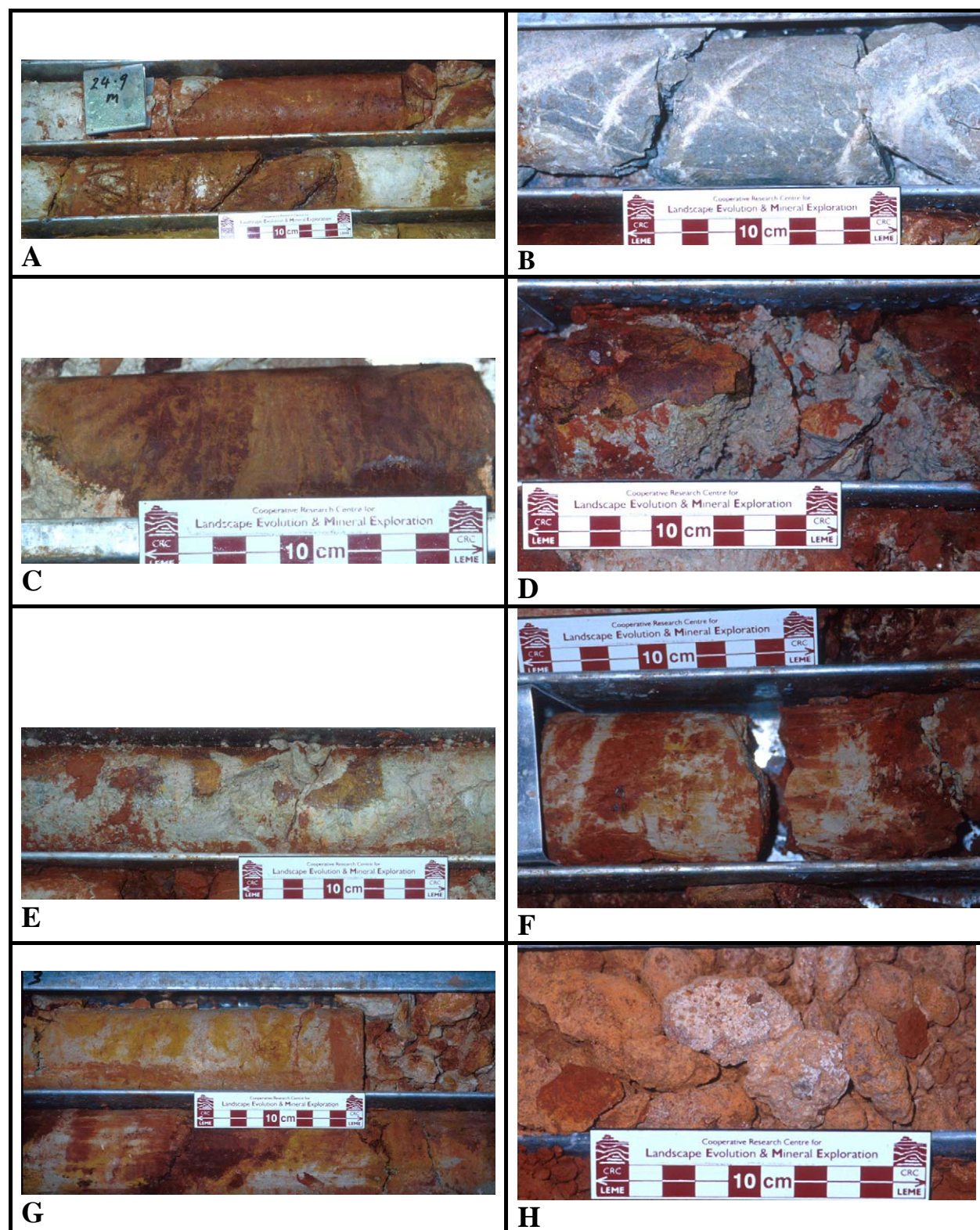


Figure 11: Regolith drill core from Mullina Well (TMWRDD-1).

Note: Mullina Well core is reversed to normal and runs right to left.

Petrography

Drillhole KLHRDD-1

Depth 49.7 m. ULTRAMAFIC BEDROCK.

Pale, acicular tremolite, probably after pyroxene, forms a mesh of randomly oriented needles in which lie patches of chlorite and tremolite, after olivine (Figure 12E, F). Grains of anhedral chromite, ilmenite or magnetite, occur mainly in the chlorite or between chlorite and tremolite and some form parallel bands, probably outlining an original olivine spinifex structure. Weathering is very minor and occurs along cracks that are partly filled with goethite and some goethite has lightly stained the amphiboles adjacent to the cracks. Specimen R406683.

Depth 28.75 m. Fe-STAINED SAPROCK OF ULTRAMAFIC.

The fabric and mineralogy of this saprock is similar to the bedrock below but large, diffuse patches have been stained by goethite developed along grain margins. Cracks in the fabric are infilled with clays and the material around the cracks appears bleached of iron staining, suggesting a cycling water table which placed this saprock alternately in an oxidising and then in a reducing environment. The iron oxides show a slight parallel alignment, suggesting some palimpsest olivine spinifex structures as in the rocks below. Specimen R406682.

Depth 17.0 m. LOWER SAPROLITE OF ULTRAMAFIC WITH SPINIFEX FABRIC.

The saprolite consists of a very fine mesh of hydromuscovite, smectite and chlorite, in which there are remnant needles of unaltered tremolite. However, this fine mesh still preserves the distinctive bladed pyroxene spinifex structure in which illitic clay has replaced the pyroxene and the very fine, dusty iron oxides have picked out the interstices of the spinifex structure (Figure 12C, D). Some of the pyroxene pseudomorphs are cored with a concentration of Fe-oxides. Weathering has lightly stained the rock. Specimen R406681.

Depth 13.75 m. COLLUVIAL SEDIMENT.

Subround to subangular grains, mainly of quartz with minor chert, sericitized plagioclase, clay pellets and goethite-quartz nodules, are loosely packed into a matrix of kaolinite, smectite and hydromuscovite (Figure 12A). This has been mottled to yellow and brown by goethite that has variably stained the matrix. Some voids have been infilled by banded cryptocrystalline aluminosilicate (Figure 12B). Specimen R406680.

Depth 13.47 m. COLLUVIAL SEDIMENT.

Clasts of quartz are dispersed in a clay-hydromuscovite matrix. This section varies from loosely packed at the base to closely packed at the top. Feldspars are absent. Mottling by goethite and some hematite has variably stained the matrix throughout. Sinusoidal veins of cryptocrystalline silica meander throughout the matrix and are probably related to hardpanization. Specimen R406679.

Depth 12.15 m. COLLUVIAL SEDIMENT.

Round, large grains (3 mm) and smaller angular grains (0.5 mm) are loosely packed in a kaolinite-smectite-hydromuscovite matrix that has been mottled by Fe-oxides (Figure 13H). Some quartz clasts are a strained compound mosaic of sutured to granoblastic grains. Specimen R406678.

Depth 10.65 m. COLLUVIAL SEDIMENT.

The sediment consists of fine-grained, angular quartz (1-2 mm), coarser (5 mm) subround strained quartz, minor sericitized plagioclase, a trace of fresh microcline and chert, loosely packed into a flaky phyllosilicate (kaolinite-smectite-hydromuscovite) matrix. A few larger fragments (10 mm) are of gneiss (highly strained quartz and sericitized plagioclase). Parts of the matrix are brown and mottled with goethite. Specimen R406677.

Depth 9.33 m. COLLUVIAL SEDIMENT.

Smaller (0.5 mm) subangular grains of quartz and sericitized plagioclase and larger grains (1-1.5 mm) of subrounded quartz, sericitized feldspar and ferruginous silcrete are loosely packed into a matrix of flaky clay and banded aluminosilicate (Figure 13G). There is more matrix than in those at a shallower depth. Specimen R406676.

Depth 6.5 m. COLLUVIAL SEDIMENT.

The clasts are small, angular to subround and are largely of quartz, vein quartz (with some comb fabrics) and lesser sericitized feldspar and minor fresh microcline. With these are a few larger clasts (10-30 mm)

of ferricrete, silcrete, chert and weathered granite (Figure 13E). These are closely packed in an Fe-mottled phyllosilicate matrix with some banded aluminosilicate cement (Figure 13F). Specimen R406675.

Depth 4.95 m. COLLUVIAL SEDIMENT.

Closely packed subangular to subrounded grains of quartz, chert, vein quartz and lesser sericitized plagioclase, fresh microcline and ferricrete clasts, set in an aluminosilicate/phyllosilicate cement (Figure 13C, D) which is less Fe-stained than that higher in the profile. There is less microcline and feldspar and more quartz than in the sediments at a shallower depth. The feldspars are more weathered and Fe-stained (prior to sedimentation). The ferricrete contains both angular, shardy quartz grains and highly rounded grains (water worn). Specimen R406674.

Depth 2.8 m. HARDPANIZED COLLUVIUM.

Closely packed subangular to subround quartz grains, probably from a dismembered granite (relatively fresh), are set in an Fe-stained aluminosilicate cement. The grains consist of sutured quartz, fresh microcline, sericitized plagioclase (Figure 13A, B) and compound grains of these three component minerals. There is also a trace of epidote and chert grains. The dark red cement is banded in part and probably infilled voids in a sedimentary grain mesh. A small amount of the matrix consists of red-stained phyllosilicates. Specimen R406673.

Comments

- It seems likely that the sediments were deposited on soft, easily eroded ultramafic rocks that occupied low parts of the topography.
- The smectitic clay of the matrix was probably largely from erosion of mafic-ultramafic rocks and the kaolinite and hydromuscovite from weathered granitic materials. The upper part of the sediment is cemented to a hardpan by banded aluminosilicate. The matrix of the sediments below the hardpan consists of phyllosilicate and becomes more abundant with depth. Where it is less stained, it is a flaky mixture of phyllosilicates (XRD and petrography indicates kaolinite, smectite and hydromuscovite) and varies in birefringence from grey to first order yellow.
- The quartz clasts appear to have been derived locally from deeply weathered granites (characterized by small shardy grains), however some larger grains are more rounded, probably also granitic and have been transported further. Vein quartz was another source.
- Predominance of quartz clasts in the lower part of the sediments and the appearance of microcline and sericitized feldspar towards the top imply the progressive erosion of and provenance from a deeply weathered granitic/gneissic profile that progressively exposed less weathered materials with time.
- The bedrock intersections are relatively undeformed, allowing some of the original igneous fabrics to persist into the saprolite. It seems likely that different parts of the ultramafic flows have been intersected to show both olivine and pyroxene spinifex structures.

Drillhole THHRDD-1

Depth 38.63 m. HIGHLY DEFORMED FRESH ULTRAMAFIC BEDROCK.

A highly schistose fine-grained mat of acicular tremolite and flakes of chlorite in which chlorite and a dusting of Fe-oxide picks out at least two acutely intersecting, closely spaced cleavages. Coarser granules of Fe-oxide are scattered throughout. Coarser tremolite and chlorite occur in a few small lenses and boudins. There has been only slight staining along some cleavage planes. Specimen R406691.

Depth 16.13 m. SAPROCK OF ULTRAMAFIC.

Large islands, consisting of a mat of chlorite and talc, contain acicular pseudomorphs after either metamorphic tremolite or after pyroxene spinifex structures. These are surrounded by broad, meandering veins of coarse, flaky kaolinite in which lie small, unconsumed remnants of the talc-chlorite mat (Figure 14C, D). Fragments of pale, delicately banded aluminosilicate cement has filled voids and been later brecciated (Figure 14D). Specimen R406690.

Depth 13.35 m. SAPROCK OF ULTRAMAFIC.

Patches of largely opaque material, heavily dusted with Fe-oxides, pseudomorph olivine grains cut by serpentine/antigorite veinlets in what was probably an adcumulate (Figure 14A, B). This is surrounded by chlorite and talc. The whole is cut by meandering veinlets of cryptocrystalline silica and fibrous brucite

(Figure 14A). Weathering along specific bands has altered the fabric to stained clay (smectite and kaolinite) obliterating the original fabric. Specimen R406689.

Depth 9.78 m. POROUS SAPROLITE.

The saprolite consists of a fine-grained flaky mat of smectite and kaolinite with some remnant talc and chlorite, all dusted with Fe-oxides. This has been veined by early gypsum or brucite and later brecciated by near-surface weathering. Voids are now filled with sediment from above, containing a polymict assemblage of saprolite, Fe-oxide granules and small quartz grains in a clay matrix (Figure 15G, H). A few voids and cracks in this porous material are filled with banded, light brown aluminosilicate cement. Specimen R406688.

Depth 8.65 m. CLAYSTONE-QUARTZ ARENITE.

A highly complex sediment consisting mainly of large clasts (5-20 mm) largely of a dark claystone, some of which itself contain smaller clasts of claystone and subangular to subround quartz grains (Figure 15E). Other, less abundant, clasts are Fe-oxide granules. These are set in a matrix of fine-grained angular quartz and dark-brown stained kaolinite. Parts of the matrix have been broken and re-cemented and coated by brown, banded aluminosilicate that also lines voids. Some of the aluminosilicate has also been broken and re-cemented. Some of the larger claystone clasts show evidence of infilled burrows (Figure 15F), which might explain the bimodal nature of the materials in this claystone by bioturbation and mixing of originally separate, stratified and sorted materials. Specimen R406687.

Depth 8.28 m. CLAYSTONE-QUARTZ ARENITE.

A polymictic sediment of poorly sorted, rounded fragments of claystone, quartz and Fe-oxide nodules (Figure 15C, D) tightly packed into a clay matrix that has been brecciated and partly dissolved and the voids filled with several generations of banded aluminosilicate. The claystone fragments contain quartz clasts but are not as complex as those from higher in the profile. Specimen R406686.

Depth 8.08 m. CLAYSTONE-QUARTZ ARENITE.

A highly complex sediment consisting mainly of large clasts (5-20 mm) largely of a dark claystone which itself contains smaller clasts of claystone and subangular to subround quartz grains (Figure 15A). Other less abundant clasts are of Fe-oxide granules and ferricrete. These are set in a matrix of fine angular quartz and deep brown-stained kaolinite. Parts of the matrix have been broken and re-cemented and coated by brown, banded aluminosilicate that also lines voids. Some of the aluminosilicate has also been broken and re-cemented (Figure 15B). Specimen R406685.

Depth 4.52 m. HARDPANIZED COLLUVIUM-ALLUVIUM.

Larger grains (2 mm) of rounded quartz and smaller grains (0.5 mm) of angular to shardy quartz with minor microcline and granules of Fe-oxides are loosely packed into a brown-stained phyllosilicate (kaolinitic) matrix (Figure 12H) which contains numerous voids lined and some filled with a finely banded, brown aluminosilicate cement. Among the larger rounded grains are a few rounded clasts of ferricrete (Figure 12G) containing angular quartz. There is evidence of erosion and redeposition of this material as some clasts have the same quartz clasts and stained phyllosilicate matrix as the main part and are coated with banded aluminosilicate that also forms veins in the matrix. Specimen R406684.

Comments

- The ultramafic bedrocks show significant but variable deformation and metamorphism that have largely obscured their character, although some hints of cumulate fabrics remain. The top of the saprolite contains cavities filled with sedimentary materials.
- The majority of the overlying sediments consist of fragments of claystone that imply a pre-existing claystone, consisting of clays and quartz, that have been mixed by bioturbation, before being broken up and redeposited on the ultramafic saprolites.
- Only the top of the sediments are different and probably had a granitic provenance.
- The aluminosilicate cementing material had a complex history, showing evidence of several cycles of cementation, break-up and re-cementation.

Drillhole TMWRDD-1**Depth 39.15 m. RELATIVELY FRESH MAFIC BEDROCK.**

Fine-grained acicular tremolite and fibrous chlorite forms a mesh with interstitial plagioclase and minor quartz. The whole is dusted with granular Fe-oxides and brown rutile. The proportions of mafic and felsic minerals varies. Some parts are schistose, with a cleavage of aligned mafic minerals and small lenses of granular quartz. Cracks have developed, some along the cleavage, and these are lined with clay and goethite. Goethite has spread from these to a limited extent, to stain the mafic minerals. Specimen R406702.

Depth 34.45 m. SAPROCK OF ULTRAMAFIC.

A mat of talc and chlorite, dusted with fine-grained Fe-oxides contains some acicular structures pseudomorphed by the talc. Small diffuse patches and veinlets within the metamorphic fabric have altered to very fine-grained flaky clay (smectite and kaolinite) that has lost the acicular structure. The clays are very faintly stained and the metamorphic fabric is unstained. Specimen R406701.

Depth 30.08 m. SAPROLITE OF ULTRAMAFIC.

A mat of talc and chlorite with veinlets and patches of granular metamorphic quartz has been intensely altered to very fine-grained clay (smectite and kaolinite) in numerous diffuse patches (Figure 16H) that contain unconsumed or partly consumed remnants of the metamorphic assemblage. Iron staining, which has largely penetrated from fractures, cleavages and along quartz vein margins has spread into the metamorphic fabric to a limited extent (Figure 16G, H). Specimen R406700.

Depth 23.70 m. SAPROLITE OF PRESUMED ULTRAMAFIC.

The ultramafic has been altered pervasively, leaving only minute remnants of the talc fabric in a mass of circular patches of very fine-grained, flaky clay and vermiform clay stacks between, dusted with opaque Fe-oxides and rutile (Figure 16E, F). Clays have penetrated between the grains of the veins and patches of metamorphic quartz, producing a loose jig-saw structure or patches of disaggregated grains. Iron staining is confined to cracks and these and voids are filled with brown, banded aluminosilicate. Specimen R406699.

Depth 18.80 m. MOTTLED GRITTY SEDIMENT OF SAPROLITE FRAGMENTS.

A complex matrix-supported polymictic gritty sediment (Figure 16D). It contains large subangular clasts, mainly of the underlying saprolite (characterized by patches and 'blasts' of fine-grained clay, disaggregated quartz crystals and relics of the metamorphic fabric) and lesser quantities of clasts of claystone with quartz inclusions. This is set in a matrix of rounded similar materials but with claystone and quartz dominating, all in a clay matrix. Part of the specimen, probably representing a large mottle (Figure 16C), is intensely ferruginized to goethite, obscuring much of the fabric. Specimen R406698.

Depth 15.80 m. MOTTLED CLAYSTONE.

A mottled claystone with numerous subround to subangular quartz clasts (0.1-0.5 mm) and a few ferruginous granules (2 mm). Coarse mottling has stained the clays brown in diffuse zones (Figure 16B). There is faint evidence for curved burrows about 5 mm diameter and 15 mm deep. Specimen R406697.

Depth 12.92 m. MOTTLED CLAYSTONE.

This is similar to the sediment below but minor microcline occurs among the sand-sized quartz clasts and these are more unevenly distributed throughout. Goethite mottling has stained some clays and minor goethite has been deposited along cracks (Figure 16A). Specimen R406696.

Depth 12.45 m. GRITTY SEDIMENT OF CLAYSTONE FRAGMENTS.

Mottling of the matrix of this matrix-supported grit has accentuated its fabric (Figure 14G). It consists of clasts of quartz-bearing claystone, talc-chlorite-clay saprolite with a variety of fabrics and weathering states and quartz. These are set in a matrix of Fe-stained clay (Figure 14H). Specimen R406695.

Depth 10.90 m. MOTTLED GRITTY SEDIMENT.

Large rounded to subround and small angular to shardy quartz grains are densely packed into a matrix of ferruginous clay which has been partly replaced by a deep brown aluminosilicate cement. Specimen R406694.

Depth 9.15 m. GRAVELLY SEDIMENT.

Polymictic gravel containing rounded clasts of ferricrete, claystone and saprolite set in a matrix of clay scattered with quartz and ferruginous nodules. Specimen R406693.

Depth 8.05 m. CALCRETE CEMENTED CLAYSTONE.

This section consists of two samples each of two different materials (Figure 14E).

- i) The first material is a complex sediment of clasts of clay-rich material and both angular and round quartz set in a clay and fine quartz matrix. The clays of both the matrix and the clasts are stained brown by goethite. Numerous cracks and voids within the matrix have been lined with a delicately banded aluminosilicate cement that also forms papules. This fragment has a partial cutan of brown aluminosilicate. The other fragment is similar but has been more intensely stained a deep red-brown.
- ii) The second material consists of clasts of a broad range of sizes of the first material, ferruginized to varying degrees, set in a very fine-grained carbonate matrix (calcrete) with clasts of angular to subround quartz and minor rounded very fine-grained granular carbonate (Figure 14F). Specimen R406692.

Comments

- The mafic-ultramafic bedrocks show significant deformation, which have largely obscured their character, although some hints of cumulate fabrics remain. The top of the saprolite contains cavities filled with sedimentary materials.
- Although the base of the sediments is a breccia of saprolite fragments, succeeding layers are of a claystone, similar to that of the palaeochannel sediments on the Yilgarn Craton, consisting of a bimodal mixture of clays and quartz. These have been broken up and redeposited higher in the succession.
- Logging of even diamond core of regolith, and locating the unconformity between transported and *in situ* materials are very difficult in places. The core can have different appearances when wet and dry and can show different features in these two states. Thus, it is inevitable that the core needs revisiting and initial logs need revision, particularly when additional chemical, mineralogical and petrographic evidence becomes available.

Figure 12: explanation. Petrography of samples from cored drillholes KLHRDD-1 and THHRDD-1.

<p>A. Subrounded to subangular grains of quartz (QZ) and clay pellets (CP) loosely set in a pale grey clay matrix (MX). The clay has been mottled yellow-brown with a goethite stain (GO). Close up photograph of colluvial sediment. Specimen R406680: Drillhole KLHRDD-1, Depth 13.75-13.80.</p>	<p>B. Loosely packed nodules of goethite and quartz (GO), angular to subrounded quartz (QZ), chert (CT), and sericitized plagioclase (PL) in a matrix (MX) of flaky kaolinite, smectite and hydromuscovite. The matrix has been stained brown by goethite. Some voids are infilled with banded aluminosilicate (AL). Photomicrograph of colluvial sediment under transmitted light with crossed polarizers. Specimen R406680: Drillhole KLHRDD-1, Depth 13.75-13.80.</p>
<p>C. Yellow-green hydromuscovite pseudomorphs after bladed pyroxene spinifex fabric (SP) surrounded by massive, bright green, plasmic, smectitic clay (SM) with remnants (RM) of the previous illitic material. Close up photograph of saprolite of ultramafic rock with spinifex fabric. Specimen R406681: Drillhole KLHRDD-1, Depth 17.0-17.07.</p>	<p>D. Bladed pyroxene spinifex structure (SP) now pseudomorphed by illitic clay and the interstices (IS) and pyroxene cores (PC) are accentuated by dusty Fe-oxides. Photomicrograph of saprolite of ultramafic rock with a spinifex fabric under plane polarized transmitted light. Specimen R406681: Drillhole KLHRDD-1, Depth 17.0-17.07.</p>
<p>E. A fresh mass of pale, acicular tremolite (TM) and patches of dark green chlorite (CL). Cracks are partly filled with goethite (GO) from which a staining has spread. Close up photograph of ultramafic bedrock. Specimen R406683: Drillhole KLHRDD-1, Depth 49.70-49.77.</p>	<p>F. A mesh of acicular tremolite (TM) after pyroxene with patches of chlorite (CL) after olivine. Minor goethite staining (GO) along cracks. Photomicrograph of ultramafic bedrock under plane polarized transmitted light. Specimen R406683: Drillhole KLHRDD-1, Depth 49.70-49.77.</p>
<p>G. Larger subrounded grains of ferricrete (FC) and quartz (QZ) and smaller, angular to shardy quartz grains (QS) loosely packed into a brown-stained kaolinitic matrix (MX). Cracks are partly lined by siliceous clay (CL). Close up photograph of hardpanized colluvium-alluvium. Specimen R406684: Drillhole THHRDD-1, Depth 4.52-4.58.</p>	<p>H. Ferruginous nodules (FN) and large, subround to subangular clasts of creamy claystone (CS) containing smaller white claystone clasts (CL) and clear subangular quartz grains (QZ). These are set in a in a matrix of fine-grained angular quartz and deep brown stained kaolinite (KA). Close up photograph of hardpanized sedimentary breccia. Specimen R406685: Drillhole THHRDD-1, Depth 8.08-8.15.</p>

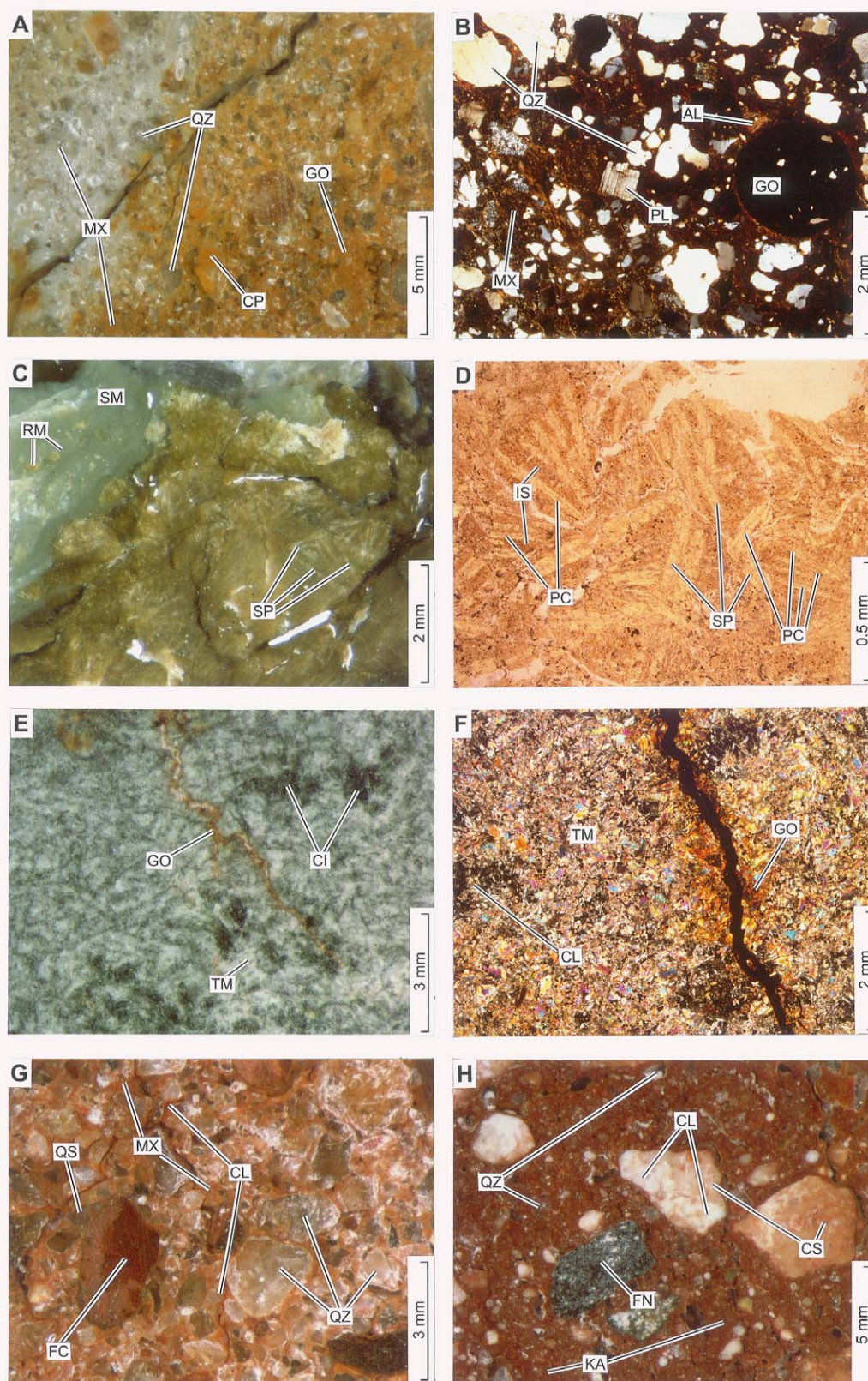


Figure 12: Petrography of samples from cored drillholes KLHRDD-1 and THHRDD-1.

Figure 13: explanation. Petrography of samples from cored drillhole KLHRDD-1.

<p>A. Grains of vein quartz (VQ), granitic quartz (QZ) and feldspar (FS) in a red hardpanized aluminosilicate and phyllosilicate matrix (MX). Cementation by siliceous, banded clays (BC) has taken place along cracks. Close up photograph of hardpanized colluvium. Specimen R406673: Drillhole KLHRDD-1, Depth 2.80-2.87.</p>	<p>B. Closely packed grains of fresh microcline (MC), quartz (QZ) and sericitized plagioclase (PL) set in a dark red matrix of Fe-stained aluminosilicate and Fe-stained phyllosilicates (AL). Photomicrograph of hardpanized colluvium under transmitted light with crossed polarizers. Specimen R406673: Drillhole KLHRDD-1, Depth 2.80-2.87.</p>
<p>C. Angular to subrounded grains of white vein quartz (VQ), quartz (QZ) closely packed into a matrix of Fe-stained phyllosilicates (PH) and aluminosilicate patches (AL). Close up photograph of colluvial sediment. Specimen R406674: Drillhole KLHRDD-1, Depth 4.95-5.02.</p>	<p>D. Close-packed subangular to subrounded compound grains of quartz (QZ), chert (CT), vein quartz (VQ) and minor sericitized plagioclase, fresh microcline and ferricrete clasts in a slightly Fe-stained aluminosilicate-phyllosilicate matrix (MX). The ferricrete contains both rounded and shardy quartz. Photomicrograph of colluvial sediment under transmitted light with crossed polarizers. Specimen R406674: Drillhole KLHRDD-1, Depth 4.95-5.02.</p>
<p>E. Angular to subrounded clasts of dark brown ferricrete (FC), yellow silcrete with a partial white weathered rind (SC) and quartz (QZ) in a matrix of grey clay (CL) and banded aluminosilicate cement (AL). Close up photograph of colluvial sediment. Specimen R406675: Drillhole KLHRDD-1, Depth 6.50-6.58.</p>	<p>F. Large, lithic clasts of ferricrete (FC), consisting of angular quartz grains (QZ) in a hematite cement (HT) and smaller mineral grains comprising quartz, vein quartz, lesser sericitized feldspar (FS) and minor fresh microcline (MC) set in an Fe-mottled matrix of phyllosilicates (PH). Photomicrograph of colluvial sediment under plane polarized transmitted light. Specimen R406675: Drillhole KLHRDD-1, Depth 6.50-6.58.</p>
<p>G. Subrounded clasts of Fe-stained silcrete (SC) ultramafic saprolite (US) and grains of quartz (QZ) loosely packed into a matrix of slightly mottled clay (CL). Close up photograph of colluvial sediment. Specimen R406676: Drillhole KLHRDD-1, Depth 9.33-9.40.</p>	<p>H. Larger subrounded and smaller angular grains of quartz (QZ) in an abundant matrix of grey-green kaolinite-smectite-hydromuscovite clay (CL) slightly mottled (MO) with goethite. Close up photograph of colluvial sediment. Specimen R406678: Drillhole KLHRDD-1, Depth 12.15-12.20.</p>

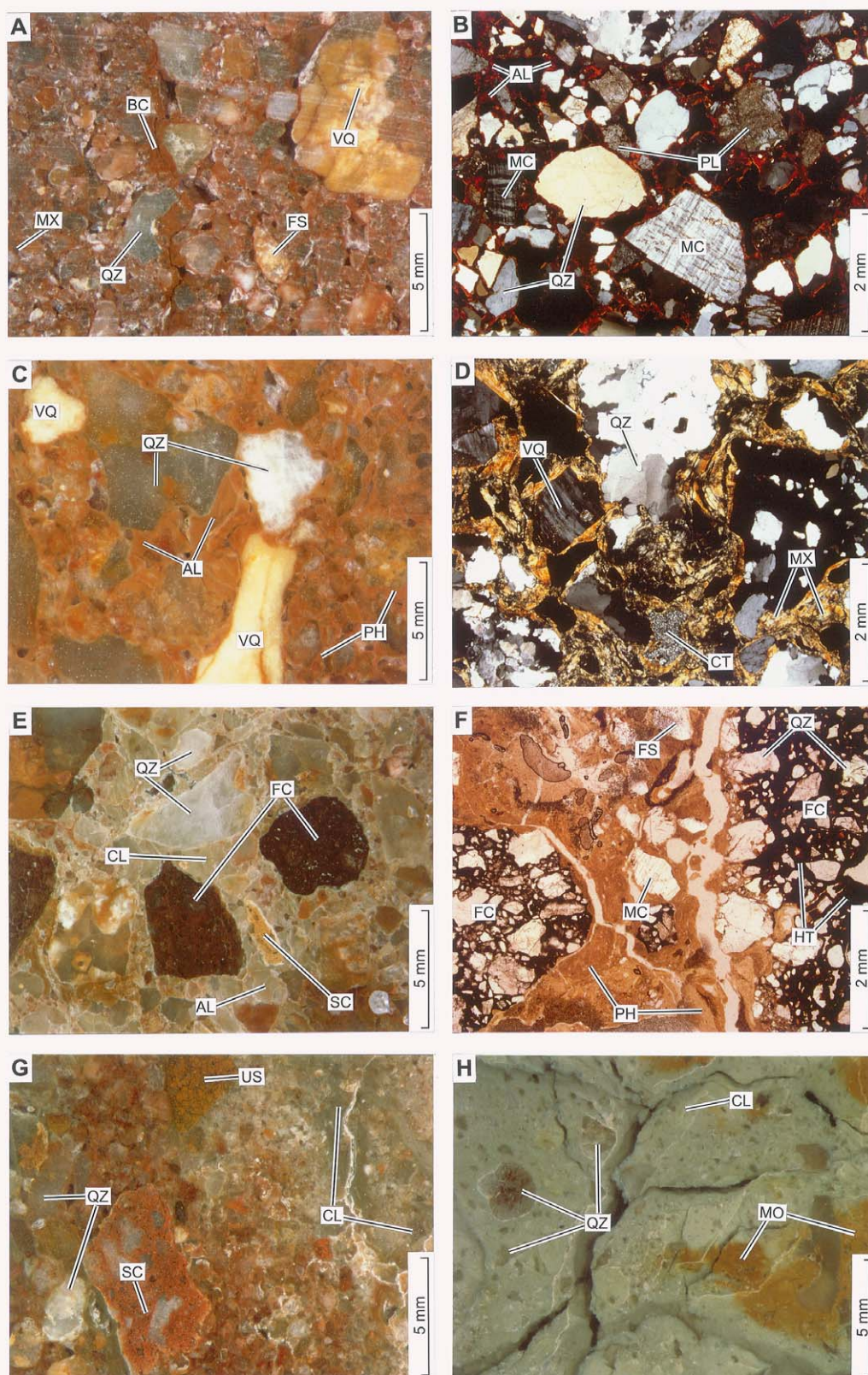


Figure 13: Petrography of samples from cored drillhole KLHRDD-1.

Figure 14: explanation. Petrography of samples from cored drillholes THHRDD-1 and TMWRDD-1.

<p>A. Dark serpentine pseudomorphs after olivine (OL) outlined by a dusting of Fe-oxides set in a mass of chlorite and talc (CT). This has been cut by veinlets of asbestiform minerals (AS) and voids have been filled by opaline silica (OP). Minor weathering has stained the margins of cracks with goethite (GO). Close up photograph of ultramafic saprock. Specimen R406689: Drillhole THHRDD-1, Depth 13.35-13.45.</p>	<p>B. Serpentine pseudomorphs after olivine grains (OL) shown by a dusting of Fe-oxides cut by serpentine/antigorite (AN) with the fabric of an adcumulate, surrounded by chlorite and talc (TC). Photomicrograph of ultramafic saprock under plane polarized transmitted light. Specimen R406689: Drillhole THHRDD-1, Depth 13.35-13.45.</p>
<p>C. Green chlorite and talc (CT) saprolite cut by white veins of kaolinite (KA). Close up photograph of ultramafic saprock. Specimen R406690: Drillhole THHRDD-1, Depth 16.13-16.22.</p>	<p>D. A mass of chlorite and talc (CT) with acicular pseudomorphs cut by veins of coarse flaky kaolinite (KA). Some veins have been lined by brown, delicately banded aluminosilicate (AL) that has been subsequently brecciated. Photomicrograph of ultramafic saprock under plane polarized transmitted light. Specimen R406690: Drillhole THHRDD-1, Depth 16.13-16.22.</p>
<p>E. A fragment of a quartz-claystone arenite (QC) cemented by clay and quartz and two fragments of calcrete cemented sediment clay-quartz arenite (CX). Close up photograph of claystone-quartz arenite. Specimen R406692: Drillhole TMWRDD-1, Depth 8,05-8.10.</p>	<p>F. Clasts of ferruginized claystone-quartz arenite (QC) set in a matrix of smaller quartz (QZ) and feldspar (FS) grains and very fine-grained carbonate (CC). Photomicrograph of calcrete cemented claystone-quartz arenite under transmitted light with crossed polarizers. Specimen R406692: Drillhole TMWRDD-1, Depth 8,05-8.10.</p>
<p>G. Claystone (CL), quartz (QZ) and variably weathered ultramafic saprolite (UM) clasts in a matrix (MX) of fine quartz and clay that is variably stained with Fe-oxides. The fabric of this rock is accentuated by Fe-staining of the matrix. Close up photograph of claystone-quartz arenite. Specimen R406695: Drillhole TMWRDD-1, Depth 12.45-12.50.</p>	<p>H. Clasts consist mainly of quartz-bearing claystone (CS) with minor saprolites of ultramafic rocks (UM) in various states of weathering and ferruginization, set in a clay matrix (MX) that has been mottled by Fe-oxides (border MO). Photomicrograph of claystone-quartz arenite under plane polarized transmitted light. Specimen R406695: Drillhole TMWRDD-1, Depth 12.45-12.50.</p>

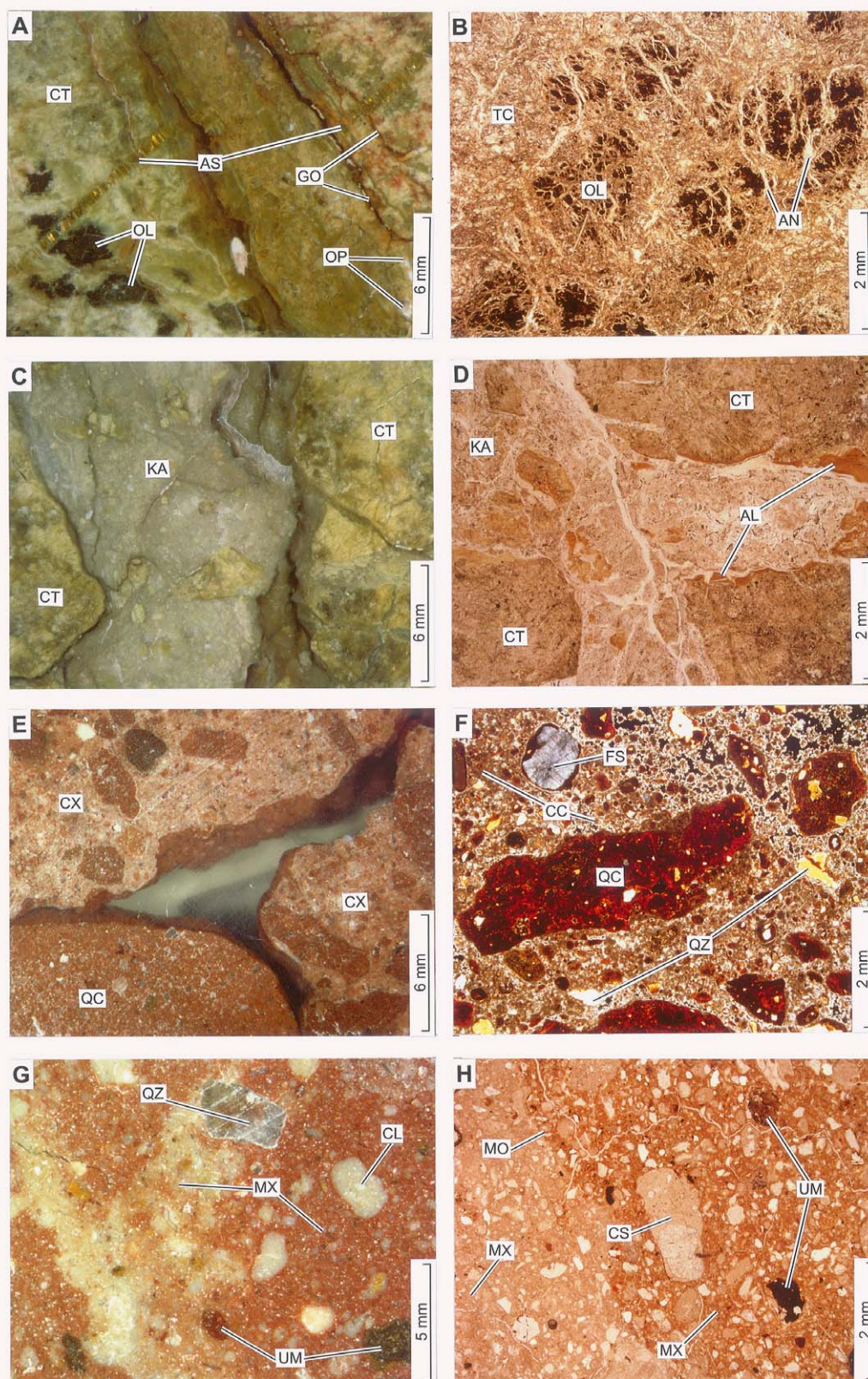


Figure 14: Petrography of samples from cored drillholes THHRDD-1 and TMWRDD-1.

Figure 15: explanation. Petrography of samples from cored drillhole THHRDD-1.

<p>A. A large clast of claystone containing smaller clasts of claystone (CL), ferricrete (FC) and subangular to subround quartz (QZ). The matrix consists of quartz grains (QZ) set in brown, Fe-stained kaolinite (KA) with cracks and voids (VO). Photomicrograph of a sedimentary breccia under plane polarized transmitted light. Specimen R406685: Drillhole THHRDD-1, Depth 8.08-8.15.</p>	<p>B. Part of the matrix, consisting of ferruginous granules (FG) and quartz (QZ) in stained kaolinite (KA) which has been partly dissolved and re-cemented by banded aluminosilicate (AL). The aluminosilicate has been further brecciated (AB) and again re-cemented. Photomicrograph under plane polarized transmitted light. Specimen R406685: Drillhole THHRDD-1, Depth 8.08-8.15.</p>
<p>C. Rounded to angular fragments of a variety of claystones (CL), quartz grains (QZ) and Ferricrete (FC) in a clay matrix (MX). Close up photograph of polymictic sediment. Specimen R406686: Drillhole THHRDD-1, Depth 8.28-8.34.</p>	<p>D. Ferruginous granules (FG) and clasts of claystone (CL) in a finer-grained groundmass of ferruginous granules and clay pisoliths (CP) in a clay matrix (MX). Voids (VO) have been lined with banded aluminosilicate (AL). Photomicrograph of polymictic sediment under plane polarized transmitted light. Specimen R406686: Drillhole THHRDD-1, Depth 8.28-8.34.</p>
<p>E. Complex claystone clasts containing an earlier generation of pale claystone clasts (CO) and Fe-oxide granules (FG) in a matrix (MX) of angular quartz and brown-stained kaolinite. Close up photograph of sedimentary breccia. Specimen 406687: Drillhole THHRDD-1, Depth 8.65-8.73.</p>	<p>F. A claystone clast (CL) containing part of an infilled burrow (BR). This is set in a matrix (MX) of clay and claystone granules. Photomicrograph of sedimentary breccia under plane polarized transmitted light. Specimen 406687: Drillhole THHRDD-1, Depth 8.65-8.73.</p>
<p>G. A saprolite (SP), consisting of kaolinite and smectite, has been brecciated by near-surface weathering processes. Voids are now filled with a polymictic assemblage of saprolite (SP), hematite granules (HM) and small quartz grains set in clay (CL). Close up photograph of porous saprolite. Specimen R406688: Drillhole THHRDD-1, Depth 9.78-9.85.</p>	<p>H. Brecciated saprolite fragments (SP) in a clay matrix (MX) with quartz (QZ) and pieces of Fe-oxides. Photomicrograph of porous saprolite under transmitted light with crossed polarizers. Specimen R406688: Drillhole THHRDD-1, Depth 9.78-9.85.</p>

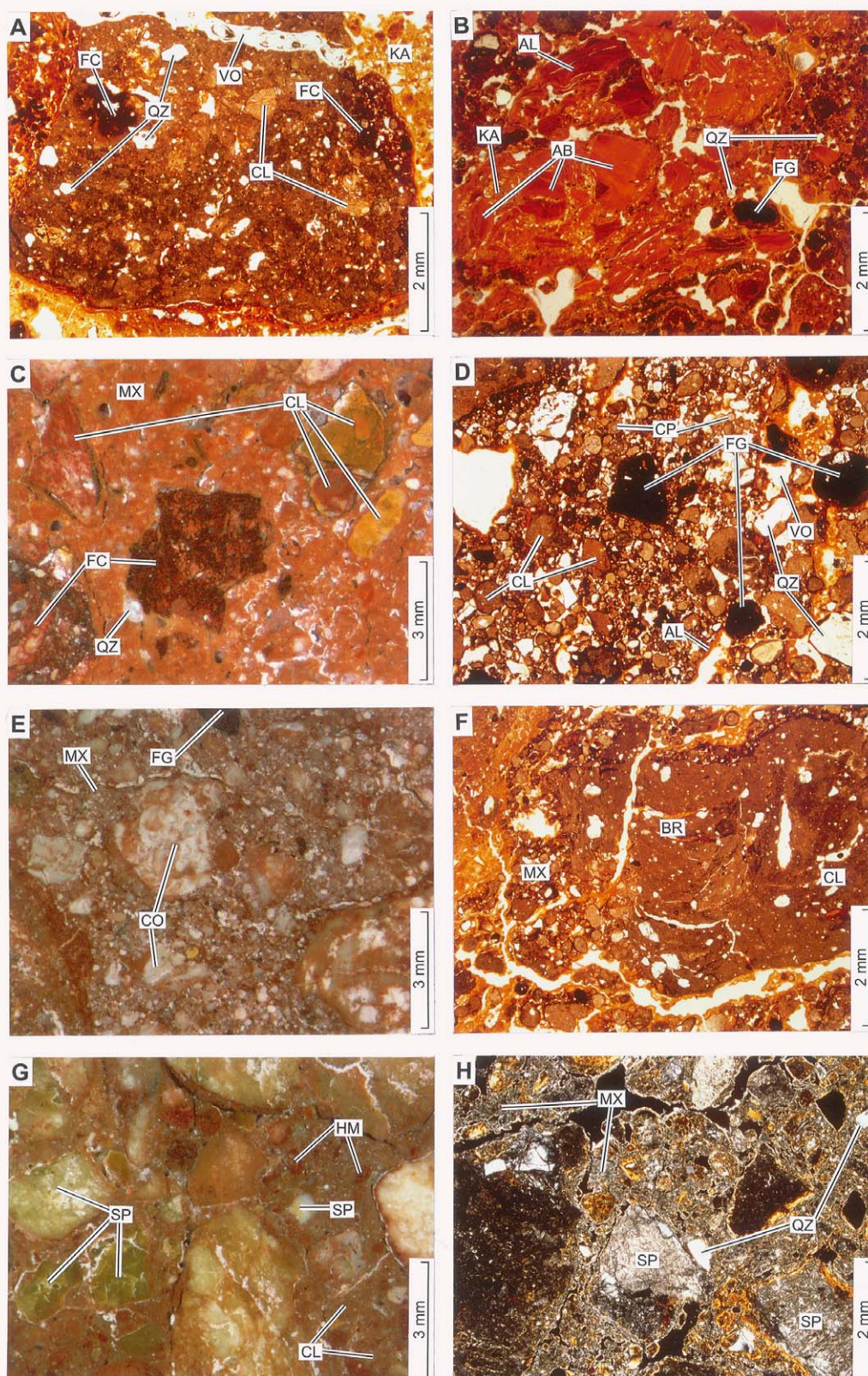


Figure 15: Petrography of samples from cored drillhole THHRDD-1.

Figure 16: explanation. Petrography of samples from cored drillhole TMWRDD-1.

<p>A. Pale grey claystone (CL) with minor quartz grains (QZ) distributed throughout and a few claystone fragments (CF). The rock is stained and mottled by goethite (GO) and hematite (HM) has penetrated along cracks. Close up photograph of claystone. Specimen R406696: Drillhole TMWRDD-1, Depth 12.92-12.97.</p>	<p>B. A mottled claystone, consisting of pale yellow-grey kaolinite and fine quartz with a variety of brown ferruginous nodules (FN) and clasts (FC). Mottling by Fe-oxides has stained parts of the rock red (HM) and yellow (GO). Close up photograph of claystone. Specimen R406697: Drillhole TMWRDD-1, Depth 12.92-12.97.</p>
<p>C. A gritty sediment of greenish subangular clasts of quartz-kaolinite saprolite (SP), clasts of grey claystone (CL) and small quartz crystals in a matrix (MX) of finer, similar materials and clay. Part is a large, clearly defined yellow and brown mottle (MO) where much of the saprolite clasts and the clay rich matrix are obscured by Fe-oxides, leaving only a few recognizable saprolite relics and quartz grains. Close up photograph of claystone arenite. Specimen R406698: Drillhole TMWRDD-1, Depth 18.80-18.87.</p>	<p>D. Quartz-clay saprolite (SP) clasts, claystone (CL) and ferruginous claystone (FC) clasts in a matrix of quartz (QZ) and lightly stained clay (KA). Photomicrograph of claystone arenite under plane polarized transmitted light. Specimen R406698: Drillhole TMWRDD-1, Depth 18.80-18.87.</p>
<p>E. Greenish ultramafic saprolite (SP) with clay filled voids (KA). Close up photograph of ultramafic saprolite. Specimen R406699: Drillhole TMWRDD-1, Depth 23.70-23.78.</p>	<p>F. Remnants of talc (TC) and vermiform clay stacks (VC) in a mesh of equant patches of very fine-grained flaky kaolinitic clay (CL) all dusted with opaque Fe-oxides (FO). Photomicrograph of ultramafic saprolite under transmitted light with crossed polarizers. Specimen R406699: Drillhole TMWRDD-1, Depth 23.70-23.78.</p>
<p>G. Greenish saprolite (SP) has been penetrated and stained by yellow-brown goethite marking a complex cleavage network (NT). Close up photograph of ultramafic saprolite. Specimen R406700: Drillhole TMWRDD-1, Depth 30.08-30.18.</p>	<p>H. Patches (CL) of fine-grained clay (smectite and kaolinite) with unconsumed remnants (ME) of the metamorphic assemblage (talc, chlorite and quartz). Iron staining (GO) has penetrated from fractures and cleavages. Photomicrograph of ultramafic saprolite under transmitted light with crossed polarizers. Specimen R406700: Drillhole TMWRDD-1, Depth 30.08-30.18.</p>

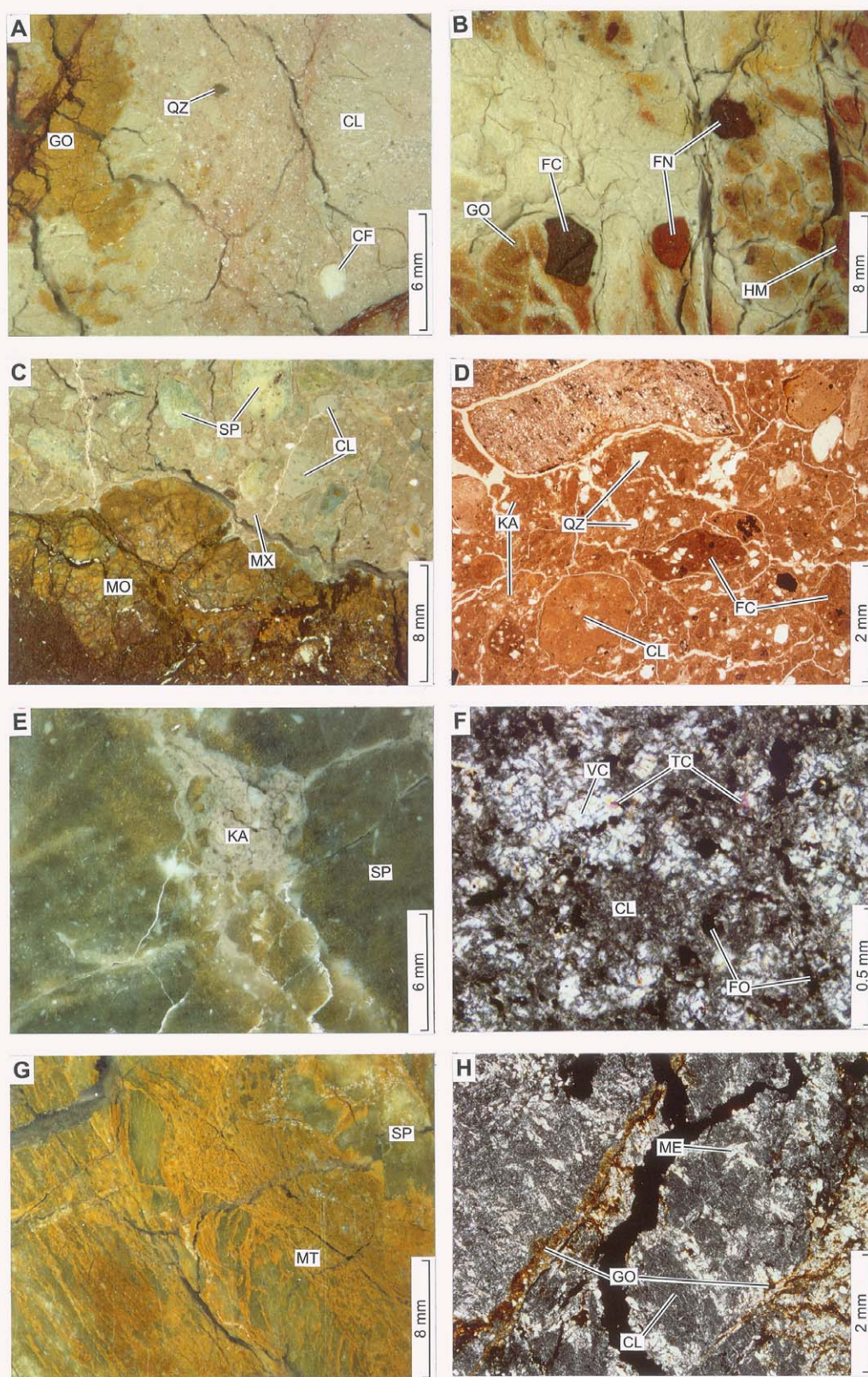


Figure 16: Petrography of samples from cored drillhole TMWRDD-1.

Mineralogy

Samples from the described atlas materials and small specimens from the diamond drilling were selected for XRD mineralogical analysis. The methods are described above.

Results

The XRD mineralogy and chemistry of the atlas materials are given in Appendix 2., Table A2.3 and have been integrated with the petrography. The XRD mineralogy of selected specimens from the diamond drilling are consolidated in Table A3.1, Appendix 3. The first eight minerals have been ordered according to their weatherability. This shows the expected concentration of easily weathered minerals, such as amphiboles, towards the base of the profile, with increasing abundance of weathering products (smectite, Fe-oxides and kaolinite) towards the top. Halite and K-halite indicate seeping ground water from the lake. The presence of muscovite and perhaps rutile below the unconformity in TMWRDD1 on a mafic-ultramafic bedrock would indicate that the major unconformity between transported and *in situ* regolith was incorrectly placed in the original logging.

Geochemistry

Half core spot samples, up to 100 mm long, were taken at selected points from the HQ diamond core to indicate chemical variations but, at the same time, preserve at least the other half core as a record. Thus, the geochemistry is not continuous. Results are given in Table A2.2, in Appendix 2. Downhole plots are provided below and as pdf files in item A2.2 of Appendix 2.

Drillhole KLHRDD-1: Lake Harris

A ternary plot of the major components (Si-Al-Fe; Figure 17A) indicates that ferruginisation is the major weathering trend in the residual part of the profile. However, it must be kept in mind that structurally and stratigraphically complex Archaean rocks were intersected and these were not necessarily originally chemically equivalent prior to weathering. Figure 18 displays the down hole log against geochemistry for this drillhole. The upper part of the residual profile is particularly rich in Ni, Co, Cu and Cr (2000-4000 ppm; 300-400 ppm; 120-170 ppm; & 4000-6000 ppm, respectively). The petrography and XRD indicate less weathering throughout the saprolite than implied by the logging and this is supported by the high Mg contents. However, the petrographic and geochemical materials represent only a small part of the logged core. The high Mg contents reflect both remnant primary minerals (clino-amphibole and chlorite) and secondary smectite. It is suggested that at least some of the residual profile is lower saprolite to saprock, as weathering, penetrating along grain fracture boundaries and consuming comparatively little of the bulk of the rock, can lead to a very friable material. High Na in the upper saprolite is correlated with Cl, implying saline water and halite (confirmed by XRD mineralogy).

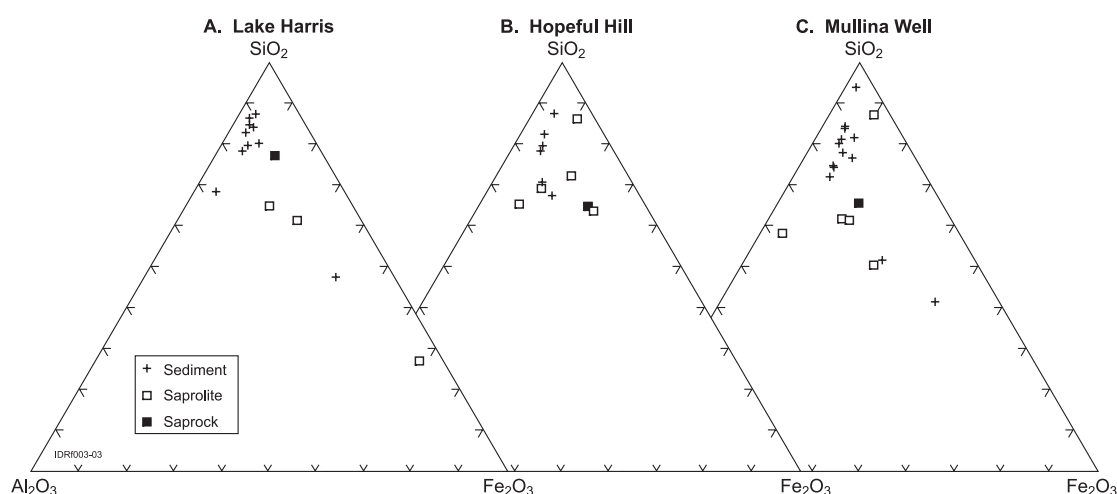


Figure 17: Ternary plots of major elements (Si, Al, Fe) for (A) the Lake Harris drillhole, (B) the Hopeful Hill drillhole and (C) the Mullina Well drillhole showing weathering trends in the weathered basement rocks and sedimentary and weathering trends in the overlying sediments.

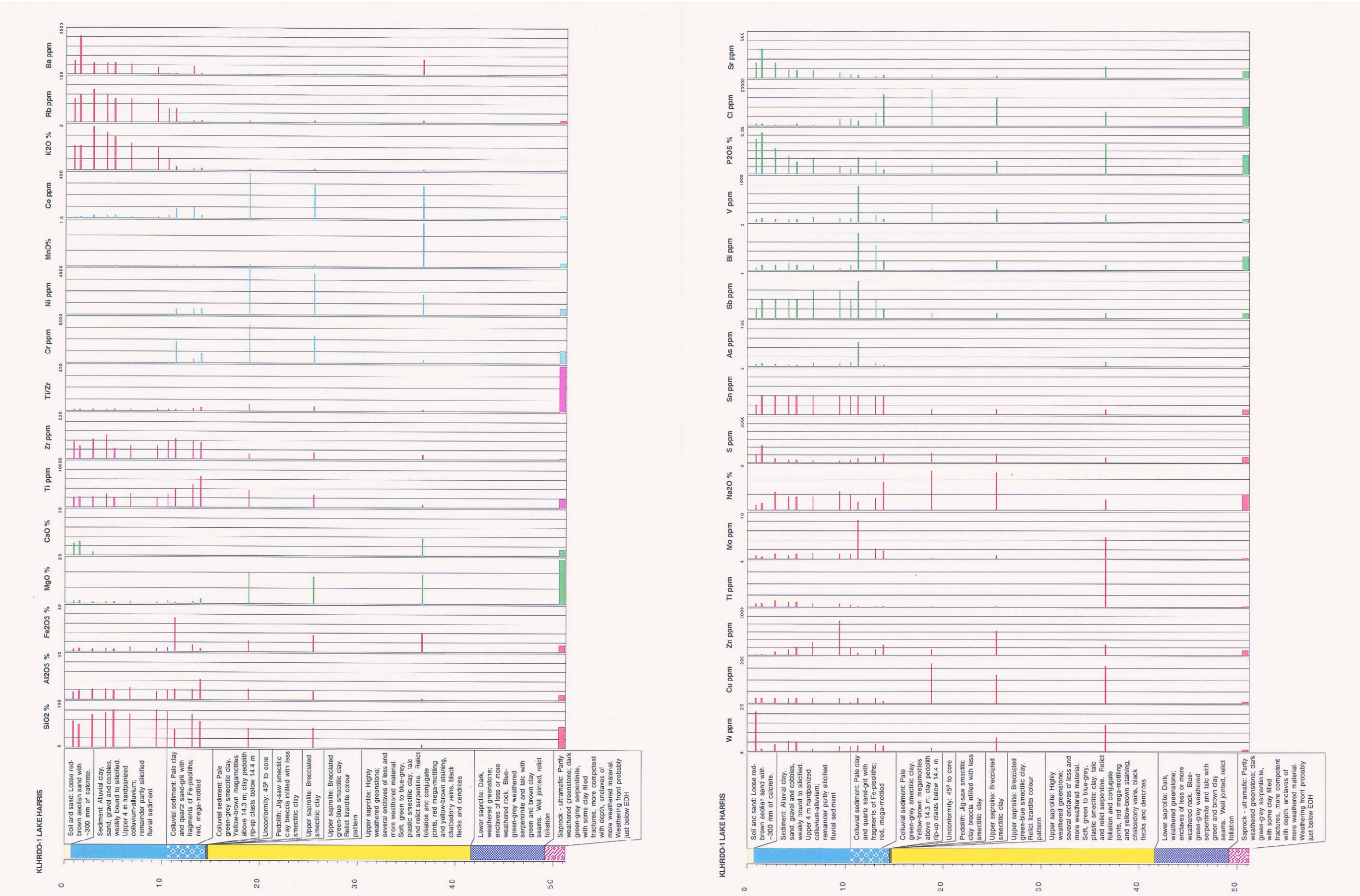


Figure 18:
Log and geochemistry of drillhole KLHRDD-1 at Lake Harris. [fold out sheet].

The sediments have a similar Si-Al spread (Figure 17A) to the other sites, due to varying sand and clay contents; one of the sediments is ferruginous. The observed increase in relatively fresh granitic detritus towards the top of the sedimentary column is supported by progressive increases in K, Rb and Ba. In contrast, the Si and Zr contents are variable but consistently high in the sediment, reflecting weathering-resistant quartz and zircon. Calcification of the top two metres is also reflected in Ca and Sr. Maxima in As, Sb, Bi and V are associated with high Fe. The clay-rich material at the base of the sedimentary column is comparatively rich in Ni, Cr and Co, suggesting at least some input from a greenstone saprolite provenance.

Drillhole THHRDD-1: Hopeful Hill

A ternary plot of the major components (Si-Al-Fe; Figure 17B) indicates that loss of Fe and possible congruent dissolution and precipitation of smectite then alteration to kaolinite as being the major weathering trends in the residual part of the profile. Figure 19 displays the down hole log against geochemistry for this drillhole. The weathered greenstones are intermediate in Cr, Co and Ni contents and low in Cu. The Mg content indicates a substantial difference in the degree of weathering between the upper and lower saprolite. However, throughout, the Ti/Zr ratio is typically basaltic.

The sediments have a similar Si-Al spread (Figure 17B) to the other sites, due to varying sand and clay contents. Core logging indicates the unconformity as being at 9.05 m, beneath the claystones. Because the clays were probably partly derived from nearby weathered ultramafics, their chemistry is equivocal. The upper part of the colluvial-alluvial sediments is rich in K and Rb. Again, Si and Zr are variable and Zr is substantially more abundant than in the underlying greenstones.

Drillhole TMWRDD-1: Mullina Well

A ternary plot of the major components (Si-Al-Fe; Figure 17C) indicates that minor ferruginisation and clay formation are the major weathering trends in the residual part of the profile. The saprock is richer in kaolinite than at the other sites. Figure 20 displays the down hole log against geochemistry for this drillhole. The Mg, Ca and Na contents decline significantly low in the profile, implying more intense weathering and the landscape position may be an important factor here. These rocks are relatively poor in Cr and Ni, implying a fractionated komatiite. These weathered greenstones are much richer in Ti, K, Rb and Ba than at the other sites although the Ti/Zr ratio is typically basaltic.

The sediments have a similar Si-Al spread (Figure 17C) to the other sites, due to varying sand and clay contents; one of the sediments is ferruginous. The upper part of the sedimentary profile is substantially calcified. Elevated levels of As, Sb, Bi and V are associated with high Fe.

Distinguishing cover from basement

Probably one of the most useful distinctions is between cover and basement. Normally, chemically distinguishing granite-derived sedimentary cover from a weathered ultramafic basement would present little difficulty. However, the lower part of the sediment at Mullina Well is clay rich and was probably at least partly derived from the weathered saprolite of mafic and ultramafic rocks. Also, the greenstones at Mullina Well are Ni- and Cr-poor. This results in some overlap of some characteristic elements. If the drillholes are considered separately, good univariate distinctions can be made. Pooling the data from the three drillholes makes the distinction more difficult. However, Zr is still able to separate the two groups at all three sites on a univariate basis (Table 13). Although this would only be useful where the basement is known to include ultramafic lithotypes.

Bivariate treatment of the pooled data shows slightly imperfect separation using K-Mg (Figure 21A) and K-Ni, both of which show independent orthogonal trends of the two fields (sediment and greenstone basement) with overlap at low values. Potassium-Sr (Figure 21B), As-Cu (Figure 21C) and Mn-Rb show broader fields with good separation. A particularly good separation is achievable using a rotated Rb-Sr-Mn plot (Figure 21D). Multivariate data analysis was not attempted, as the number of cases are too few (sediment 30, basement 16) for the number of variables (30) to be meaningful.

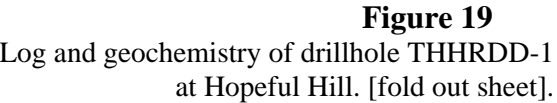




Figure 20:
Log and geochemistry of drillhole TMWRDD-1 at Mullina Well. [fold out sheet].

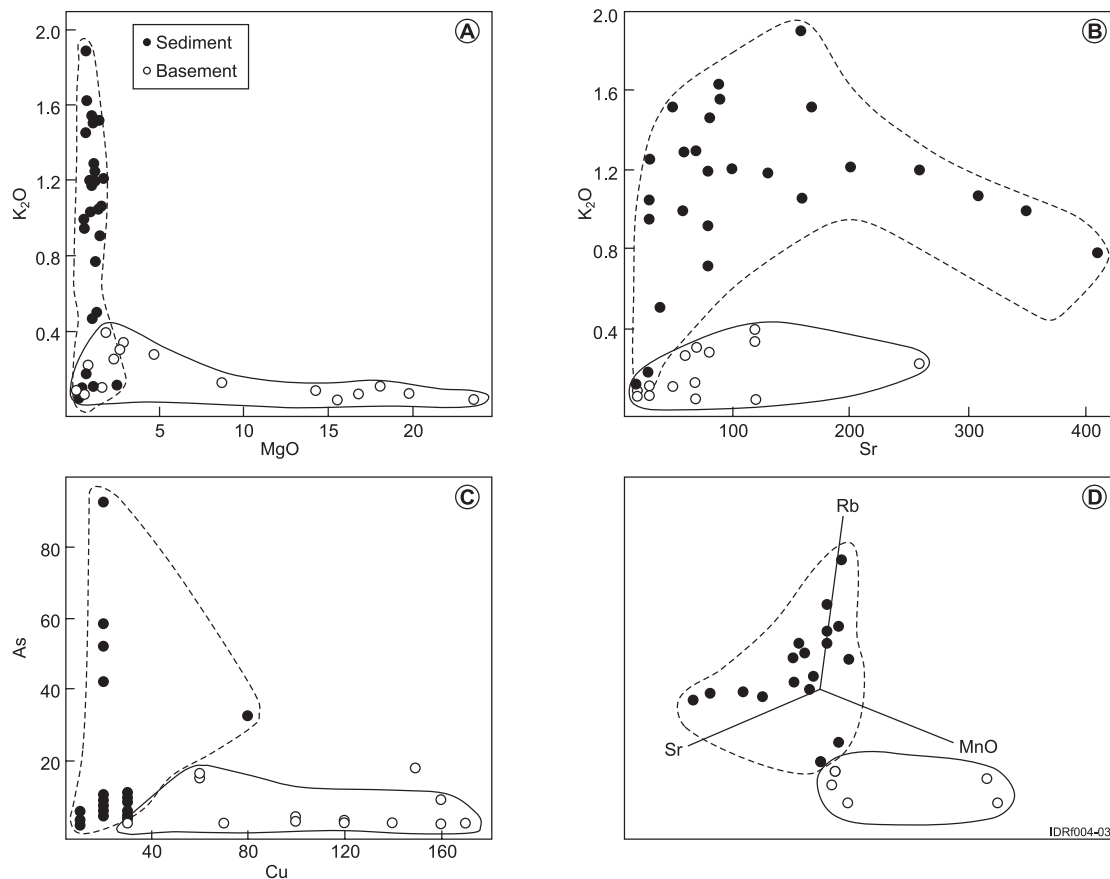


Figure 21: Bivariate plots (A-C) and a trivariate plot (D) illustrating how basement rocks may be largely distinguished geochemically from the covering sediments.

Basalt classification and prospectivity

Provided there has been minimal mobility of the generally stable elements (Ti, Zr and Al), Al/Ti-Zr/Ti plots and Ni/Ti-Ni/Cr plots might be used to determine the affinities of these mafic-ultramafic rocks (S.J. Barnes, pers. comm., 2003). The basalts from Mullina Well appear to be komatiites (Al/Ti-Zr/Ti plot; Figure 22A) and, more specifically, fractionated komatiitic basalts on the Ni/Ti-Ni/Cr plot (Figure 22B). Those greenstones from Hopeful Hill and Lake Harris appear to be komatiites (Ni/Ti-Ni/Cr plot; Figure 22B) typical of thin, differentiated flows, possibly contaminated, increasing their Ni prospectivity. Although some outlying points are probably due to Al mobility in the regolith, the quite good fit with data from fresh rocks would support the hypothesis of incomplete weathering proposed for some of the lower saprolite at the Lake Harris and Hopeful Hill sites.

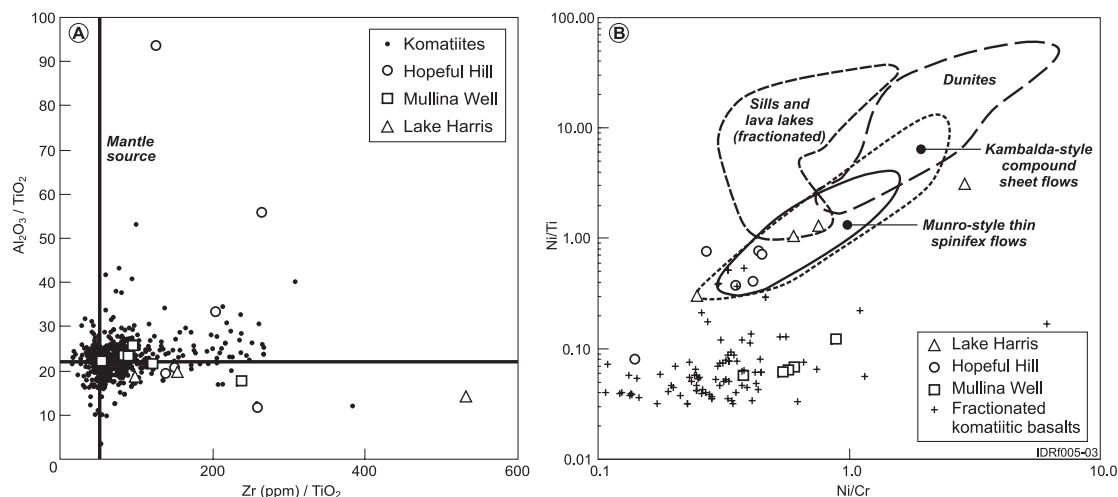


Figure 22: Bivariate ratio plots of minimally mobile elements to illustrate classification of mafic basement rocks at the two sites (after Barnes pers. com, 2003).

Table 13: Thresholds for Distinguishing Greenstones from Sediments.

MgO	<i>In situ</i> greenstones	Sediments
Lake Harris	>14%	<2.5%

K₂O	<i>In situ</i> greenstones	Sediments
Lake Harris	<0.09%	>0.09%
Hopeful Hill	<0.4%	>0.4%

Rb	<i>In situ</i> greenstones	Sediments
Hopeful Hill	<40 ppm	>40 ppm

MnO	<i>In situ</i> greenstones	Sediments
Lake Harris	>0.06%	<0.05%
Mullina Well	>0.03%	<0.03%

Ni	<i>In situ</i> greenstones	Sediments
Mullina Well	>50 ppm	<50 ppm
Hopeful Hill	>150 ppm	<60 ppm
Lake Harris	>570 ppm	<520

Zr	<i>In situ</i> greenstones	Sediments
Mullina Well	<90 ppm	>90 ppm
Hopeful Hill	<90 ppm	>90 ppm
Lake Harris	<90 ppm	>90 ppm

Key regolith zonal components

The following points draw together common themes from the three greenstone areas studied, however the regolith of the Lake Harris locality has received more attention than the other two areas and so this might bias some conclusions. Significantly, the bulk composition, fabric, foliation and weathered mineral components of the greenstones strongly contrast with the adjacent combined granite, felsic gneiss and felsic volcanic terranes.

***In Situ* – Protolith**

Protolith was penetrated in about 80% of the aircore drillholes sampling the greenstones. General characteristics are: dark grey to near black aphanitic serpentinite or serpentinized basalt, variably fractured and veined by chalcedony or hydrothermal quartz, foliated and retaining remnant primary fabrics – although these are generally difficult to see with the naked eye. The more felsic crystalline host rocks vary in colour from grey to brown-grey and brown, their fabrics range from fine- to coarse-grained to megacrystic, and most display a metamorphic fabric ranging in strength from mild to extreme – often displaying multiple overprinting from several orogenies. This zone is a good and easily interpreted sampling medium but depths range over the tested areas from shallow (about 6-12 m) to medium (about 25-40 m) to deep (about 65->80 m).

– Saprock

Variably developed, saprock ranges from <2 to about 10 m in thickness over altered meta-basalts and from <2 to about 20 m thick over altered metakomatiite. However, the profile is found to be more complex when seen in core, as the weathering is generally incomplete, leaving enclaves of saprolite and corestones of protolith within the saprock envelope. There is much less clay and more altered serpentinite in this zone but the weathered weatherable minerals form 5-20% of the bulk. Saprock is gradational with both the lower saprolite and protolith. Metamorphic foliation and relict primary fabrics are apparent. This zone has a variable hardness due to the primary lithotype, variable fracturing and weathering. Colours are generally dark green to dark olive-grey or even dark bluish green. Some Fe-staining persists along fractures.

– Saprolite

This is more highly weathered than the saprock. Greenstone **saprolite** ranges from <2 to about 56 m in thickness and in some drillholes has been much reduced by erosion (Hopeful Hill area). Two sub-zones have been recognized in this study, an upper and a lower.

The **upper saprolite** sub-zone tends to be moderately or brightly coloured in green to bluish green and red to brown. It is megamottled or stained, very clay-rich, smectitic, sticky and plastic when manually moulded and may have a greasy feel due to talc and related minerals. Remnant foliation and fabric generally occurs and chalcedony veins are abundant.

The **Lower saprolite** sub-zone is darker in green to olive green-grey or blue-green with red, yellow and brown staining and bright green to yellow-green clays filling fractures. Generally this sub-zone is stiffer or is more competent than the upper saprolite but is still highly weathered. The main components are sticky, plastic smectite, talc and relict serpentinite. Metamorphic foliation and primary fabrics remain and chalcedony veining is abundant. Saprolite colour and clay type are distinctive enough to form a useful lithotype indicator during reconnaissance drilling where depth—cost constraints are important.

– Pedolith (plasmic) zone

This zone has undergone advanced weathering. Within the greenstones the plasmic zone ranges from 0 to >8 m in thickness; it is partly eroded in all the drilling and, at a few sites, is absent. At the Lake Harris outcrop locality there are very thin ferruginous cappings preserved in a few small areas, indicating that most of the profile is preserved here. The cappings are generally unstructured Fe-accumulations with a blocky or fragmentary pedogenic fabric, but they are not full lateritic profiles. Geochemical analysis shows elevated metal contents (Ni, Cr and Mn) in these cappings (see later sections and Appendices). Where a plasmic zone is present it is comprised of dominantly fine-grained minerals, including clay minerals, variably to strongly coloured by Fe-oxides, it may be partly silicified or friable, and the clays are plastic to highly plastic when manually moulded. Some contain remnant chalcedony veining and, in natural exposure, they show evidence of overall profile collapse. This zone could be a useful sampling horizon, due to selective metal enrichment although, other metals are generally depleted (see geochemistry section). However, its value as a geochemical medium is limited by its variable preservation.

Transported Cover

Colluvium (basal to the alluvium) is generally <1- ~3 m thick, is locally derived, pale to medium coloured in browns and greys, consists of weathered polymictic lithic fragments, quartz and silty clays. It may contain chromite or Ti-Fe-spinel grains and chalcedony plates and fragments over greenstone terrain and can be silicified with variable pedogenic features like mottling and near vertical cracking preserved. It is derived from locally eroded regolith and may contain the remnants of an old lag developed on this regolith. Thus, sampling the base of this material (interface sampling) could take advantage of target enlargement by mechanical dispersion, making it a worthwhile sample medium, although anomalies in it are likely to be subtle.

There is, however, a more substantial colluvial unit revealed in the Mullina Well regolith core, the >5 m thick debris flow deposit, a bouldery to sand fragmentary material with mud infill and ranging from clast to matrix supported. It contains both weathered greenstone and felsic derived clasts. Due to recognition difficulties in drill cuttings (see above), it is not possible to estimate the extent of such deposits within the Harris Greenstone Belt cover units.

Alluvial sediments are <1- ~30 m thick, consist of clay to pebbles, rounded quartz dominated clasts, are matrix to clast supported and some carry chromite and Ti-Fe-spinel grains over or near greenstone terrain. Without a sound understanding of the palaeotopography, these would not be a good sample medium but may indicate a more localised area for further prospecting on a large tenement.

Silcrete is generally <1-3 m thick over basement but can form many thin bands within the Tertiary sediments. It is the dominant palaeo-duricrust, is generally quite hard and can yield eroded clasts that form gravel to pebbles within the sediments or lags on their surfaces or be exposed as outcrop edges in the present landscape. Some carry chromite grains and chalcedony plates or fragments over greenstone terrain where greenstones are vertically and laterally adjacent (Photo 3) and can be geochemically anomalous (see below).

Red-brown Hardpan is <1-3 m thick, strongly coloured, dominantly colluvial, matrix supported, possibly a suitable sampling medium over greenstones, where the basement is within 5 m of the surface. Any lag developed on its surface could yield useful heavy or magnetic sample media.

Calcrete is generally 0.2-0.5 m thick, as earthy to pisolithic to nodular or aggregated nodular to laminated forms, enriched in CaCO_3 , as a distinct pedogenic horizon and normally occurring within the surficial 0-1 m interval. Colours vary from off-white to pale brown or pale orange. Calcrete cements or infills voids within its host materials and therefore is diluting their bulk composition, although through evapotranspiration processes calcrete can be a zone where other mobile elements are similarly deposited. It is an easily recognized and proven soil profile sampling medium for Au, Ag and Cu but is an unproven medium for Ni or related greenstone mineralization pathfinder elements.

Aeolian sand is <1-5 m thick, is siliceous but can contain 5-20% feldspar grains, is fine- to medium-grained, mantles the terrain and therefore can obscure palaeotopography and hide basement inliers. Aeolian sand often forms low dunes that are partly stabilized by vegetation. It is loose to partly indurated by calcrete or gypcrete, has a very low organic content and rarely displays any pedogenic horizon development other than the calcrete. It is a major sample diluent but can be removed from soil samples by size fractionation (see below).

Photo 3: Part of a silcrete block (polished) from the Lake Harris greenstone outcrop area, collected near the lake shore where it forms low stony rises and a blocky capping on weathered greenstone. Angular laths of a translucent-grey-brown to greenish grey chalcedony are enclosed in a colluvial sand derived from both granitic and ultramafic source rocks. The greenstone—Glenloth Granite sheared contact lies only ~30 m from where this sample was collected in 1997. Bulk assay of a portion from this specimen revealed: Cr = 63 ppm, Ni = 6 ppm, Ti = 1.83%, V = 39 ppm and Y = 11 ppm. Sample R367509.



Description of surficial materials at Lake Harris site

Sand Cover

Red dune sand

Most of the dunes are red-brown, siliceous and only partly stabilized by grasses and small shrubs (Figure 23A). They are very lightly cemented in their upper parts and loose, with a few coarse grains concentrated in their swales (Figure 23B). Activities of rabbits, wombats and ants are very evident, implying that bioturbation of the sand is important. The red dune sand laps onto the basement as thin sandy sheets that are also partly covered by a thin, orange-brown soil with an aeolian component.

The dune sand consists of subangular to angular grains, largely of strained quartz, with lesser microcline and sericitized plagioclase. The smaller grains are angular to shardy, indicating derivation from a degraded granitic terrain. A few grains are of Fe-stained saprolite and some are granules of Fe-oxides, probably derived from weathered greenstones. There is also a trace of tourmaline and epidote. Each quartz grain has a very thin hematite-stained rim (Figure 23C, D) indicating significant residence in the regolith.

As this dune sand is a major component of soils and creek sediments in the area and has a very broad provenance, it acts as a sample diluent. Thus, it needs to be accurately defined, to facilitate the design of removal procedures. Size fractionation (dry sieving) indicated a range from 75-710 μm (Figure 23F). The coarser material (710-2000 μm and some even coarser) has probably been transported from the basement by bioturbation of the sand and concentrated in the swales by deflation. It mostly consists of quartz, much of it frosted, K-feldspar, gypsum and desiccated parts of ants. There are also small, black to dark brown lozenge-shaped granules and casts, consisting of clusters of fine dune sand, cemented by Fe-oxides, carbonates and organic materials (Figure 23E) of a probable entomological origin, possibly micro-coprolites. Oxide chemistry of the micro-coprolites is given in Table 14.

Figure 23 explanation: Surface regolith – Dune Sand and petrography.

A. Sand dunes (SD) with a veneer of dune sand (DS) lapping onto the basement (BS). 514624E 6566515N.	B. Dune sand (DS) in swale with a slight concentration of the coarse fraction (CF). 514624E 6566515N.
C. Dune sand. Reddened angular and slightly frosted quartz grains (QZ), with part of an insect carapace (IC) and a fragment of ferruginized wood (FW). 500-710 μ m fraction, 514624E 6566515N. Close up photograph of specimen R622564 in oblique reflected light.	D. Subangular grains of quartz (QZ), minor feldspar (FS) and ferruginous granules (FG), each with a thin coating of hematite (HM). Photomicrograph of specimen R622564 in plane polarized light. 514624E 6566515N.
E. A scanning electron micrograph of a small, black cluster of angular quartz grains (QZ) cemented by Fe-oxides, carbonates and organic materials (GN). Specimen R622564, 514624E 6566515N.	F. Size fraction distribution of red dune sand of Specimen R622564.
G. A gypsum crust (GC) mantled by yellow dune sand (DS), exposed by wind deflation and gypsum heave. The crust forms a roof to rabbit warrens and wombat burrows. Lake Harris (LH) in the background. 519586E 6568066N.	H. A scanning electron micrograph of the fabric of the gypsum crust showing subangular quartz grains (QZ) in a matrix of fine, crystalline gypsum (GY). Specimen R622568, 519586E 6568066N.

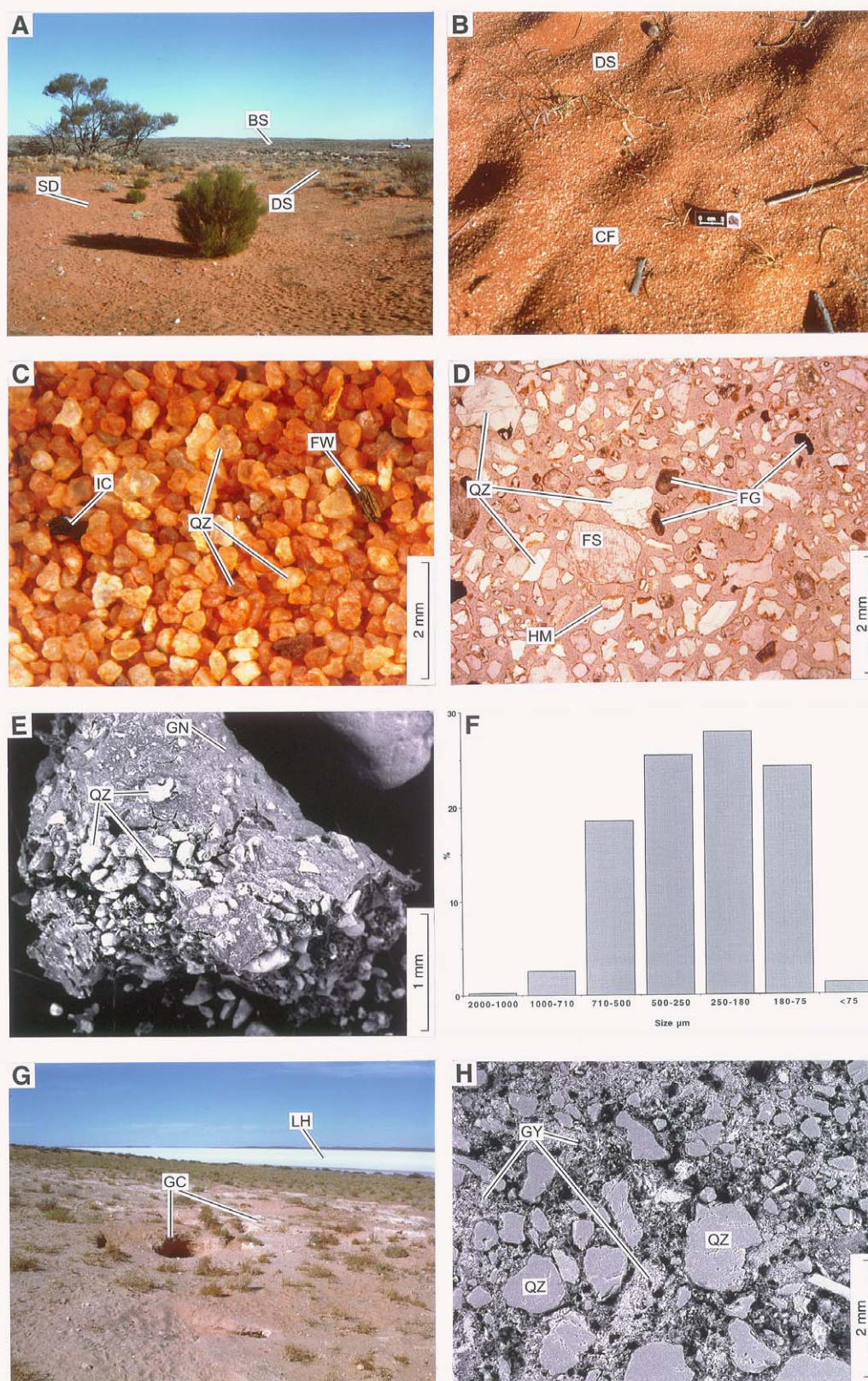


Figure 23: Surface regolith – Dune Sand and petrography.

The mineral content is largely quartz and feldspar, from the dune sand, bonded by gypsum, carbonate and organic materials. Their low Fe content, low SG and likely biological origin suggest little value as a prospecting material.

There is, however, a minute proportion of ferruginous chips within the sand, probably ferruginized clay saprolite, containing about 26% FeO, that might be worth extracting by gravity means. It would be necessary to select a coarse fraction, outside that of the normal aeolian range (>1000 or $>2000\ \mu\text{m}$), to ensure local derivation from the basement beneath the dune (by bioturbation). This could only be achieved by sieving a very large quantity of sand on site and would only be effective where the dune is thin (dune swales could be selected as sample sites). Gravity separation could be by heavy liquid, panning or jig.

Table 14: Energy Dispersive Spectroscopy Analysis of micro-coprolite ferruginous cement.

Oxide	Wt%
MgO	6.2
Al ₂ O ₃	19.6
SiO ₂	50.5
SO ₃	4.7
K ₂ O	2.0
CaO	12.4
TiO ₂	0.6
FeO	4.0
Total	100.0

Yellow dune sand and gypsum crust

Some pale dunes, on islands in Lake Harris and elsewhere, where small playas have developed, contain gypsum. In places, a gypsum crust has developed beneath a pale yellow dune sand and the hardened gypsiferous layer is favoured by rabbits and wombats as a roof for their warrens. This has been exposed by a combination of aeolian deflation and gypsum heave (Figure 23G).

The gypsum crust consists of a crumbly mass of matrix-supported grains of quartz with minor microcline and compound granules of fine-grained gypsum, weakly cemented by a mesh of crystalline gypsum and minor carbonate (Figure 23H). Many quartz and feldspar grains have red-coated rims. This material does not respond well to thin sectioning due to the hardness contrast between gypsum and quartz, despite epoxy impregnation.

The composition of the overlying yellow dune sand is similar to that of the red dune sand but it is richer in K-feldspar and the red coatings on the grains are less well developed. It consists of angular to shardy strained quartz with lesser amounts of fresh microcline and sericitized Na-plagioclase. A few of the larger grains are round and there are traces of black Fe-oxides, chert grains and very small grains of tourmaline. Most grains have an extremely thin coating of hematite or goethite. The lighter colour suggests a shorter period of stable residence in the regolith, relative to the red dune sand, due to active sand dune migration.

LAG

Lag on Gawler Range Volcanics

Outcrops of the Gawler Range Volcanics (GRV; Figure 24G) are well developed in places near the edge of Lake Harris. They are dark red-brown and partly mantled with boulders and scree. Elsewhere, the GRV is covered with an almost monomictic, very coarse lag (10-50 mm). This consists of rough, angular to partly smooth, subround, partly weathered fragments of the GRV with smaller, minor fragments of quartz and silcrete on a yellow earth (Figure 24H).

The lag consists of lava clasts containing phenocrysts and glomerocrysts (Figure 25A, B) of partly sericitized euhedral plagioclase and crystals of clinopyroxene or amphibole, (now completely altered to chlorite). This is set in a fine-grained matrix of hematite-stained chlorite, quartz and feldspar (plagioclase and microcline). The chlorite comprises lizardite and clinocllore. The weathering is to saprock stage.

Figure 24 explanation: Surface regolith – Silcretes + GRV lag, and petrography.

A. The massive, grey, rounded and jointed blocks of the upper part of the silcrete (SL) veined with pink calcrete (CC). 514681E 6566206N.	B. Pale grey-green blocks of silcrete (SL) at the top of the breakaway invaded by pink calcrete (CC), shedding a lag of silcrete and minor vein quartz (QZ). 514681E 6566206N.
C. Elongate, shardy quartz grains (QZ) set in a creamy QAZ cement (CM). Silcrete developed on granite. Specimen R622567. 513413E 6567185N. Close-up photograph of polished block in oblique reflected light.	D. Outcrop of massive silcrete (SL) containing tabular clasts of chalcedony (CH) from a pre-existing ultramafic rock. 513413E 6567185N.
E. Tabular pieces of chalcedony (CH) and grains of strained metamorphic quartz (QZ) in an opaque cement of quartz, anatase and zircon (CM). The colour differences in the cement are related to variable staining by a minute amount of goethite (GT). Specimen R622560, 513413E 6567185N. Close-up photograph of polished block in oblique reflected light.	F. Tabular pieces of chalcedonic quartz (CH) and grains of strained metamorphic quartz (QZ) in an opaque cement of quartz, anatase and zircon (CM). Specimen R622560, 513413E 6567185. Thin section photomicrograph in plane polarized light.
G. Outcrop of Gawler Range Volcanics (GV) on an island in Lake Harris (LH), shedding a brown lag (LG). 522899E 6567394N.	H. Detail of the partly weathered lag (LG) of Gawler Range Volcanics on a yellow, sandy soil (SL). 510885E 6669728N.

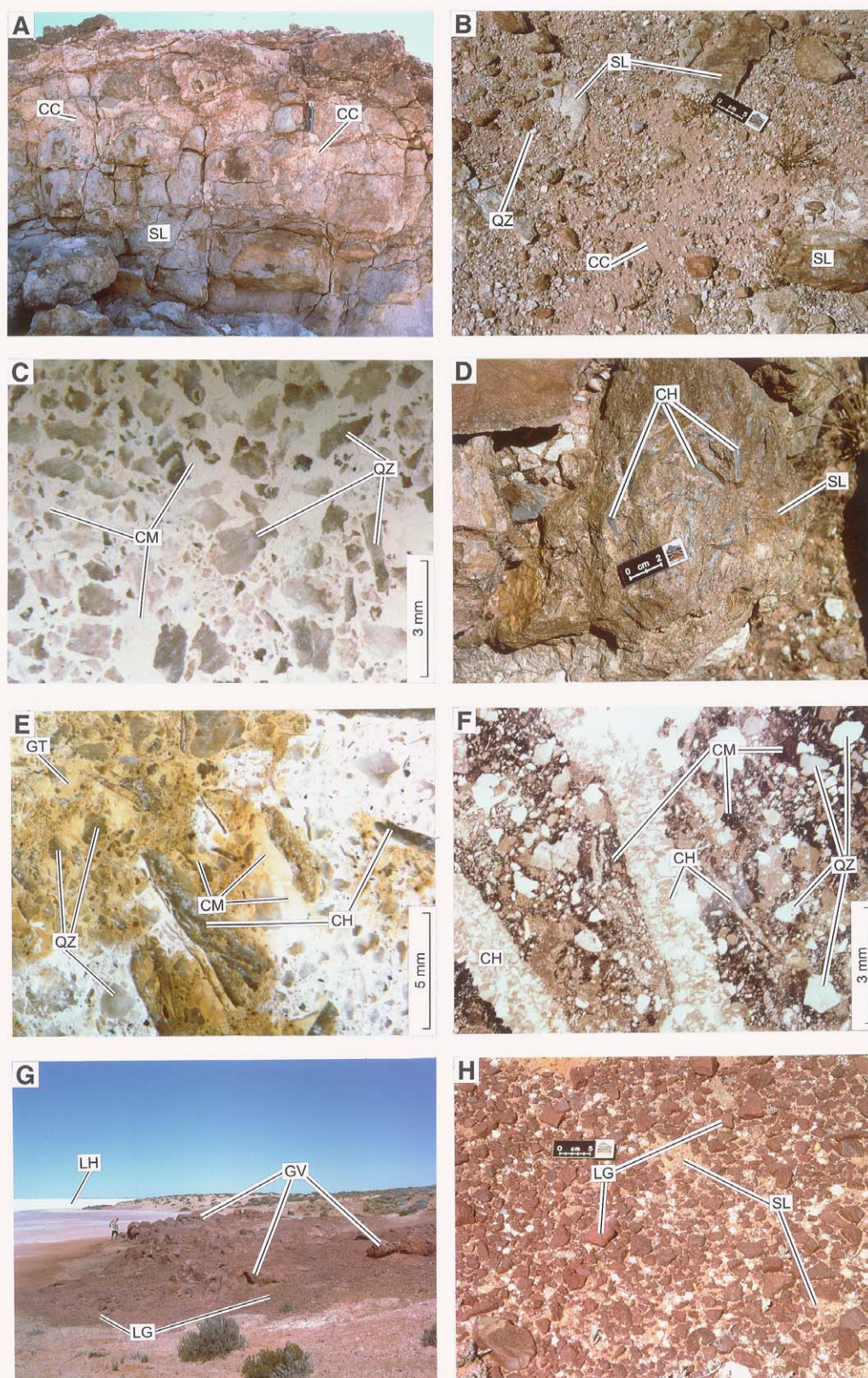


Figure 24: Surface regolith – Silcretes + GRV lag, and petrography.

Figure 25 explanation: Surface regolith – GRV lag, Silcrete lag, Ultramafic lags, and petrography.

A. Feldspar phenocryst (FP) in a fine grained pink lava matrix (MX) - Gawler Range Volcanics. Specimen R622566, 510885N 6669728N. Close-up photograph of polished block in oblique reflected light.	B. Feldspar phenocryst clusters (FP) in the fine-grained, slightly weathered matrix (MX) of the Gawler Range Volcanics. Specimen R622566, 510885N 6669728N. Thin section photomicrograph in transmitted plane polarized light.
C. Lag of yellow-green silcrete (SL) and brown ferruginous silcrete (FS) fragments with clasts of white vein quartz (QZ). 512932E 6567318N.	D. Internal structure of silcrete with shardy quartz in a white QAZ cement. Specimen R622567. 509836E 6566876N. Close-up photograph of polished block in oblique reflected light.
E. Internal structure of ferruginous silcrete lag fragment, consisting of angular fragments of vein and granitic quartz (QZ) in a variably ferruginized QAZ cement (CM). 512932E 6567318N. Close-up photograph of polished block in oblique reflected light.	F. Close-packed compound quartz grains (QZ) and shardy fragments (SF) in an opaque QAZ cement (CM). Specimen R622575, 512932E 6567318N. Thin section photomicrograph in transmitted light with crossed polarisers.
G. A coarse lag of ferruginous saprolite of an ultramafic rock, with minor vein quartz, in an erosional area. 513154E 6566977N.	H. A monomictic, lithic lag of tabular ultramafic saprolite fragments. 513012E 6566880N.

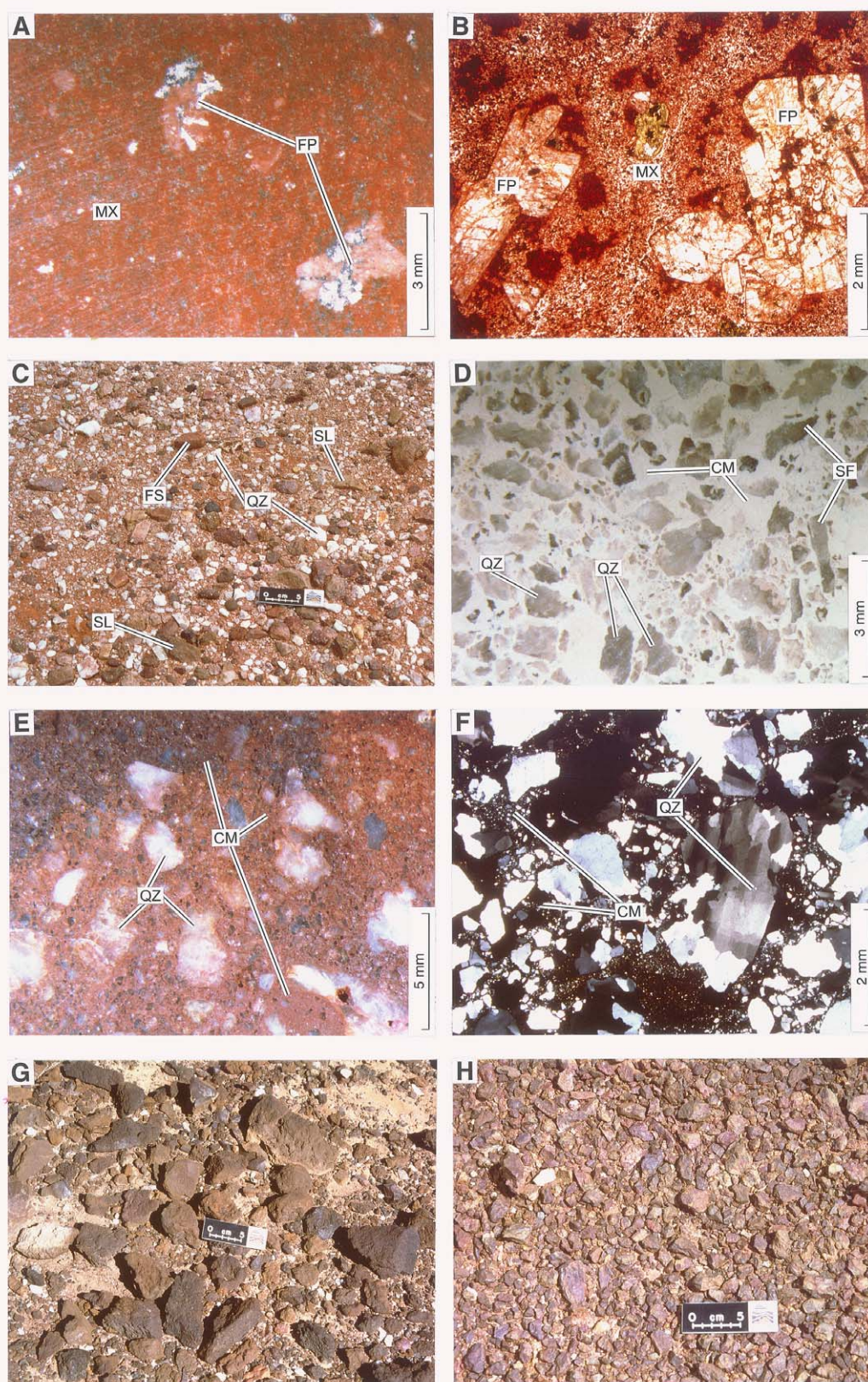


Figure 25: Surface regolith – GRV lag, Silcrete lag, Ultramafic lags, and petrography.

Lag on granite

Granitic areas are mantled by a lag of pale yellow-green to grey silcrete, white vein quartz and brown, ferruginous silcrete on an orange-brown soil (Figure 25C). Outcrops of weathered granite are rare, except where creeks have incised the regolith or close to playas, where they form breakaways.

Internally, the silcrete lag fragments consist of compound, strained, metamorphic quartz grains, with a sutured to polygonal fabric, and smaller clasts of angular to shaly, strained quartz set in a creamy but opaque, granular, QAZ (quartz-anatase-zircon) cement. Parts of the cement are slightly stained with Fe-oxides. The ferruginous silcrete is similar, but the QAZ cement has been largely replaced by hematite. Chemically the silcrete lag is almost identical to outcropping silcretes. Analyses of the silcrete lag and ferruginous silcrete lag are included in Table A2.6 (Appendix 2) for comparison and major elements are plotted in the Silcrete section below (Figure 30).

Lag on ultramafic rocks

The ultramafic rocks weather deeply and do not readily crop out. Where they do, in erosional areas, the ground is covered with large or small, dark brown fragments of ferruginous saprolite, many with faces blackened by Mn-oxides (Figure 25G). This lag is monomictic, apart from a few chips of white quartz, and consist of tabular, lithic fragments (Figure 25H). Where the ultramafic saprolites have weathered away, a characteristic lag of brown, tabular vein chalcedony fragments has accumulated (Figure 26A) and some of this has been incorporated into silcrete (see silcrete).

Elsewhere, the ultramafic rocks are almost entirely mantled by a veneer of hardpanized colluvial detritus and silcrete. Mixing of this detritus has brought small but characteristic granules of black, magnetic Fe-oxides to the surface. These round ferruginous granules are incorporated in a polymictic, coarse lag of yellow-green silcrete, white vein quartz, brown chalcedony slabs and brown ferruginous silcrete on a yellow-brown, sandy soil (Figure 25B, D). The granules consist largely of massive maghemite and hematite. A few granules have weakly differentiated thick hematite cutans. A few contain quartz clasts. They comprise porous, massive hematitic goethite, a few with a fingerprint fabric after a smectitic mafic/ultramafic saprolite (Figure 26C). This has been extensively ferruginized, with some fabric loss. Some voids are rimmed by weakly banded goethite.

The black granules are very rich in Fe (78-81% Fe_2O_3) and their ultramafic origins are shown by enrichment in Cr (1250-17200 ppm), Ni (530-640 ppm) and V (720-1200 ppm) as shown in Table A2.8. Selective sampling of this ferruginous material may be effective where the colluvial veneer is thin (<7 m). However, it has been demonstrated by Baumgartner and Neuhoﬀ (1998) over covered kimberlites in Africa that bioturbation by termites can move indicator minerals through significant transported cover (many 10's of metres). They concluded that the minerals: garnet, ilmenite, chromite and clinopyroxene, are transported to surface through thick Kalahari cover (~ 35 m aeolian sand + ~20 m of calcrete & silcrete duricrusts + ~30 m of epiclastic kimberlitic sediment), where additional concentration of grains occurs in association with the development of calcrete and silcrete. They also note that many grains would occur on the surface where only 10 m of cover existed. In the HGB regolith study, silcretes developed over the greenstones do have elevated Cr and Ni, as well as containing ultramafic sourced chalcedony fragments containing even higher Cr and Ni values, although chromite grains have not been seen in the silcrete (see later section).

GYPSUM

Gypsum is a major component of some dunes (Figure 27H). It generally forms a crust in the upper layer, providing an excellent roof for burrowing mammals (Figure 27G), making vehicle traversing of gypsiferous parts of dunes somewhat hazardous. The gypsum, here, is fine and powdery and of sand size or finer. As much of this gypsum has been transported and concentrated by aeolian action, and is likely to have been repeatedly cycled in the landscape, its isotopic chemistry would be of little help to prospecting.

Gypsum also occurs as a coarse encrustation on saprolites (Figure 28A) and in soils exposed on the edges of playas (Figure 28B), where it forms from evaporation of seeping ground waters. Here it forms plates and booklets of very coarse crystals. Although recycling of gypsum in the landscape is important here too, these evaporation sites could retain some of the soluble elements that move in the groundwater. The S isotopic composition of the gypsum here might also be a guide to sulphides within the groundwater regime.

Figure 26 explanation: Surface regolith – Lags, Calcrete, Ultramafic saprolite, and petrography.

A. A lag of tabular chalcedony (CH) fragments, a few ferruginous nodules (FN), fragments of ferruginous ultramafic saprolite (UM) and sand (SO) on deeply weathered ultramafic saprolite in an erosional area. 513154E 6566977N.	B. A polymictic lag of silcrete (SL) and vein quartz (QZ) on a transported sandy veneer (SO), with small, round granules of Fe-oxides (FN) indicating an underlying or nearby ultramafic. 513377E 6567230N.
C. Goethite pseudomorph of phyllosilicate (PH) – probably smectite – in porous goethite (GO) by ferruginization of the saprolite of an ultramafic rock. Ferruginous lag fragment. Specimen R622577, 513244E 6567375N. Polished section photomicrograph in plane polarized, normally reflected light.	D. A polymictic lag of silcrete and ferruginous silcrete (SL) and vein quartz (QZ) on a transported sandy veneer, with small, round granules of Fe-oxides (FN) indicating an underlying or nearby ultramafic. 513377E 6567230N.
E. A layer of calcrete (CC) on saprolite (SP) is intermittently exposed among stream sediments in a small creek. 511520E 6566767N.	F. Saprolite of tremolite schist (UM) coated and veined with calcrete (CC). 513082E 6566983N.
G. Pinkish calcrete (CC) permeating and partly capping silcrete (SL) on granite. 514681E 6566206N.	H. Large and small nodules and pisoliths of calcrete (CC) set, with grains of hematite-coated sand (QZ), in a matrix of hematite-coated sand cemented by younger carbonate (MX). This is veined by still younger white carbonate (WC). Specimen R622583. Thin section photomicrograph in transmitted plane polarized light. 511520E 6566767N.

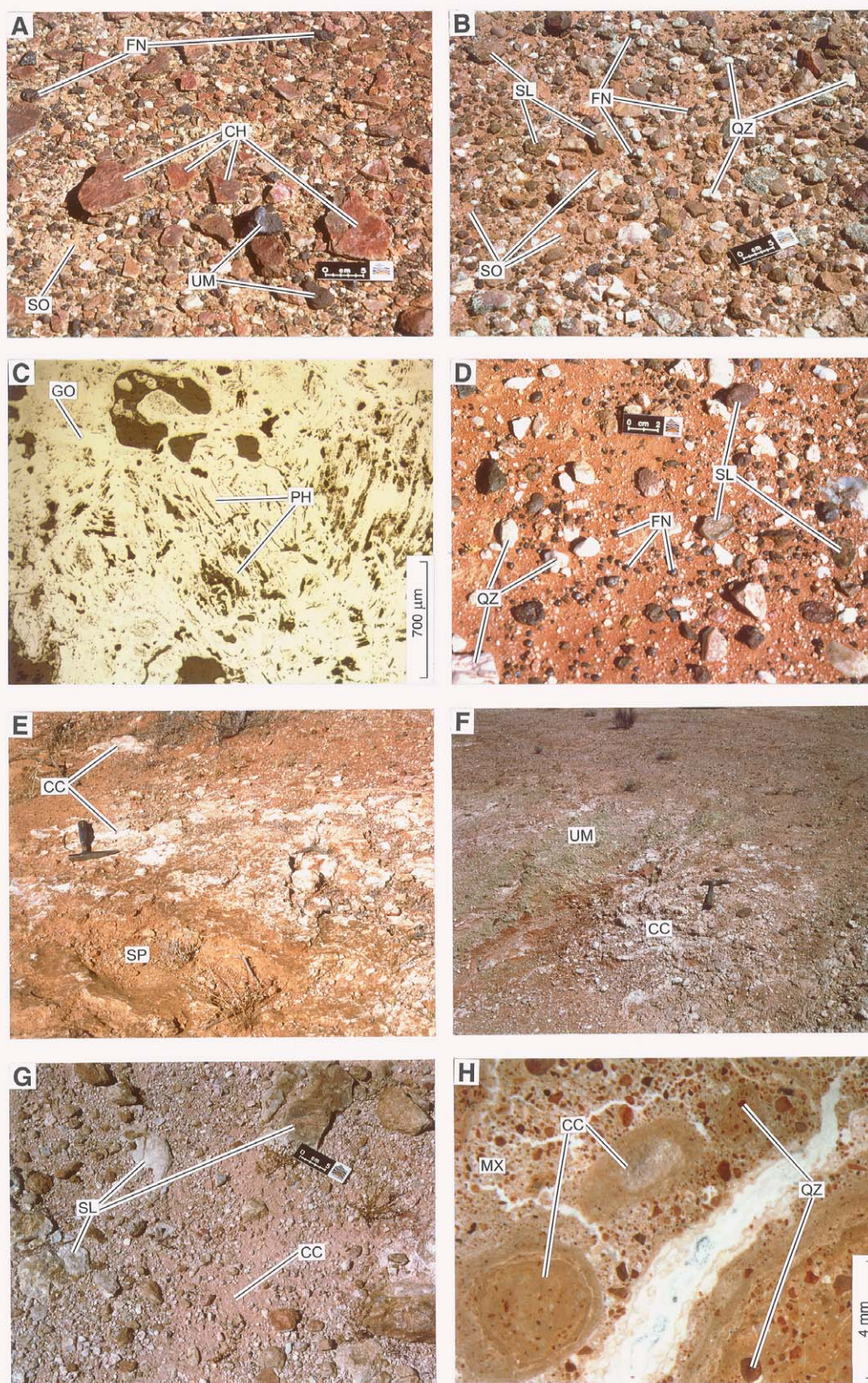


Figure 26: Surface regolith – Lags, Calcrete, Ultramafic saprolite, and petrography.

Figure 27 explanation: Surface regolith – Granite saprolite, Colluvium, Hardpan, Gypsum, and petrography.

A. Angular to subangular fresh granite vein quartz (VQ), silcrete (SL) and ferruginous silcrete (FS) clasts in a brown, quartz-rich gritty-sandy matrix (MX) with coarse bedding. 512961E 6566754N.	B. Colluvial detritus (CD) draped over granite saprolite (GS) with a gravelly lag at the base (GB). 512961E 6566754N.
C. Gravelly beds of subround to subangular vein quartz (VQ), ferruginous silcrete (FS) and silcrete clasts (SC) with laminae of calcrete (CC). 513036E 6567865N.	D. Course, angular grains of quartz (QZ) and rounded grains of granitic saprolite (GS) set in a red-brown sandy matrix (MX). Specimen R622570. 512961E 6566754N. Close-up photograph in oblique reflected light.
E. A hardpanized veneer of polymictic detritus (PD) on tremolite schist saprock (TS), overlain by a lag (LG) of both these materials. 513082E 6566983N.	F. Hardpanized detritus (HD) developed on ultramafic schist. Angular ultramafic saprolite fragments (US), a few ferruginous granules (FG) and gritty-sandy quartz clasts in a brown, silty matrix (MX). 513082E 6566983N.
G. A crust (GY) developed on a gypsum dune, excavated by rabbits and/or wombats. Island in Lake Harris (LH). 519586E 6568066N.	H. Gypsum crust (GY) on a dune (DN). Island in Lake Harris. 522771E 6567249N.

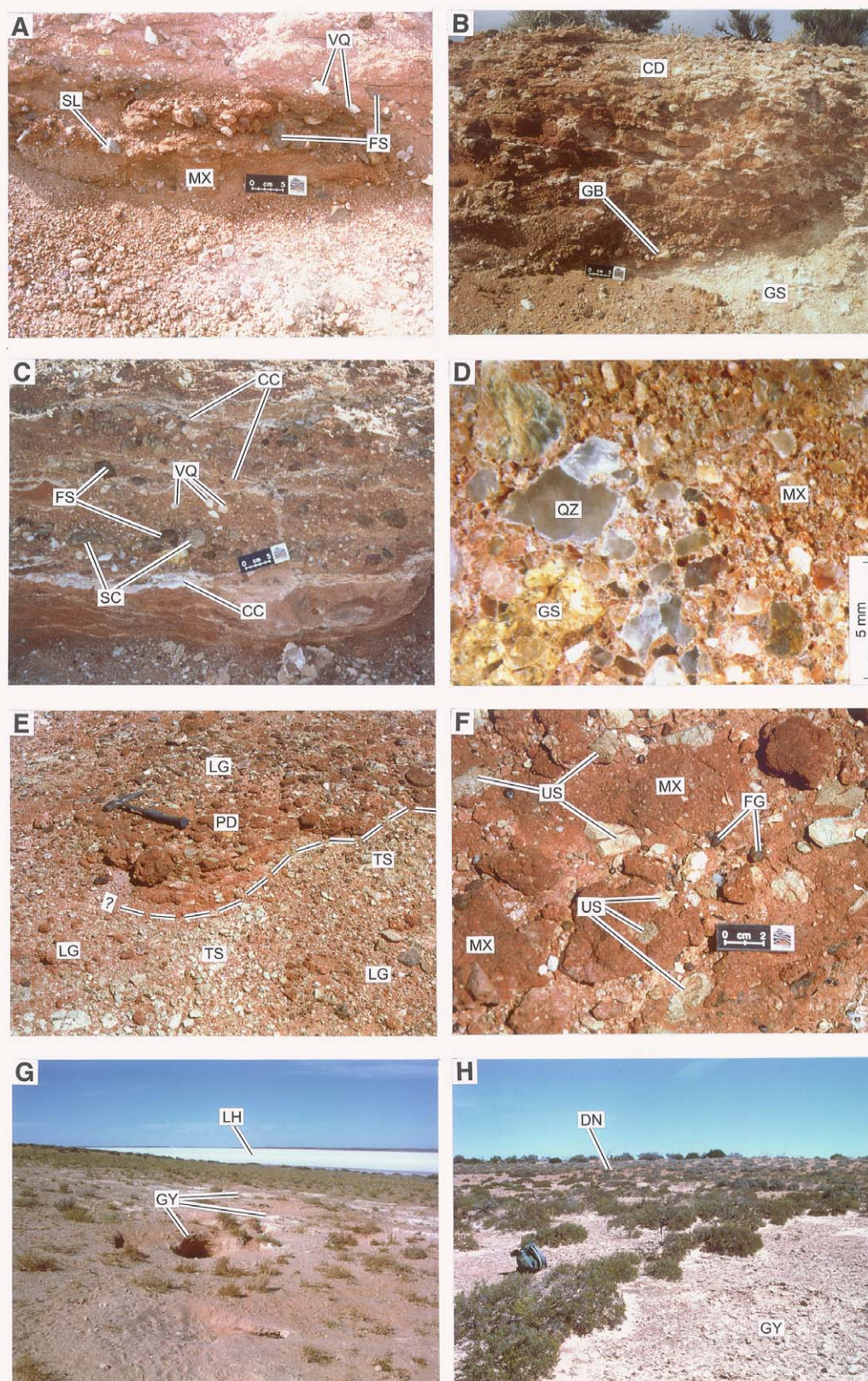


Figure 27: Surface regolith – Granite saprolite, Colluvium, Hardpan, Gypsum, and petrography.

Figure 28 explanation: Surface regolith – Gypsum, Stream sediments, Silcrete, and petrography.

A. A gypsum pod (GY), formed by evaporation of ground water seeping from granite saprolite, beneath a silcrete (SL) on the edge of Lake Harris. 508573E 6562733N.	B. Booklets of coarse, platy gypsum (GY) developed in sandy soil (SL) in a drainage entering a playa. 510837E 6569266N.
C. Size distribution in sample R406779. Stream sediment sample, Lake Harris area.	D. Size distribution in sample R406800. Stream sediment sample, Lake Harris area.
E. The magnetic component of the heavy fraction of the 1000-2000 μm fraction of specimen R406800. It consists of dark hematite- and maghemite-rich grains (HM) and a few are coated with or attached to goethite-stained clay (GC). Close-up photograph of polished block in oblique reflected light.	F. The non-magnetic component of the heavy fraction of the 1000-2000 μm fraction of specimen R406800. A wide-variety of lithic fragments including silcrete (SL), ferruginous silcrete (FS), hematite- and goethite-stained saprolite (FP), goethite nodules (GN) and various compound grains (CG). Close-up photograph of polished block in oblique reflected light.
G. A breakaway of silcrete crust (SL) on granitic saprolite (GS) near the edge of Lake Harris. The saprolite is partly covered by silcrete cobbles and gravel (SG). 514681E 6566206N.	H. The transition between silcrete and saprolite, consisting of silcrete blocks (SL) in saprolite (GS), veined with calcrete (CC). 514681E 6566206N.

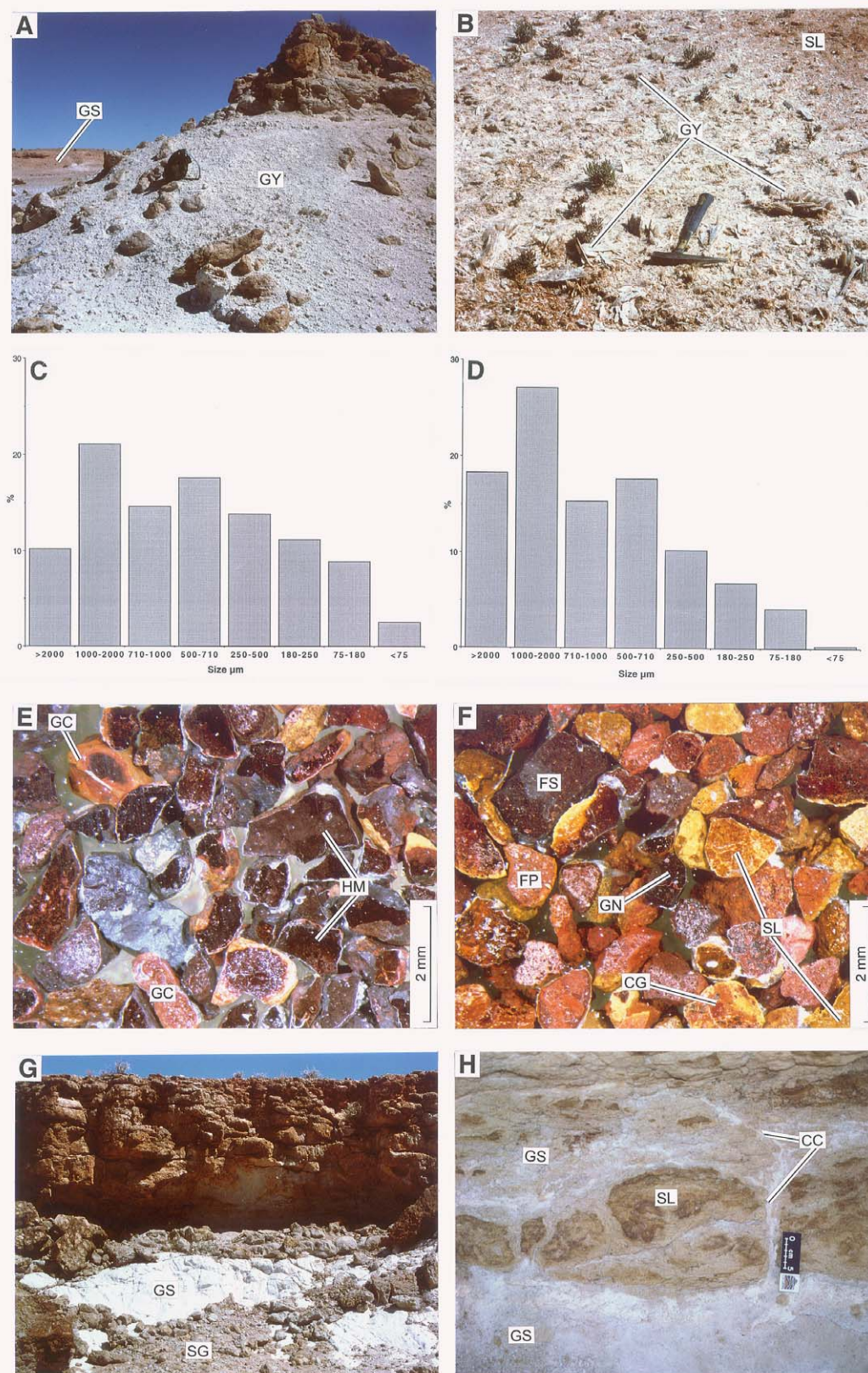


Figure 28: Surface regolith – Gypsum, Stream sediments, Silcrete, and petrography.

CREEK SEDIMENTS

The drainages are generally poorly defined in this arid region of low topographic relief, except near Lake Harris where erosion has cut back into the landscape, forming breakaways and creeks with relatively steep banks. Elsewhere in the HGB, stream channels can be difficult to define without careful on-the-ground inspection and may require judicious care with respect to the interpretation of modern or palaeolandscape drainage—flow regimes. Stream sediment prospecting is a popular prospecting method for quickly assessing large areas. Consequently, understanding the composition and provenance of stream sediments may provide guidelines to their proper use and enhancement.

The physical attributes of sediments from two streams were investigated in detail. Size fraction analysis (Table 15 and Figure 28C, D) shows that they differ from the dune sand in that they have a much more abundant coarse fraction. The coarser fractions consist of dominantly angular quartz and some K-feldspar, with minor silcrete and ferruginous silcrete, indicating fresh and weathered granite and their overlying colluvial deposits as likely provenances. The granitic materials would be expected to be largely barren of indicator elements, apart from pegmatophile elements (Ti, Nb, Sn, K, Rb, Li, Cs). Finer fractions contain a progressively increased proportion of thinly red-coated and slightly frosted quartz grains, indicating aeolian input; this is also likely to be barren. There is a very small clay fraction (probably much less than 0.5%).

However, all fractions contain a small but consistent proportion of ferruginous chips, some of which are magnetic. Heavy liquid separation (>2.85 SG) of the 1000-2000 µm fraction showed that the ferruginous material comprises about 3.5% of the whole, of which about a third is magnetic and the remainder is non-magnetic. The magnetic heavy fraction (Figure 28E) consists mostly of angular fragments of massive to porous hematite and maghemite, with some attached goethite, in which secondary fabrics dominate (dehydration cracks, coatings and void fillings). There is only a trace of relict primary fabrics after phyllosilicates (clays). In contrast, the non-magnetic fraction (Figure 28F) is much more varied. It consists of angular quartz, set in ferruginous clays, massive to porous goethite, goethite with lozenge shaped granules of hematite, goethite pisoliths in ferruginous clay and numerous goethite clasts containing fingerprint fabrics after clays. The magnetic fraction of these heavy minerals is enhanced (x 1.5-2.0) in Fe, Cr and Pb but the non-magnetic fraction is enhanced in Si, Al, Na, Ba, Co, Cu, S, Sr and Zn (Table A2.10, Appendix 2).

Magnetic extraction of the geochemically reactive ferruginous component from the stream sediments would seem to benefit the sample. Although some elements are enhanced in the magnetic heavy component, this fraction is dominated by secondary fabrics. In contrast, the non-magnetic heavy component is dominated by saprolitic fabrics, indicating a saprolitic provenance and this would be discarded by magnetic separation on its own. This indicates that the extra cost of heavy mineral separation (heavy liquid, jig or pan concentration) would be justifiable to include this important ferruginous saprolite component to enhance the stream sediment geochemistry. Separation of the non-magnetic fraction from the heavy fraction would not seem justified.

CALCRETE

Where calcrete is exposed, its basement substrate can be found with careful search, in places, but, in others, the calcrete may be thick and completely mask the substrate, or has formed in soil or transported materials. At one locality, calcrete is exposed in the floor of a small stream at 511520E 6566767N, with no indication of the substrate (Figure 26E). Thin section and XRD study shows the calcrete has formed around ferruginous kaolinite set with subrounded to subangular quartz and minor microcline. The calcrete has been invaded by many veinlets of fine-grained carbonate (Figure 26H, 29A). Thin section study reveals the substrate may be either a saprolite or recent detritus of mixed provenance. Calcrete also commonly coats, veins and permeates ultramafic rocks in the upper few metres of the residual regolith (Figure 26F) and permeates and caps silcretes on granite (Figure 26G).

Calcrete, developed in soil, consists of a matrix-supported, slightly corroded grains of quartz and minor microcline, sericitized plagioclase and chert embedded in several generations of calcite (Figure 29B). The quartz grains are red and hematite coated (Figure 26H). The calcite varies from dark brown and fine-grained to pale, slightly coarser grained and slightly banded. One clast is of very fresh quartz-plagioclase porphyry. Linear and sinuous veins of coarse carbonate cut the fabric. This calcrete appears to have formed in granite-derived detritus.

Figure 29 explanation: Surface regolith – Calcrete, Granite saprolite, Ultramafic amphibolites, and petrography.

<p>A. Compound carbonate pisoliths and nodules (CN) invaded and fragmented by a younger generation of white carbonate (WC). Specimen R622565. 511520E 6566767N. Thin section photomicrograph in transmitted plane polarized light.</p>	<p>B. Clasts of quartz (QZ) and minor microcline (MC) set in several generations of fine carbonate (CC). Specimen R622583. Thin section photomicrograph in transmitted light and crossed polarisers.</p>
<p>C. Upper part of granite profile. Blocks of granitic saprolite (GS) veined and brecciated by pink calcrete (CC). 512962E 6566754N.</p>	<p>D. Distinct coarse fabric of kaolinite from K-feldspar (KM), finer kaolinite from Na-plagioclase (KP) and stringers of metamorphic quartz (QZ) preserve the fabric of the granite. Staining in the kaolinite by Fe-oxides (GO) and slight separation of quartz grains by clay (CL) indicate advanced weathering. Specimen R622572, 512962E 6566754N. Thin section photomicrograph in transmitted light and crossed polarisers.</p>
<p>E. Outcropping pods of dark green, massive amphibolite (AP) and pale green tremolite schist (TS) intruded by grey vein quartz (QZ) and partly mantled by a red, sandy soil. 512977E 6566783N.</p>	<p>F. A fabric of magnesian amphiboles with minor albite (MA), cut by a schistosity (SH) that has been penetrated and stained by Fe-oxides and smectites. Specimen R622573, 512977E 6566783N. Thin section photomicrograph in transmitted light and crossed polarisers.</p>

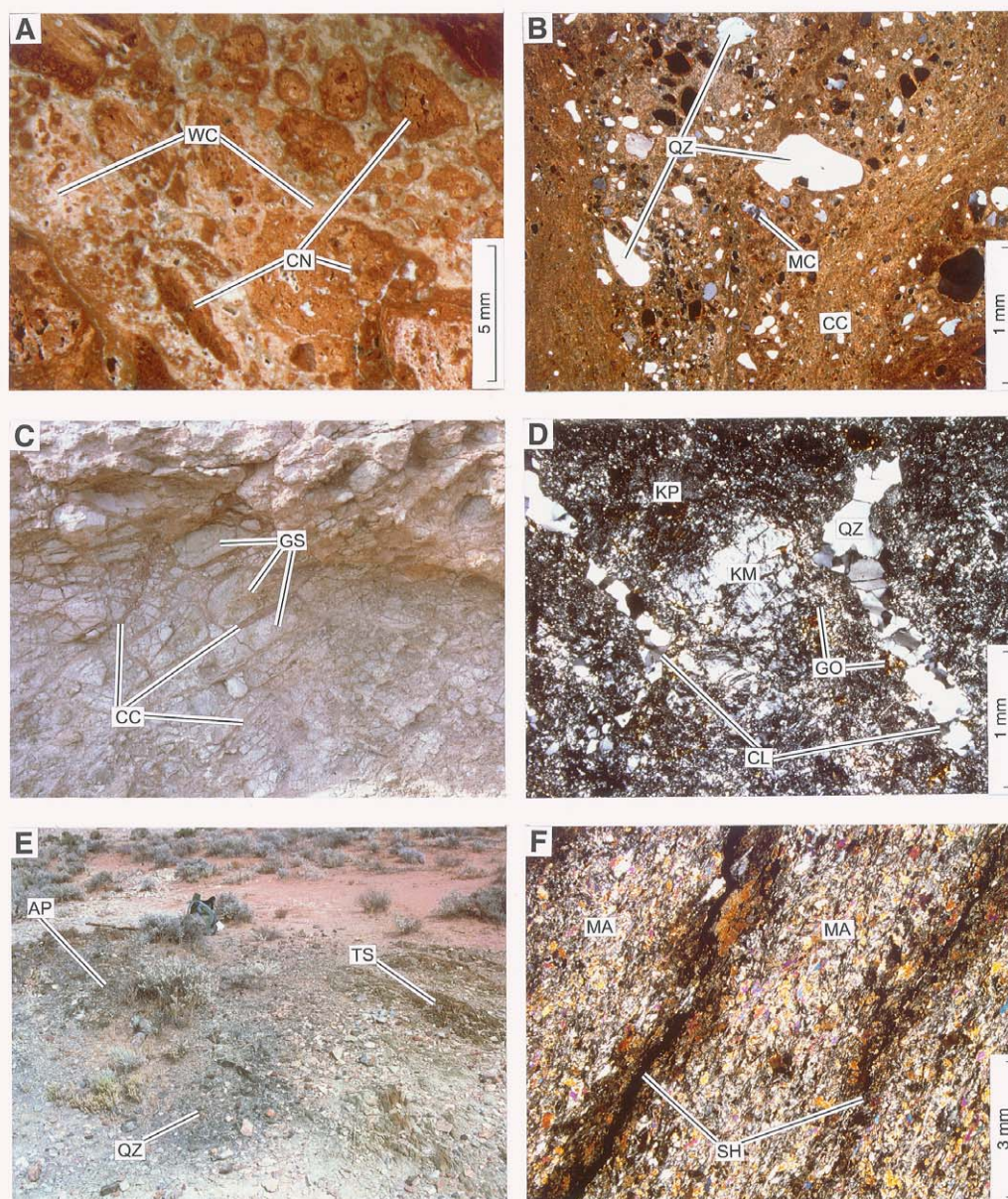


Figure 29: Surface regolith – Calcrete, Granite saprolite, Ultramafic amphibolites, and petrography.

Calcrete was confirmed as a prospecting material in this area by sampling calcrete developed in the upper metre of the regolith, exposed in costeans, pits and mine openings at the Glenloth Royal Gold Mine (~5 km S of cored drillhole KLHRDD-1). These calcretes are strongly anomalous in Au (300 ppb), Ag (4 ppm) and Ba (1500 ppm) (Table A2.7, Appendix 2). However, their Ti/Zr ratios are low (14) indicating that the enclosed lithic and mineral fragments have derived from a felsic regolith (weathered Glenloth Granite).

Table 15: Stream Sediment Size Distributions.

Sample Size in μm	R406779 Wt%	Materials
>2000	10.17	Largely angular vein quartz and large fragments of hardpanised granitic detritus. A very few pieces of ferruginous cellular material.
1000-2000	21.08	Mostly angular white quartz with a few grains of silcrete and some compound grains of hardpanised granitic detritus.
700-1000	14.61	Quartz dominates; most is clear granitic quartz but about a third is white vein quartz. Minor clasts are ferruginous silcrete and ferruginous lithic clasts.
500-710	17.63	Similar quartz content with a few cleavage flakes of microcline. Slightly ferruginous silcrete and some ferruginous lithic clasts form a very minor component.
250-500	13.84	Similar to coarser fraction.
180-250	11.22	Similar to coarser fraction.
75-108	8.93	Similar – trace of gypsum fibres and flakes
<75	2.53	Similar – very minor clay component
Sample Size in μm	R406800 Wt%	Materials
>2000	18.28	Dominant angular fragments of white quartz with lesser amount of silcrete, ferruginous silcrete and lithic ferruginous clasts and cellular ferruginous material
1000-2000	27.10	Similar to above. Dark material about 1-2%, consisting of magnetite or maghemite and some non-magnetic cellular material.
700-1000	15.38	Similar – much of the quartz is as opaque, pinkish angular grains. A few pieces of pink K-feldspar-quartz assemblage
500-710	17.70	Similar to coarser fraction - mainly degraded granite with some K-feldspar grains and quartz–K-feldspar assemblages
250-500	10.28	Similar – a few granules and chips of dark brown ferruginous material
180-250	6.84	Similar but a few quartz grains are rounded and many are reddened and frosted, indicating aeolian transport. Ferruginous chips are present
75-108	4.17	Similar but proportion of reddened grains slightly increased
<75	0.26	Similar with and a small proportion of clay and some fibres of gypsum and curled salt crystals.

SILCRETE

Small breakaways on the edge of Lake Harris expose silcretes. There are two types; i) those developed on granitic rocks (Glenloth Granite), which are rich in angular granitic quartz fragments set in a creamy quartz-anatase-zircon (QAZ) cement, and (ii) those developed from ultramafic rocks which are similar but are rich in additional tabular pieces of vein chalcedony.

On granite

On the margin of Lake Harris, the silcrete forms an amphitheatre-like breakaway, floored by granitic saprolite (Figure 28G) and edged by silcrete with a carbonate-veined silcrete breccia between (Figure 28H). The carbonate post-dates the silcrete. The upper part of the silcrete is also brecciated with calcrete (Figure 24A) and this calcrete shows on the surface, among the silcrete lag (Figure 24B). In other places, the remnants of nearly *in situ* quartz veins occur in the silcrete as linear structures of coarse, angular vein fragments, some in jig-saw fit relationships.

The silcrete consists largely of strained, metamorphic quartz set in a granular QAZ cement that has been partly replaced by a younger, brown aluminosilicate cement. Some of the larger subangular quartz grains are compound; other smaller ones are shardy and consist of single, strained crystals (Figure 24C). The cement is probably now kaolinite stained with Ti and Fe-oxides.

On Ultramafic rocks

The brown silcrete on ultramafic rocks contains numerous chalcedony veinlet fragments of sizes ranging from 2-150 mm (Figure 24D). The silcrete, which forms a discontinuous layer of blocky outcrops, overlies the saprolite of an ultramafic rock and is overlain, in part, by calcrete-cemented colluvium with silcrete fragments. The whole is capped by a lag of subangular fragments of silcrete, ferruginous silcrete and white vein quartz.

The silcrete on the ultramafic consists of clasts of slabby vein chalcedony in a matrix of angular, strained metamorphic quartz grains, cemented by quartz and anatase (Figure 24E, F). The chalcedony consists of layers of comb-textured, unstrained quartz that form layers and line voids within the chalcedony slabs, which are now largely filled with fine-grained quartz and anatase. The quartz of the matrix is very fine grained and the quartz-anatase ratio is variable.

Silcrete chemistry

The bulk chemistry of the two types of silcrete is remarkably similar in terms of their Si-Al-Fe relationships. All show evidence of Al depletion (Figure 30) at a consistently high Si/Fe ratio. A fully developed silcrete contains about 95% silica, 2.5% titania and very little else; some of the silica may be displaced by Fe-oxides, where there has been ferruginization. All are rich in Ti and Zr, reflecting their QAZ cement. Although the Ti/Zr ratio in the silcrete on the ultramafic is high (45), Ti/Zr ratios can be unreliable in the pedolith (Robertson and Butt, 1997). However, the most significant differences between silcrete on granite and ultramafic rocks lie in the trace elements (Table A2.6, Appendix 2). The silcrete developed on the ultramafic is strongly enriched in Cr (2200 ppm compared to 15 ppm on the granite), Co (10 ppm compared to 4), Ni (35 ppm compared to 2), V (115 ppm compared to 40), Zn (160 ppm compared to 1) and W (10 ppm compared to 2) and, to a lesser extent, in Mn (0.24% compared to 0.008) and Ba (425 ppm compared to 200).

The petrology and chemistry of the silcrete developed on the ultramafic rock suggests a composite origin. The tabular chalcedony fragments were probably derived by collapse of a partly silicified ultramafic saprolite. This contributed some of the Si and most of the Cr, Ni, V, Zn, Ti and Mn. This was incorporated in a soil and mixed with granite-derived colluvial detritus, which contributed more Si and most of the Zr before silicification. This observation is consistent with the location for this type of silcrete which is within about 50 m of the sheared contact between granite and ultramafic exposed along the modern creek line (refer to Regolith-Landform Map, Appendix 6).

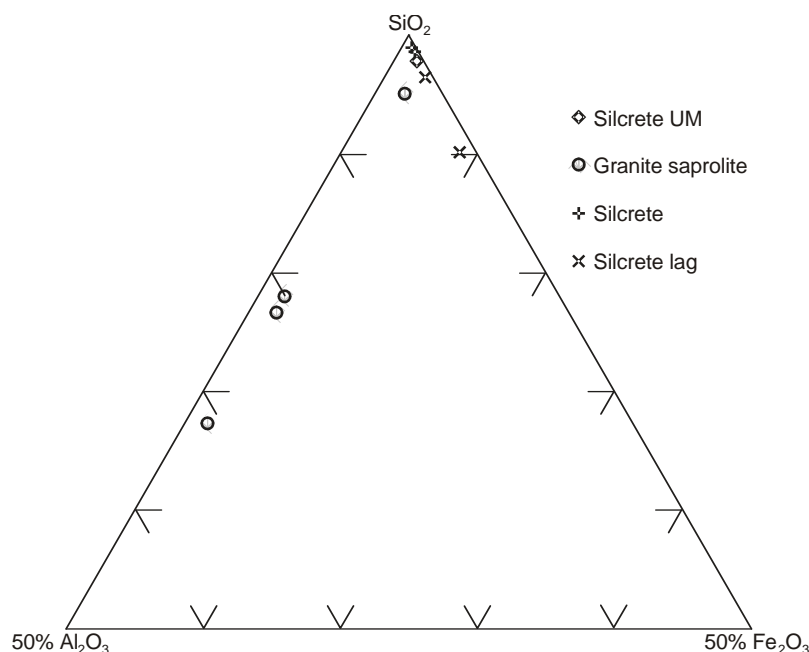


Figure 30: Ternary Si-Al-Fe diagram showing the silcretes and the weathered granites from which some of them developed. The silcrete with chalcedony fragments (silcrete UM), lying on an ultramafic saprolite, is similar. A ferruginous silcrete is similarly Al depleted but has a higher Si:Al ratio.

GRAVELLY DETRITUS

A substantial portion of the Harris Greenstone Belt is mantled by a veneer of brown, gravelly detritus beneath soil and sand. This consists of round to subangular gravel to cobble-sized clasts of silcrete, ferruginous silcrete, vein quartz and saprolite in a brown sandy-silty matrix. Some of this has been hardpanized (cemented with hyalite and Fe-oxides) and then veined and permeated by sub-horizontal laminae of calcrete. A pebbly lag lies at the base (Figure 27B) and the material fines upwards but can contain gravelly layers (Figure 27C).

Where it has been developed on a calcrete-infused granitic saprolite, the detritus is slightly hardpanized, and consists of angular silcrete, ferruginized silcrete, quartz and granite saprolite fragments in an orange-brown, gritty-sandy matrix. The upper part is permeated with calcrete and the lower part has a pebbly lag of silcrete and quartz (Figure 27A, B). In detail, it consists of a grain-supported mass of granitic detritus (strained quartz, fresh microcline, sericitized plagioclase and granitic clasts) cemented by Fe-stained kaolinite (Figure 27D).

Where developed on meta-ultramafics (Figure 27E), it is similar but the saprolite fragments are pale green and clay rich (Figure 27F). On ultramafics, ferruginous granules occur as well. In detail, this material is a polymictic, matrix-supported sediment. It consists of compound clasts of strained, sutured quartz, microcline, sericitized plagioclase, fresh granite, Fe-oxide granules and weathered magnesian schist (hornblende, anthophyllite and plagioclase slightly stained with goethite) set in a matrix of Fe-stained kaolinite and montmorillonite. Input to this sediment has been from various lithologies (granite and greenstones) and from various parts of the weathered profile, from fresh to deeply weathered.

SAPROLITE AND SAPROCK

On granite

Granite saprolite is exposed in the white, lower part of breakaways on the edge of Lake Harris (Figure 28G), or occurs where creeks have incised the regolith beneath a silcrete crust. Although feldspars have been completely replaced by white kaolinite, the granitic fabric, any gneissic structures and the form of the quartz grains and clusters are retained.

In detail, parts consist of fibrous to flaky kaolinite, probably after K-feldspar, partly stained and cemented by aluminosilicate that forms delicate bands in voids. Set in this are angular to subangular grains of strained quartz. Other parts consist of fine kaolinite with a few flakes of hydromuscovite, probably after Na-plagioclase, also set with strained, metamorphic quartz. The whole has been lightly stained by a brown, titaniferous material. XRD indicates significant halite, lost in sectioning, probably reflecting the salinity of seeping and evaporating ground water.

Where silcrete has been eroded from the upper part of the profile, the granitic saprolite is veined and brecciated by calcrete. Here, blocks of greenish-grey granitic saprolite is cut and surrounded by linear to meandering, light-brown carbonate veinlets (Figure 29C).

In detail, this saprolite consists of patches and sinuous lenses of fresh, strained quartz, with a sutured to granoblastic polygonal structure (Figure 29D). These are set in a mass of flaky kaolinite and hydromuscovite (after Na-plagioclase) and worm-like kaolinite probably after microcline. The boundaries between the types of kaolinite are blurred, suggesting some recrystallisation of clays. The whole has been veined with granular carbonate. In other places, the fabric is similar but the two types of kaolinite are very distinct. The XRD also indicates significant halite.

On ultramafic rocks

A particularly green ultramafic saprolite occurs at surface where the cover has been locally removed. This is overlain by a red-brown hardpan, containing angular clasts of ultramafic saprolite. Both the saprolite and the hardpan have been coated and veined by calcrete. A lag of silcrete, ferruginous silcrete, vein chalcedony slabs, vein quartz and brown, ferruginous nodules mantle all this (Figure 27E, F). Where erosion has incised the regolith to saprock, this is clearly recognizable where it crops out as pods of massive dark-green hornblende amphibolite and schistose, pale-green tremolite schist. It has been intruded by granite and grey vein quartz, near the southern contact of the Harris Greenstone Belt, close to Lake Harris. These low outcrops are partly mantled by an orange, sandy soil (Figure 27E).

The pale-green amphibolite has a schistose fabric of flaky magnesian hornblende and finer magnesian anthophyllite with patches of albite. This is cut by fractures along which weathering has penetrated, altering the ferromagnesian minerals to smectite (nontronite) stained with Fe-oxides (Figure 29F).

Chemistry

The saprock has retained some of its silicate Ca and Mg (8% CaO and 11% MgO). These elements have been almost entirely leached in the saprolite (all <1%), leaving a regolith also poor in Si and Al but rich in Fe (46-70% Fe₂O₃; Table A2.9, Appendix 2). Despite these changes, high Cr and Ni contents are retained.

Soil Geochemistry

A large number of elements (Table A2.1, Appendix 2) have been analysed largely to establish background levels. A few were consistently, or almost consistently, below detection; these have not been considered further (Ag, Cd, Sn and Te). To determine the most useful elements, minima, maxima, means and the maximum/mean ratios were calculated (see Table A2.5, Appendix 2). Elements selected for further processing are shown in bold in this table. A log-log plot of the mean and ranges of these elements, which show anomalies with contrasts close to an order of magnitude, is shown in Figure 31.

These data are presented as dot maps (Appendix 2) showing the upper and lower soil samples separately. Higher values are encountered in the deeper samples for some elements (As, Au, Bi, Ca, Cu, Mg and U). High Ca is related to a calcrete layer. The reverse is true for Fe, Mn and Cr, due to surface lag accumulations by aeolian deflation, particularly over the exposed basement. As upper and lower samples were not collected at every site, it is difficult to determine if one or the other medium resulted in improved background to anomaly contrasts, though this is likely. All komatiite lithology-indicating elements (Mg, Cr, Ni, As, Co, Fe, Mn and V) are elevated over exposed basement or where basement is mantled by thin cover (e.g. Figure 32 and Table A2.3, Appendix 2). Mineralization-related elements (Au, Bi, Cu, Pb and W) are elevated here too (e.g. Figure 33), indicating prospective ground. The stream sediment samples (6) do not indicate anything significant as their catchments drain covered terrain. Zinc data are all close to background.

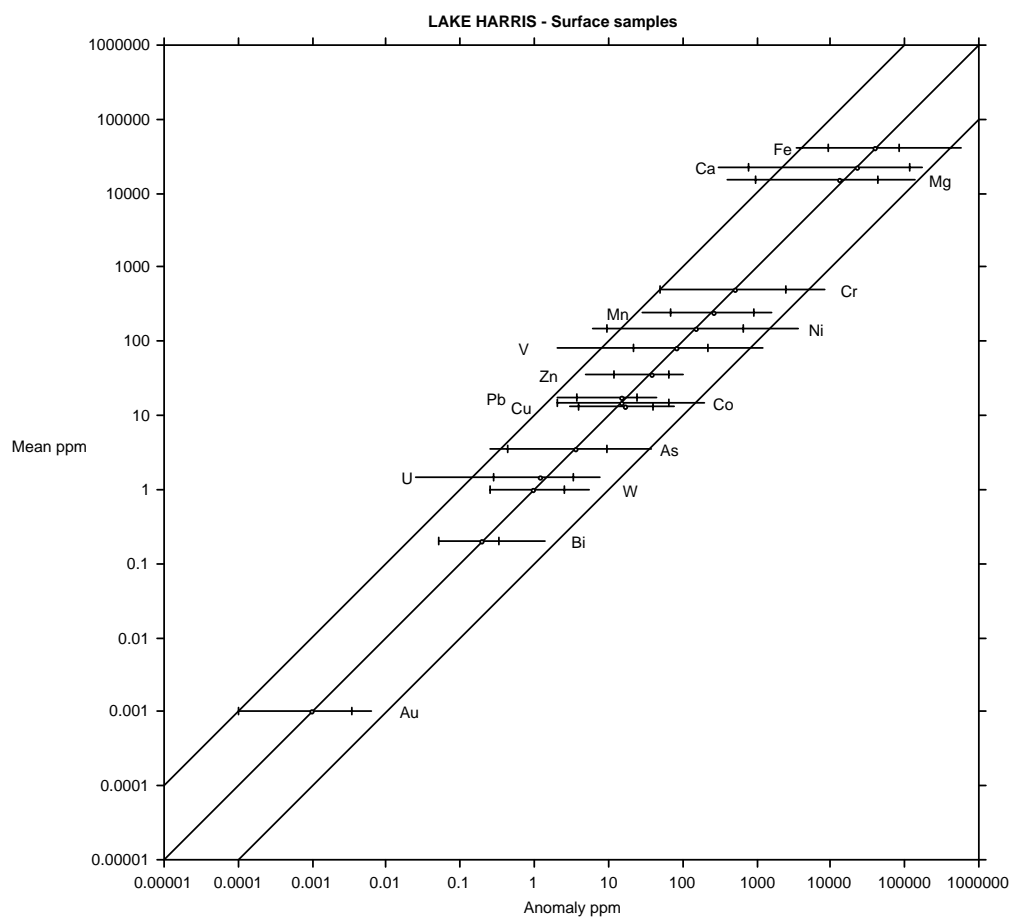


Figure 31: A log-log plot of ranges against means of anomalous elements (As, Fe, Mg, Cr, Ni, V and Co) indicate exposed komatiitic lithologies elsewhere covered by transported overburden with a largely granitic provenance.

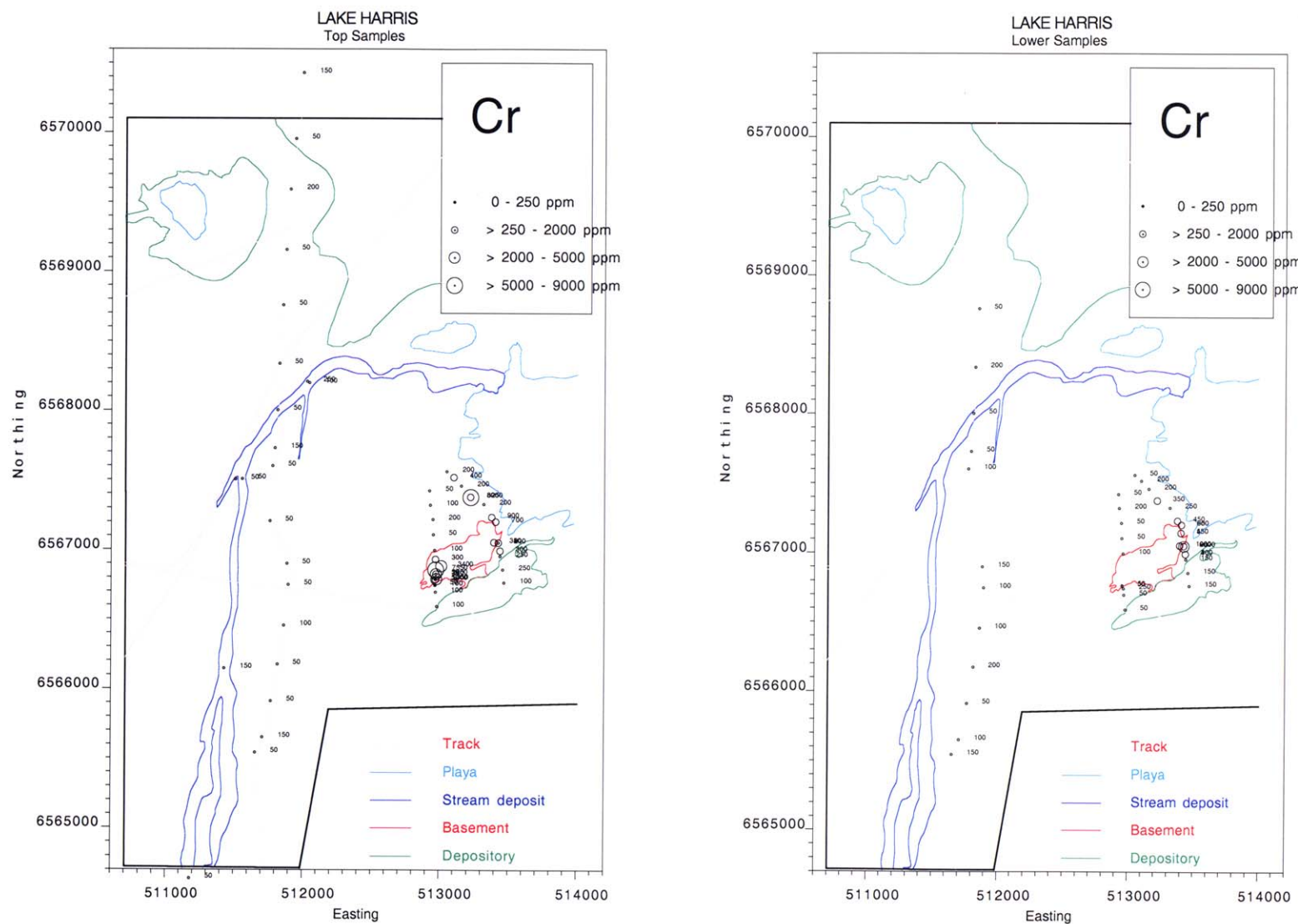


Figure 32: Chromium content of soil samples at Lake Harris showing both the upper (20-150 mm) and lower (200-250 mm) media in relation to major geomorphic units.

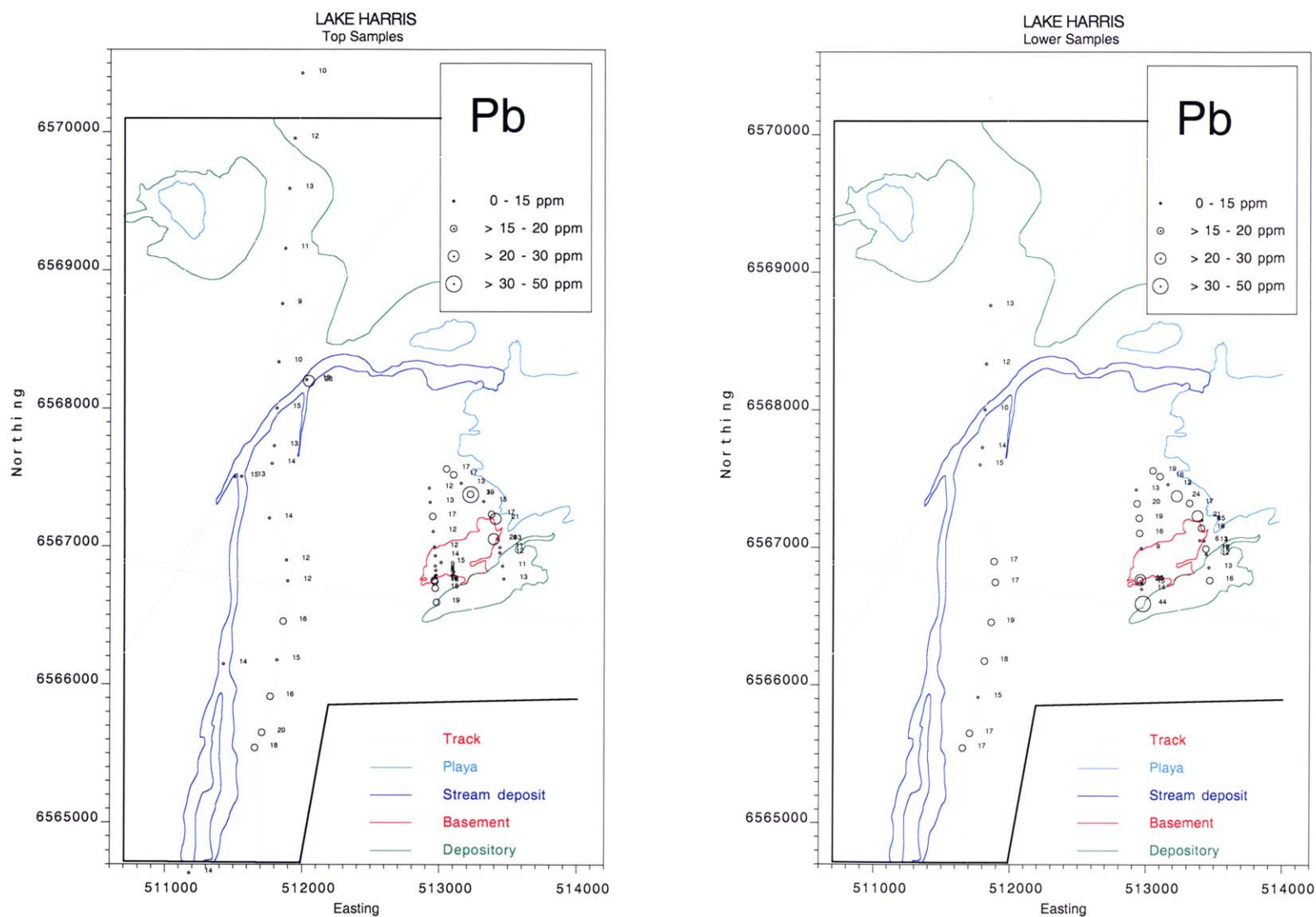


Figure 33: Lead content of soil samples at Lake Harris showing both the upper (20-150 mm) and lower (200-250 mm) media in relation to major geomorphic units.

Regolith-Landform Map and Explanatory Notes

Only a few areas of the Gawler Craton, within the Christie Domain, have been regolith mapped relatively recently (Craig and Wilford, 1997; Wilford *et al.*, 1997; Craig, 2001). They used mapping methods and formats adopted by Geoscience Australia (RTMAP) that had been used widely elsewhere in the eastern and western parts of Australia. However, these particular Gawler Craton maps have met with very limited uptake by the exploration industry. Suggested reasons from exploration company people and others for this include the following:

- Transported cover on deeply weathered basement in South Australia is particularly thick and varied, obscuring the basement. This needs emphasis.
- Some outcrop patterns are hidden or disguised by the choice of map units, colour schemes, overprints and map unit—polygon tag complexity.
- The polygon tagging is cumbersome without constant reference to the key and needs simplification.
- 3D information is lacking (depth of transported cover and/or depth to unweathered basement), despite abundant exploration drilling since the 1980's.
- Cross-sections, block models or regolith unit relationships diagrams would aid understanding and interpretation.
- On the other hand, an improved understanding of regolith terminology by the exploration industry would improve acceptance and uptake of regolith mapping in general.

Thus, it was decided, in late 2001, to revisit the earlier and highly practical approach to regolith mapping developed by CSIRO Exploration and Mining for the Yilgarn Craton (Anand *et al.* 1993a, b) *i.e.* the 'RED scheme' (Relict-Erosional-Depositional).

The original RED scheme, was modified for this project's use to better fit regolith presentation on the Gawler Craton by incorporating aspects from other regolith mapping methods. A later Regolith-Landforms scheme of mapping (RTMAP), as used by Craig (1996a and b) for AMIRA Project 409, was compared with similar more recent work over parts of the Gawler Craton (Craig and Wilford, 1997; Craig, 2001). Alternative regolith-landform presentations were considered, such as: the 'resource inventory' approach of Marnham *et al.* (2000) and the 'regolith exploration' approach of Taylor and Joyce (1997a, b) and Taylor (1997, 1999). Useful elements from all of these were considered and tempered with feedback from Gawler Craton explorationists to improve map readability and ease of use. The list of regolith mapping deficiencies (above) was also taken into consideration. A revised RED scheme resulted and this is set out in Table 16 as a trial system.

An **important difference** from the original RED scheme, is the changed use of the term **relict**. Herein, it implies neither a residual Fe-cemented weathered rock, nor a lateritic profile. The term relict, used on the accompanying Map (Appendix 6), means "*remnant basement (fresh or weathered) lying within a broader area of younger, transported cover*". The Gawler Craton generally lacks ferruginous cappings, ferricretes and complete lateritic profiles, as defined for the Yilgarn Craton where the term relict has become synonymous with lateritic profiles. However, in South Australia and in particular on the Gawler Craton, the dominant duricrust is Tertiary silcrete, generally of three separate generations. Each successive siliceous input has overprinted any earlier silcrete to form a major duricrust of increased internal complexity (Benbow *et al.*, 1995b; Lintern and Sheard 1999; Mason and Mason, 1998). Worrall and Clarke (2004) have suggested that, during the Tertiary, highly acidic groundwaters stripped Fe out of the weathered zone and redeposited it further down the flow path into zones that have been termed laterites on the Yilgarn Craton. At the same time, on the Gawler Craton, Fe released by weathering was almost totally removed in the acidic ground- and surface-water, and discharged into the sea. Conditions in the Gawler Craton subsurface appear to have been of a sufficiently low pH, to strip out Fe and a significant amount of silica. The silica was mobilised and re-precipitated in porous media to form silcrete. These siliceous profiles are commonly overlain or impregnated by Quaternary calcrete and, to a lesser degree, by gypcrete, that further complicate these duricrusts.

In exploration, it is important to distinguish basement (weathered or fresh) from transported cover. It is not easy for new fieldworkers to make this important field distinction in the Gawler Craton regolith. This important distinction has not been made by many explorationists during the last decade, with consequent poor interpretation of geochemical anomalies. The many broad scale or regional Au-in-calcrete anomaly

maps covering large areas of the Gawler Craton, produced in the late 1990s to 2001, are an example. Many lack this provenance distinction or any data from which it could be drawn at a later stage. This led to costly drilling of largely false anomalies on inliers of weathered basement with inherently higher Au backgrounds than those of transported cover with inherently lower Au backgrounds. Data from these contrasted regimes require separate analytical and interpretive treatment and the data should *never* be pooled for analysis.

Table 16: Regolith Landform Map unit symbol notation.

Landscape Class	Brief Explanation and Notation
Relict	<p><i>In situ</i> fresh or weathered basement remnant as a resistive inlier within a broader area dominated by near surface younger transported cover or erosional terrain.</p> <p>┌ Landscape Class</p> <p>RfvP</p> <p>└┐ Regolith Zone (P = Protolith, S = Saprolith).</p> <p>└┐ Lithotype (fv = felsic volcanic, g = granite, uv = ultramafic volcanic).</p>
Erosional	<p>Terrain where erosion is the dominant landscape modifying component, can include currently eroding weathered <i>in situ</i> crystalline basement and/or transported cover deposits.</p> <p>┌ Landscape Class</p> <p>EgS</p> <p>└┐ Regolith Zone (P = Protolith, S = Saprolith) or where sedimentary (unit's name abbreviation [hp = hardpan] or a sequential number).</p> <p>└┐ Unit's gross descriptor (f = felsic volcanic, g = granite, u = ultramafic, a = alluvium, and a dash [-] = complex landform or provenance).</p>
Depositional	<p>Terrain where deposition dominates over other geological processes.</p> <p>┌ Landscape Class</p> <p>Dahp</p> <p>└┐ Unit's name abbreviation or sequential number (hp = hardpan).</p> <p>└┐ Unit's gross descriptor (a = alluvial, e = aeolian, l = lacustrine).</p>

The mapping component of this regolith study aimed to achieve a simple, practical map notation to highlight the essential aspects of the modified RED scheme. Bold colours were used to highlight outcropping basement. Full colours represent relatively unweathered rocks (protolith) and equivalent half tones for exposed weathered and eroding equivalents (pedolith, saprolith, etc). Overprints are added for significant duricrust (silcrete, calcrete and gypcrete) for simplicity. Blues depict alluvial deposits, yellows aeolian deposits and lacustrine deposits are in grey. Complex, dominantly erosional landforms are depicted in shades of green. There are commonly mosaics of distinct landforms that can have overlapping units with differing provenance (*i.e.* , E-3 on Dahp, or De-1 on E-3, or DI-2 + Da-1). These mosaics are generally too complex for each distinct component to be expressed individually at 1:10 000 scale and so are represented by stacked or piggy-back tags (*i.e.* E-3/Dahp). Where such tags are used in areas of very thin cover, such as thin aeolian sand on a known substrate (*i.e.* De-1/RfvP) then the substrate colour is used, although the polygon tag displays the actuality. This unit colour precedence protocol follows a long-established PIRSA cartographic practice, and Taylor (1997, 1999) provides a detailed account of this for the Victorian Geological Survey.

The area mapped (about 5 x 12 km) was selected to cover the widest variety of regolith at the chosen scale for the Lake Harris area where at least some of the Greenstone Belt crops out. It covers areas of weathered greenstone, adjoining granitic and felsic volcanic basement, erosional terrain and several varieties of transported cover. Topographic relief for this area is generally subdued (<15 m) except for the two islands in Lake Harris where relief is >20 m above the lake floor. The higher ground to the north and west rises >60 m above the lakes. Portions of the digital air photograph have been included on the Map periphery as an additional landscape reference.

The Lake Harris Regolith Landform Map (Sheard and Robertson, 2003; Appendix 6) contains 26 units that include 4 relict, 8 erosional, 10 depositional and 7 induration modifiers. A text-only copy of the map symbol reference is provided in Table 17 and displays unit descriptions that summarise all rock types, regolith zones, mineralogy, fabric and granularity, landforms, likely substrates and vegetation. Detailed descriptions of these are given in this text (previous sections). Of these units, the erosional set consists of 3 weathered basement lithotypes, 1 colluvial-alluvial unit, and 4 complex landforms. Thicknesses of transported cover are taken from drilling, outcrop or terrain incisions and soil sampling pits. A series of soil pit traverses are depicted on the map; they form two geochemical traverses N and E of DME Benchmark 1457, and one along the line of drilling. Depths to unweathered basement are also shown along the drill line parallel to the Kingoonya–Glenloth track.

Regolith zones for the drilled section were taken from the aircore drill logs. These were modified to include accurately located unconformities from the diamond core (KLHRDD-1) and geochemical evidence from aircore drilling (Ti/Zr, Fe, W, As, K, Rb and Ba; see also Appendix 2).

Table 17: Modified RED scheme units symbols as used on the Lake Harris Regolith Landform Map.

Relict Landscape Class	
Basement: \pm Protolith \pm Saprock \pm Saprolite \pm Pedolith \pm Duricrusts	
Rfvp	Felsic volcanics as flows, breccias, tephra \pm ?epiclastic equivalents (undifferentiated). Aphanitic to porphyritic, red to dark reddish grey. Protolith to saprock with an angular lag of parent lithotype. Gawler Range Volcanics: CHITANILGA VOLCANIC COMPLEX rhyolite and rhyodacite. Mesoproterozoic, weathering Mesozoic-Cainozoic.
Rqd	Significant quartz blows or veins , hydrothermal fracture infill, white to pale grey. These stand above the host rock surface and outcrop is generally surrounded by an apron of quartz talus. Age – post Glenloth Granite emplacement.
RgS	Highly weathered granite , medium-grained quartz + kaolinite, white to creamy, generally cut by white to grey vein quartz. Saprolite to pedolith , upper portions are largely silicified to silcrete. GLENLOTH GRANITE, Palaeoproterozoic, weathering Mesozoic-Cainozoic.
RuvS	Weathered mafic to ultramafic metavolcanics (greenstones) , mostly komatiitic and serpentinised, rich in tremolite, actinolite, chlorite, Ni- and Cr-coloured weathering products, talc, smectite, relict amphiboles and antigorite; contains numerous chalcedony veins 1-15 mm thick. Layering is subvertical, relict foliation is subvertical and near layer parallel. Commonly coloured light, bright and dark green + green-grey + yellow-green and with rare turquoise in chalcedony veining. Saprolite \pm pedolith , variably ferruginous near top where it is dark brown, weakly mottled brown, or yellow-brown. Recently exhumed by fluvial erosion near Lake Harris. Harris Greenstone Belt Lake Harris komatiite and Lake Harris basalt. Archaean, weathering Mesozoic-Cainozoic.
Erosional Landscape Class	
Eroding Mesoproterozoic Basement: \pm Protolith \pm Saprock	
EvP	Eroding felsic volcanics (undifferentiated, <i>c.f.</i> unit Rfvp) aphanitic to porphyritic, red to dark reddish grey. Protolith to saprock with a gibber of angular parent lithotype. Mostly forms low rises and slopes covered with poorly developed thin soil or very thin aeolian sand, sparsely vegetated by low shrubs. Gawler Range Volcanics rhyolite and rhyodacite (undifferentiated).
Eroding Highly Weathered Archaean Basement: Saprolite \pm Pedolith \pm Duricrusts	
EgS	Eroding highly weathered granite (<i>c.f.</i> unit RgS) medium-grained quartz + kaolinite, white to creamy, cross-cut by white to grey vein quartz. Saprolith , upper portions are generally silicified to silcrete which forms a talus to colluvial lag on lower eroding slopes. Lag also contains vein quartz clasts. Slopes are deeply incised near cliffs but are more gently undulating distally. This material is generally unvegetated. Weathering and eroding GLENLOTH GRANITE.
EuS	Eroding highly weathered greenstones (<i>c.f.</i> unit RuvS) greens, browns and near black, clad by ferruginous lag with minor black chromite, silcrete gibber, platy fragments of relict chalcedony veins. Generally covered by thin gravelly colluvium and alluvium. Forms gentle slopes and undulating ground, generally unvegetated.
Eroding Colluvium-Alluvium	
Eahp	Eroding red-brown hardpan (<i>c.f.</i> unit Dahp) alluvial to colluvial clay \pm silt \pm sand \pm gravel, variably cemented by hyaline silica and pedogenic carbonate. Strongly coloured and mainly mottled. Hard to compact and forms badlands topography where eroding. Moderately steep to gentle slopes, some with a polymict lag of rounded to subangular clasts. Generally overlies older alluvium of unit Da-2 or the silcretes developed on saprolith derived from granitic or ultramafic basement.
Eroding Complex Landscapes	
E-1	Deflating and fluvially eroding terrain on deeply weathered granite , commonly capped by ‘greybilly’ silcrete and a typical lag of silcrete pebbles \pm vein quartz \pm other polymict resistate lithic fragments. Some thin patches of relict aeolian sand forms a distinctive mosaic with the gravel-pebble lag patches. Terrain is mainly near flat or gently undulating and sparsely vegetated.

Table Cont.

Table 17 continued.

E-2	Deflating and fluviially eroding colluvial-alluvial terrain on mafic basement: red-brown hardpan overlying older sediment on deeply weathered ultramafic basement. This unit often has an obvious gravel-pebble lag of silcrete ± polymict lithic fragments ± vein quartz ± platy chalcedony (from ultramafic source) + magnetic Fe-lag granules and chromite grains. A patchwork mosaic of thin, relict, aeolian sand occurs with the prominent lag patches. Terrain is broadly gently sloping but is locally very undulating due to gullies and sheet erosion. This landform is sparsely to moderately vegetated by shrubs but may contain a few small trees.
E-3	Deflating and fluviially eroding sand plains overlying red-brown hardpan + ?older sediment or resting directly on deeply weathered basement. Soil is orange to brownish, contains calcrete and/or gypcrete at 250-500 mm depth. Gravel-pebble lag only visible where sand has deflated or been alluvially stripped. Terrain is relatively flat to gently undulating and some is locally gullied or sculptured to yield steeper slopes. Unit contains many small clay pans. Moderately vegetated by trees (<i>Acacia</i> sp. And <i>Eucalyptus</i> sp) and shrubs (chenopods, <i>Maireana</i> sp. And <i>Eremophila</i> sp).
De-1/E-3	Complex landform mosaic of erosional and depositional components
Depositional Landscape Class	
Lacustrine Sediments	
DI-1	Playa lake deposits , dark brown to dark grey gypsiferous mud – clay and silt with minor sand, mostly moist and soft to weakly coherent, some is organic-rich, with a thin, white halite crust. Totally unvegetated. Quaternary – Holocene.
DI-2	Playa lake shore deposits , reworked aeolian sand ± modern fluvial sand to gravel ± lake shore strand-line gravel ± seed gypsum crystal fragments ± halite ± flotsam, uncemented. May form small, hummocky dunes near creek debouchments. Mainly pale yellow to pale brown or pale grey. Totally unvegetated. Quaternary – Holocene.
Alluvial Sediments	
Da-1	Modern creek fluvial sediment (undifferentiated) mainly loose but some is variably cemented by pedogenic carbonate and/or gypsum. Silty to sandy to gravelly to pebbly, rarely with cobbles. This landform is generally tree lined by (<i>Casuarina</i> sp., <i>Eucalyptus</i> sp, <i>Acacia</i> sp. And <i>Eremophila</i> sp). Quaternary – Holocene.
Da-2	Alluvium from older fluvial activity, coarse sand ± gravel ± pebbles and cobbles – mostly quartzose but some have polymict lithic clasts in some layers. Clasts are well rounded to subangular. Browns and brown-grey. Ranges from <1 to >10 m thick but is rarely exposed, generally only seen in drill sections. Portions of the basal components are variably silicified to silcrete. Cainozoic.
Colluvial-Alluvial Sediment	
Dahp	Red-brown hardpan , alluvial to colluvial clay ± silt ± sand ± gravel, variably cemented by hyaline silica and pedogenic carbonate. Hardpan is strongly coloured and can be mottled. Hard to compact and forms minor 'badlands topography' where eroding along the breakaways on the lake shore or creek banks, mostly hidden beneath younger aeolian sands. Poorly vegetated. Pleistocene.
Aeolian Sediments	
De-1	Sandplain veneer , orange to orange-brown, siliceous, loose to weakly cemented by pedogenic carbonate, ~0.3 to ~1.0 m thick, sand mantles palaeotopography, forming weakly undulating to near flat surfaces. Generally sparsely vegetated by chenopods and <i>Eremophila</i> sp. But, where thick enough, may be covered by <i>Acacia</i> sp. And <i>Eucalyptus</i> sp. Trees. MOORNABA SAND, Pleistocene-?Holocene.
De-2	Linear dunes , orange to orange-brown siliceous sand, loose to weakly cemented by pedogenic carbonate, ~1.0 to ~3 m thick, mantles palaeotopography forming linear dunes and undulating terrain. Can have significant <i>Acacia</i> sp. Shrubs to small trees and shrubs of <i>Eremophila</i> sp. MOORNABA Sand, Pleistocene-?Holocene.
De-3	Lunettes , mostly low, crescent-shaped, clayey to silty dune deposits on the eastern side of clay pans and playas. Pale, mainly associated with low density—powdery gypsum, mostly has dark, surficial layers, may be clayey towards the base. Up to 3 m thick in mapped area but may be up to 5 m thick just to the north or on the islands. Poorly vegetated by grasses and some low shrubs. Quaternary.
De-3g	Gypsum lunettes , generally low angle dune deposits on the eastern side of clay pans and playas. White to pale grey, composed of seed gypsum crystals and fragments, may be partly clayey towards the base. Up to ~1 m thick on mapped area but may be >3 m thick just to the north or on the islands. Vegetated only by grasses. Quaternary.
De-4	Lake side dunes , pale yellow to pale yellow-orange, siliceous and calcareous, loose. Formed on some headlands and N shores to Lake Harris or on the islands where they thickly cover basement units on the island's W and S flanks. Sparsely to densely vegetated by shrubs of many genera. Thickness: ~3 to >7 m. Quaternary.
Induration Modifiers	
Cc	Pedogenic carbonate, laminated sheets to massive zones to nodular aggregates, exposed mostly in erosional terrain along creek lines, road cuts and where recent deflation of calcrete. Generally cream to yellow or pale orange and occurs at depths of 200-550 mm within the soil zone B _{Ca} horizon.
Cg	Gypcrete, hard to crusty gypsum cement and/or crystalline matt capping various surfaces – generally very localised near the large lake or on the lee of gypsiferous lunettes. Pale grey to yellowish grey and ranging from <100 to ~500 mm thick. Quaternary.
C _{Fe}	Ferricrete, ferruginous capping (~20-200 mm thick) formed on the weathered greenstones, brown to dark brown and yellow-brown. Generally very jointed, readily forms lag aprons at eroding edges of outcrop. Limited in extent. Mesozoic-Cainozoic.

Table Cont.

Table 17 continued.

Cs	<p>Silcrete: siliceous cementation of host lithotypes, ?late Cretaceous-Tertiary.</p> <p>On or within saprolitic granite: generally 0.3–~1.5 m thick, with an underlying incipiently silicified zone to an additional 0.5–1 m thick, mostly developed within quartz grit-rich arenaceous zone of the pedolith, may have entrapped relict quartz veins. Grey, very hard and splintery, some contain anatase wisps, some with columnar structures containing internal banding parallel to the column. <i>[has a unique colour symbol on Map]</i>.</p> <p>On or within saprolitic ultramafic: generally 0.3–~1 m thick, some with darker entrapped chalcedony fragments derived from the underlying host. Yellow-grey, very hard and splintery, most contains abundant anatase wisps, outcrop is blocky and vertically jointed. <i>[has a unique colour symbol on Map]</i>.</p> <p>Within transported cover: only seen in drill section, in part it cements Tertiary alluvium in bands or the zone adjacent to the main unconformity where colluvial lags occur. <i>[has a unique colour symbol on Map]</i>.</p>
----	------------------------------------------------------------------------------------------------------------------------------------------------------------------------------------------------------------------------------------------------------------------------------------------------------------------------------------------------------------------------------------------------------------------------------------------------------------------------------------------------------------------------------------------------------------------------------------------------------------------------------------------------------------------------------------------------------------------------------------------------------------------------------------------------------------------------------------------------------------------------------------------------------------------------------------------------------------------------------------------------------------------------------------------------------------------------------------------------------------------------------------

Landscape Evolution

Regional landscape evolution

Palaeozoic and Mesozoic

Landscape development in this area after the last major deformation has generally involved erosion, exhumation, deep weathering, sedimentation, some landscape inversion and duricrust development (Daly, 1985, 1986; Parker, 1995). Substantial glaciation of this part of South Australia took place during the Permian. All previous deep weathering profiles and many sedimentary deposits were removed, leaving fluvio-glacial deposits, such as in the 4 x 90 km approximately NW trending Mulgathing Trough ~35 km ~NW of Lake Harris. Here about 800 m of fluvio-glacial deposits occur beneath later Mesozoic and Cainozoic sediments (Hibburt, 1995). Rifting within Gondwana to form the separate continental masses of Australia and Antarctica began in the Early Jurassic due to an emerging geo-tectonic regime which led to rift and intracratonic basin formation along the southern edge to, or on, the Australian land mass (Krieg, 1995). Mesozoic deposits are limited, due to erosion, near to or overlying the Harris Greenstone Belt but they include terrigenous Jurassic Algebuckina Sandstone (aeolian to fluvial), the Cretaceous Cadna-Owie Formation (terrigenous fluvial to marginal marine) and Bulldog Shale (marine). These were deposited on a predominantly crystalline basement of low relief that had become deeply weathered during the Jurassic. Much of the quartz- and kaolinite-rich Algebuckina Sandstone is derived from deeply weathered Jurassic profiles, to form aeolian dunes intermixed with fluvial sheets and channel sequences with a few small lacustrine deposits. Situated at about 70–60°S during those times, the climate was seasonal periglacial (Sheard, 1990) with coniferous forests covering some of the land (Krieg, 1995).

Early—Middle Cainozoic

Continued rifting between Antarctica and Australia initiated marine transgressions into the southern marine basins and sedimentation continued into the late middle Tertiary. These transgressions changed the existing drainage-erosion regimes and influenced climatic patterns further inland (Alley and Lindsay, 1995). As Australia gradually drifted north, the climate warmed and rainfall increased, promoting more rapid rock weathering and additional fluvial erosion. Significant river systems drained the Gawler Craton to the west and southwest in the HGB area (Hou *et al.* 2000; Hou, 2004). However, the area maintained a relatively low relief (v:h = 1:2,000; pers. comm. B. Hou, Geological Survey, PIRSA, 2004; Hou *et al.* 2000, 2003a). Sediments generally had dips of <1° although local perturbations around palaeochannel edges and protruding basement rises had slopes of >1:5 and associated sedimentary dips of >10°. Palaeochannels were dominated by sand during the Eocene but become progressively dominated by silt to clay in the Miocene. This was due to minor uplift in the Barton-Ooldea debouchment area of the eastern Eucla Basin that reduced topographic gradients even further (Hou *et al.* 2000, 2003a, b, c).

Tertiary vegetation for this part of the Gawler Craton ranged from meso-mega-thermal angiosperm-gymnosperm mixed rainforest to meso-thermal conifer dominant rainforest (Benbow *et al.*, 1995a). During the late Eocene and again in the late Miocene to early Pliocene, broad-scale pedogenic silicification of the landscape yielded extensive silcrete duricrusts on exposed surfaces (Benbow *et al.*, 1995b). Over the Gawler Craton silcrete can range in thickness from <1 to ~3 m and in the Lake Harris Domain silcretes have that range of thickness expressed. Commonly silcretes are complex, where the surface has been repeatedly overprinted, but where sedimentation has separated the silicification episodes the silcretes are generally of a simpler form (Benbow *et al.*, 1995b; Lintern and Sheard 1999; Mason and Mason, 1998).

Late Cainozoic

The climate became more arid during the Pliocene, causing the earlier river systems on the Gawler Craton to dry up and become silted. Strings of ephemeral playas and small clay pans mark the original fluvial traces (Hou *et al.* 2000; Hou, 2004). Some of these playas occur near Lake Harris and a small one is shown on the Lake Harris Regolith-Landform Map (Appendix 6). Erosion during the Pliocene to Quaternary has cut back from lower, less competent ground towards the generally higher silcrete armoured surfaces, leading to the formation of small scarps standing <5 to 50 m above the surrounding plains. They commonly expose softer pallid to brightly coloured saprolith below a silcrete capping and are colloquially termed ‘break-away’ or ‘jump-up’ country. Increasing aridity and strong winds during the Pleistocene developed extensive aeolian dune fields over much of Central Australia. Siliceous sands from the Great Victoria Desert, west of Tarcoola, gradually invaded parts of the Harris Domain (Callen and Benbow, 1995). During that time, and continuing today, there was an influx of aeolian carbonate dust, derived from extensive coastal shelf bryozoan-rich carbonates exposed to erosion during each glacial low sea stand. Pedogenic modification by meteoric water has reformed the carbonate dust into calcrete – another duricrust mantle (Phillips and Milnes, 1988; Lintern and Butt, 1993; Belperio, 1995; Lintern, 1997). Vegetation adapted to increasing aridity by becoming sclerophyll dominant, sparse and of moderate to low stature. The modern vegetation is sensitive to grazing pressure. Where the vegetation has been removed or overgrazed, there is no regeneration and the landscape is eroding. Previously vegetation-stabilised dunes are reactivating causing blow-out dunes.

Localised landscape evolution – Lake Harris

The bedrock intersections are, in places, relatively undeformed, allowing some of the original igneous fabrics to persist into the saprolite. It seems likely that different parts of the ultramafic flows have been intersected by the drill core revealing both olivine and pyroxene spinifex structures. Petrographic evidence suggests that the covering sediments were deposited on soft, easily eroded ultramafic rocks that occupied low parts of the topography (see Figure 6). Smectitic clay of the sediment matrix was probably largely derived from erosion of mafic-ultramafic rocks, and the kaolinite and hydromuscovite were largely from weathered granitic materials. The upper part of the sediment is cemented to a hardpan by banded aluminosilicate. The matrix of the sediments below the hardpan consists of phyllosilicate and this becomes more abundant with depth. Where it is less stained, it is a flaky mixture of phyllosilicates (XRD indicates kaolinite and smectite). The quartz clasts appear to have been derived locally from deeply weathered granites (small, shardy grains), however some larger grains are more rounded, probably also granitic and have been transported further in a fluvial environment. Vein quartz was another clast source. Predominant quartz clasts in the lower part of the sediments and appearance of microcline and sericitized feldspar towards the top imply progressive erosion of and provenance from a deeply weathered granitoid profile that progressively exposed less weathered materials with time.

Landscape evolution at Lake Harris is similar to that of the greenstone belts of the Yilgarn Craton. Here, greenstones are generally more deeply weathered than the surrounding granites, where both continuous and discontinuous valleys have been eroded into the greenstone units. These valleys were subsequently infilled with sediment from weathered greenstone, surrounding weathered granitoids and eroding Phanerozoic sediments (Robertson, 1998, Hou, 2004). Exemplifying this is the palaeochannel trace overlain on the greenstone distribution in Figure 34 where approximately half of all the greenstone belts have been opportunistically incised by palaeochannels. On the present surface these are indicated by a broad sinuous but weak topographic low containing chains of evaporite encrusted playas (Figure 35A). At Lake Harris, the fluvial sediment overlying weathered greenstone reaches a thickness of ~10 m in the cored hole KLHRDD-1 but is ~15-20 m thick in the palaeochannel tributary between drillholes KOK 19 and KIN 37. Commonly a thin basal colluvial unit is overlain by a thicker dominantly fluvial system with intermittent colluvial and aeolian input nearer the current land surface.

Pedogenic silcrete has cemented intervals of the sedimentary pile and any basement that outcropped at that time. Along parts of the shoreline of Lake Harris and along another parallel alignment about 5 km to the west, are silcrete capped saprolitic Glenloth Granite escarpments, both retreating westwards. The latter escarpment stands about 15-45 m above the plain (Figure 35B, C).

Granite tors and rises occur 5 km to the south and southwest, around the Glenloth Goldfield. These form the base to an exhumed weathering zone where relict corestones and protolith, that earlier had been buried

below 10-25 m of saprolite, have had this stripped away to reveal the less weathered basement. A similar process may have affected the northern outcrops of Gawler Range Volcanics, although the surficial evidence for that is less clear than for the granites to the south.

Aeolian sand dunes and later calcareous dusts have mantled the weakly undulating terrain during the Pleistocene. The modern drainage pattern may run counter to the palaeodrainages. Aeolian, fluvial, lacustrine and erosive processes are all evident around the current shoreline of Lake Harris (Figure 35D). Aeolian sands invaded during the Quaternary, producing a variety of dunes and sand sheets. Deflation of lake and clay pan floors has produced parna, seed gypsum and silts that now form lunettes in the lee of the playas. Calcrete is a ubiquitous duricrust within soil profiles, regolith and modern sediment in this area. Relatively recent erosion near the NW corner of Lake Harris along a minor creek has exhumed weathered greenstones and their southern faulted contact with weathered Glenloth Granite. Erosion has already removed up to 3-4 m of cover and pedolith here, possibly triggered by over-grazing as the majority appears to have occurred within the last century.

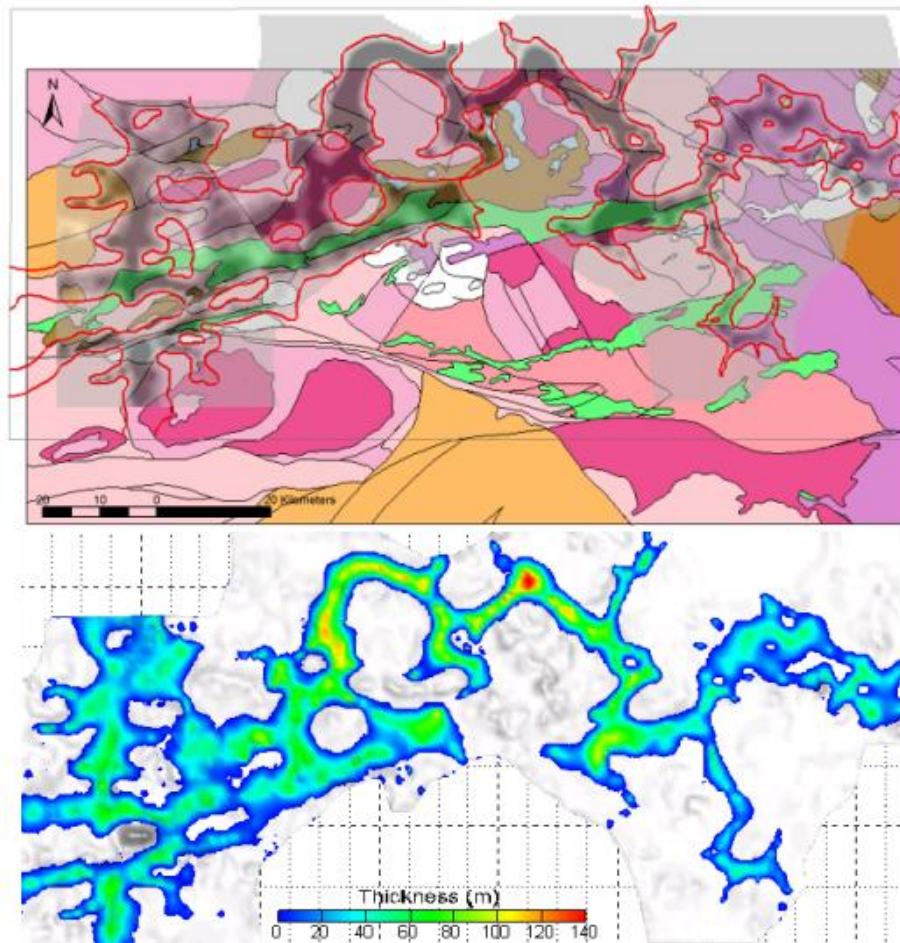


Figure 34: The **top image** displays basement geology partially overlain by an image of the Kingoonya Palaeochannel (red outline with mid-grey infill). Harris Greenstone Belt is shown in bright green, and the surrounding granites, volcanics and metasediments are shown in pinks, reds, orange, brown and purple. The **lower image** displays just the palaeochannel sediment infill thicknesses on a regional DEM background, at same scale as the top image. A strong and persisting linkage between palaeochannel and the weathered greenstone subcrop is evident for the northern most greenstone belt (>85% match). More easily eroded weathered greenstones have encouraged palaeodrainage to preferentially carve out a significant valley system over some hundreds of kilometres and in places up to ten kilometres wide. Sediment infill reaches thicknesses of ~15 to ~80 m within the greenstone linked palaeochannel segments. A small gap in that overlap linkage occurs where the 2001 Mullina Well drill line cuts the greenstones, there they form a palaeo-high ground. The 2001 Lake Harris drill line clips the eastern end of a southeastern palaeo-tributary. Both images are from Hou (2004).

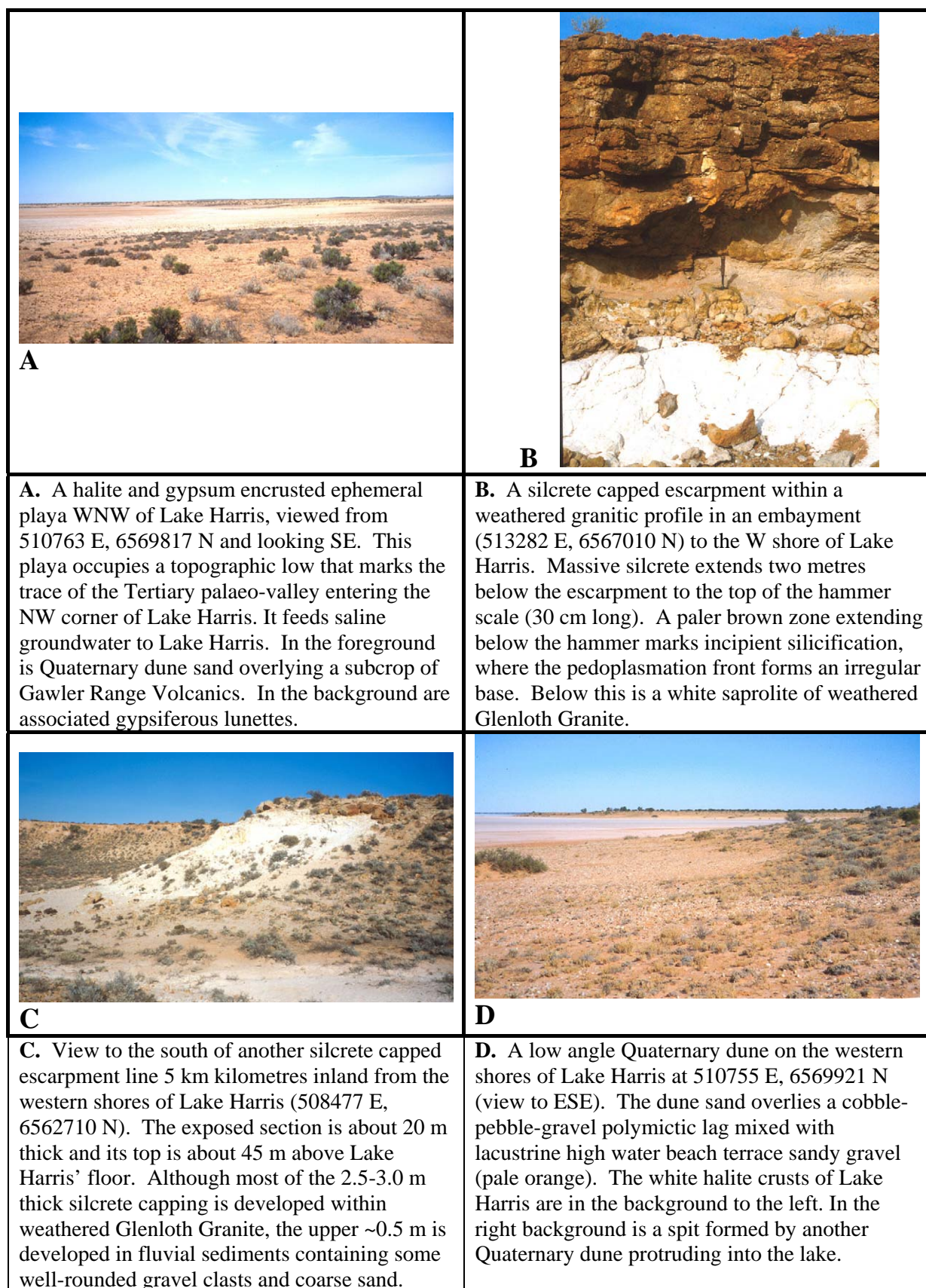


Figure 35: Landscapes of the Lake Harris area.

Localised landscape evolution – Hopeful Hill

The petrography revealed ultramafic bedrocks with significant but variable deformation and metamorphism that have largely obscured their primary character, although some hints of cumulate fabrics

remain. The top of the saprolite contains cavities filled with sedimentary materials. A majority of the overlying sediments consist of claystone fragments. These imply a pre-existing claystone, consisting of clays and quartz, that have been mixed by bioturbation, before being broken and redeposited on the ultramafic saprolites. The top part of the sediments is different and probably has a granitic provenance. The aluminosilicate cementing material has had a complex history, showing evidence of several cycles of cementation, break-up and re-cementation.

Hopeful Hill is a prominent basement inlier that rises to about 30 m above its surroundings; it is a likely major source for the transported colluvium-alluvium penetrated by the 2001-2002 drilling; however there may be other sources. Hopeful Hill outcrop includes: basalt with preserved pillow structures and related ultramafic rocks displaying gabbroic textures. There are some younger quartz veins and, a few kilometres further west, narrow units of banded iron formation outcrop (Daly, 1981, 1985; Daly and Fanning, 1993). Transported cover is generally thickest in drillholes TAR 16–19, 7 and 8; there is probably no transported cover intersected by drillhole TAR 13; TAR 12 intersected only thin cover.

Today, Hopeful Hill is surrounded and partly clad by Pleistocene aeolian sands and is covered by a sparse to closely spaced woodland of moderately tall vegetation. There is a shallow stream system within 1-2 km of Hopeful Hill draining into the major Tertiary palaeochannel that drains west from the Lake Harris area, about 7 km to the east. It appears that Hopeful Hill has been a topographic high, possibly since the early Mesozoic. Deep weathering (post Permian) has occurred on the flanks of that highland and stretch out into the surrounding plains (<35 m thick). Drilling has demonstrated some stripping of that profile near the basement highs, and basement outcrop now consists only of protolith and saprock. The highly weathered mafic-ultramafic units are not exposed. Unlike at Lake Harris, greenstones along the Hopeful Hill drill line (TAR 19-13) have been resistant to weathering, forming high ground. About 3.4 km further east along drill line TAR 7-12, where there is less topography, the greenstones have weathered to depths of about 30 m.

During the Tertiary, existing sediments were eroded and redeposited close to source, yielding the reworked claystone fabrics mentioned above. Sediment-filled cracks in the upper saprolite imply severe and deep desiccation (moist smectites can shrink by about 50% on drying). This emplaced granules, sand and silt into weathered *in situ* materials well below any pedogenic horizon. There are similar features in Quaternary materials and soils elsewhere in South Australia (Sheard and Bowman, 1996). In general most of the sediments at Hopeful Hill have a short transport history and the more sandy to gravelly upper units appear to have only had their fines removed prior to deposition. It is likely that surficial geochemistry, here, may be better at detecting greenstones through thin to moderate cover than at Lake Harris.

Development of silcrete has affected both the sedimentary cover and the pedolith along both drill transects but, along the western transect, the silcrete pinches out before reaching the high ground of weathered basement outcrop. Stratigraphically above the siliceous duricrust is a zone of incipient ferruginous duricrust (TAR 16, TAR 11-12). The true thickness, internal structure and induration remain largely enigmatic because none were cored and they do not outcrop. However, they are the only high level ferruginous duricrusts recognised in sedimentary cover near subcropping weathered greenstone here.

Sheets and dunes of Quaternary sand cover and surround the lower flanks of Hopeful Hill but do not obscure the hill outcrop. Calcrete has developed in those sands, forming a white to creamy coloured B_{Ca} horizon, and this has been used as an exploration geochemical sampling medium.

Localised landscape evolution – Mullina Well

Petrography of the mafic-ultramafic bedrocks shows significant deformation that has largely obscured their primary character, although some hints of cumulate fabrics remain. The top of the saprolite contains cavities filled with sedimentary materials. The base of the sediments is a debris flow breccia of saprolite fragments. Succeeding layers are of clay and claystone, similar to that of the palaeochannel sediments on the Yilgarn Craton, consisting of a bimodal mixture of clays and quartz. These have been broken and redeposited higher in the succession.

Today, the Mullina Well area is clad by Pleistocene aeolian sands (3-10 m thick) with no basement or Tertiary outcrop. The vegetation consists of small remnants of sparse to closely spaced woodland of

moderate stature, surrounded by grazing land. Obvious Quaternary drainages are absent within 5 km of the drill line. It would appear that the area between drillholes TAR 55-58 has formed a slight topographic high, possibly since the Mesozoic. There has been moderate weathering since the Permian over the highland but is deeper on either side of it, especially within felsic host rocks where weathering attains thicknesses of 50-70 m. Drilling has demonstrated a marked thinning of the weathered profile near the basement highs (at TAR 46, 56, 57, 61) with possible stripping near drillhole TAR 73. Unlike at Lake Harris, greenstones along this drill transect have been more resistant to weathering, forming high ground; the basaltic units have weathered more deeply (see Figure 8).

Possibly during the late Cretaceous or early Tertiary, there was a mass-wasting landslide of wet ground that produced a debris flow deposit about 5.5 m thick but of unknown lateral extent. This was revealed in the core and by petrography and was particularly difficult to recognise in the core; it demonstrated how an important detail of landscape evolution could be missed easily in drill cuttings. The cross-section from aircore drilling (Figure 8) reveals that the cored site TMWRDD-1 is on a low topographic rise that has persisted for a considerable time, and the site is also adjacent to a minor palaeovalley. Undercutting of a deeply weathered, water-saturated creek bank by storm water, or erosional over steepening of a water saturated saprolitic valley side, could cause a landslip and result in a mass-flow deposit. Sediment-filled voids in the saprolite may be related to the debris flow (newly formed surface fracturing and roughening), or imply severe and deep desiccation after exposure following the landslide. This would cause sand and silt to be deposited into the remaining saprolite (see earlier comments for Hopeful Hill).

Subsequent weathering and megamottling of the debris flow deposit have combined to firstly, leach any remaining colours to give a pallid appearance and secondly, to overprint ferruginous stains and spaced megamottles in dark reds to strong red-browns. Deposition following the debris flow consisted of clays with a similar mineralogy (saprolitic source) but eroded gradually to form claystones of greenish-grey clay. These resemble late-stage palaeochannel clays or overbank deposits. Later mottling has variably overprinted these clays to moderate reds and browns. Various colluvial to fluvial units followed and these show marked Fe-oxide colouring (strong reds and browns) in contrast to the deeper units in paler green-grey to greyish with megamottling in moderate red to brown. Silcrete is developed most intensely over the topographic highs, especially between drillholes TAR 43-55 but is also associated with the topographic low between TAR 72-48. Orange dune sands mantle the area and partially obscure pre-existing topographic expression, these sands contain calcrete duricrusts, nodules and pisoliths.

Interpretation of geochemistry

- **Bedrock and saprock outcrops** form very minor components of the landscape of the Harris Greenstone Belt. Nevertheless, where they occur, well-established rock-chip and soil sampling procedures would be effective, provided close sample spacings were used. As these outcrops occur in strongly erosional regimes, they could be detected easily by stream sediment geochemistry.
- The weathered **komatiites** show some useful geochemical fingerprints in the minimally mobile elements (Ti, Zr and Al) and it has been possible to confirm their komatiitic affinities. The basalts from Mullina Well appear to be fractionated komatiitic basalts. Those greenstones from Hopeful Hill and Lake Harris appear to be komatiites typical of thin, differentiated flows, possibly contaminated, increasing their Ni prospectivity. The quite good fit with data from fresh komatiites supports i) the hypothesis of relatively incomplete weathering proposed for parts of the lower saprolite at the Lake Harris and Hopeful Hill sites and ii) the delicate komatiitic fabrics pseudomorphed in the saprolites.
- **Distinction between cover and basement** is important and geochemistry can play a part. Although Zr can separate the two groups at all three sites on a univariate basis, the lower clay-rich sediments were probably derived partly from weathered komatiites, resulting in overlap of some characteristic elements. If the sites are considered separately, good but slightly imperfect univariate distinctions can be made for some sites using K, Rb, Mn and Ni. Using the pooled data and bivariate and trivariate plots, further quite good separations are possible using the above elements with Sr, As and Cu.
- **Stream sediment** surveys, where the stream channels are sufficiently well defined, may be able to detect ultramafic signatures in covered terrain where the cover is thin. However, dilution (by aeolian sand and granitic debris) is likely to swamp the signal from the ultramafic rocks. It may be necessary to extract and analyse a heavy mineral fraction from the >1000 µm or >2000 µm fraction to reduce the influence of these diluents.

- **Dune sand** is an important component of soils and creek sediments in this area and has a very broad provenance. It acts as a sample diluent so its size distribution (75-710 μm) has been accurately defined, to facilitate design of removal procedures. Coarse material (710-2000 μm and some even coarser) has probably not been transported far and may have been brought up from the basement by bioturbation, through the sand, and concentrated in dune swales by deflation. Although it mostly consists of quartz, K-feldspar and gypsum, there is, however, a minute proportion of ferruginous chips within the sand, probably ferruginized clay saprolite that could be extracted by gravity means. It would be necessary to sieve out a coarse ($>1000 \mu\text{m}$) fraction (to minimise aeolian material) and to preferentially sample dune swales (where the cover is as thin as possible). Separation of the heavy minerals by heavy liquid, panning or jig would minimise the influence of granitic detritus and target locally derived ferruginous material. Magnetic extraction is not recommended, as it tends to focus on secondary Fe-oxides.
- Where the ultramafic rocks are mantled by a veneer of **hardpanized colluvium**, mixing has brought small but characteristic granules of black, Fe-oxides through the colluvium to the surface. These hematite-maghemite granules form a small part of a polymictic **lag** of silcrete, quartz, chalcedony and ferruginous silcrete. Fingerprint fabrics suggest a smectitic mafic/ultramafic saprolite as an origin. They are also enriched in Cr (1250-17200 ppm), Ni (530-640 ppm) and V (720-1200 ppm). Preferential extraction of this heavy, ferruginous material from the lag may be used in a search for suitable komatiites where the colluvium is thin.
- **Silcretes** developed from degraded ultramafic rocks retain an ultramafic signature in Cr, Co, Ni, V and Zn and possibly also in Mn and Ba. These are likely to provide information on bedrock lithology where the cover is very thin. Their contained slabby chalcedony clasts can be visually identified.
- **Calcrete**, cements and permeates saprolite, dune sand, silcrete and colluvium. It has been shown elsewhere, and on the Gawler Craton, to be a satisfactory geochemical medium for Au, Ag and Cu (Lintern and Butt, 1993; Edgecombe, 1997; Lintern, 1997; Lintern and Sheard, 1999; McQueen *et al.*, 1999; Lintern *et al.*, 2000; Drown, 2003). It was not tested specifically here. Calcrete was confirmed as a prospecting material around the nearby Glenloth Au Mines by sampling calcrete over known mineralisation, with strongly anomalous results (Au 300 ppb, Ag 4 ppm and Ba 1500 ppm).
- **Gypsum** occurs as a coarse encrustation of plates and booklets on saprolites and in soils on the edges of playas, marking evaporation sites of seeping ground waters. These evaporation sites could retain some of the soluble elements that move in the groundwater. Although much gypsum is recycled in the landscape, slight distortions of the dominantly atmosphere-influenced S isotopic composition of gypsum at these evaporation sites might provide a guide to sulphides within the groundwater regime.

Conclusions

The 2001 and 2002 drilling of crystalline basement, targeting the Harris Greenstone Belt (Davies, 2002a, b) was paralleled by this regolith study using a selection from those samples but augmented by an additional three strategically cored regolith profiles. They, and the surface investigations, provided control on the earlier logging, and more detail regarding weathering and related geochemical dispersion. Together these projects have provided the exploration industry and researchers with significant new information for several parts of the Harris Greenstone Belt.

- Analysis of drill cuttings provides good orientation data but should be cross-referenced against at least one fully cored drillhole per prospect to improve confidence in regolith stratigraphy and in understanding the geochemistry.
- Deep weathering and mottling makes logging and locating the unconformity between transported and *in situ* materials difficult even for diamond core through regolith. Drill core can have different appearances when wet and dry, and can provide different information in these two states. Thus, it is advisable to revisit the core and revise initial logs, particularly when additional chemical, mineralogical and petrographic evidence becomes available.
- Two aircore holes have assays that indicate anomalous Au. The most interesting is at Hopeful Hill (TAR 10) but further drilling is needed to define this anomaly.
- Soil sample assays revealed that all komatiite lithology-indicating elements (Mg, Cr, Ni, As, Co, Fe, Mn and V) are elevated over exposed weathered greenstone basement or where weathered greenstones are mantled by thin cover. Mineralization-related elements (Au, Bi, Cu, Pb and W) are elevated there as well, indicating prospective ground.

- Ferruginous cappings on weathered greenstone are rare in the HGB. They contain, where present, Ni up to 6500 ppm and Cr up to 7500 ppm. These values are within expected limits.
- Stream sediment surveys may be able to detect ultramafic signatures in covered terrain as the cover can be thin in places (see also next point).
- Movement to the surface, by bioturbation, of greenstone-derived resistate minerals (ferruginous nodules, chromite and vein chalcedony fragments) may provide a supplementary exploration tool to ‘see’ through 5-10 m of transported cover.
- Detailed regolith landform mapping can provide an ‘outcrop vs transported cover’ framework to better target surficial geochemical sampling programs. It can also lead to landscape evolution models that may provide vectors to dispersed mineral signatures or from dispersed mineral signatures towards a primary source.

Recommendations

1. Difficulties encountered in accurately identifying the major unconformity between *in situ* and transported regolith in covered terrain, using aircore drill cuttings, are reduced markedly when compared with full regolith profile drillcore. Access to at least one targeted drillcore per mineral prospect, passing through the regolith profile, would aid regolith modelling, geochemical sampling and/or interpretation, and in more cost effective siting of further drilling.
2. Although the geochemical signal from the basement is obscured by laterally derived colluvial-alluvial deposits, vertical movement within the cover can bring a weak signal to the surface where that cover is thin (<5-10 m). This weak signal can be significantly enhanced by analysing heavy minerals.

Project Products

- Optimised regolith sample media for detection of ultramafic greenstones through thin cover (~5-10 m).
- Optimised element suites to distinguish cover sequences from weathered greenstones.
- Descriptions of weathered rock and transported cover, a Regolith Landform Map, and regolith cross-sections for three selected drilled lines.
- A Landscape evolution model for the Harris Greenstone Belt.
- Digital data on CD-ROM including: Report pdf, drill logs, assay data—logs & distributions, XRD mineral determinations, PIMA spectra, photo images. Regolith Map & cross-sections.
- A GIS data package is being prepared in early 2004 by PIRSA Geological Survey Branch to include all Harris Greenstone Belt investigation data held by PIRSA, including open file company data. All data and value added products contained herein will form an interactive Regolith layer to that GIS data package and will allow comparison with related data sets covering: geology, drilling, calcrete geochemistry, basement geochemistry, tectonics, and geophysics. PIRSA intends to release that product as “The Harris Greenstone Belt GIS data package” on a DVD in late July 2004.
- Regolith cores, drill cuttings, drill sample chiptrays, surface samples, 42 element assay data, petrography, XRD data and PIMA spectra. Drill cuttings, cores, surface samples, thin sections and polished blocks are housed permanently for reference at the PIRSA Core Store Facility, 23 Conyngham St, Glenside, South Australia.

References

- Alley, N.F. and Lindsay, J.M. (Compilers), 1995. Chapter 10, Tertiary. *In: Drexel, J.F. and Preiss, W.V. (Eds), 1995. The Geology of South Australia. Vol. 2, The Phanerozoic. South Australia. Geological Survey. Bulletin, 54:150-217.*
- Anand, R.R., Churchwood, H.M., Smith, R.E., Smith, K., Gozzard, J.R., Craig, M.A. and Munday, T.J., 1993a. Classification and Atlas of regolith-landform mapping units: Exploration perspectives for the Yilgarn Craton. *CSIRO Division of Exploration Geoscience. / AMIRA Report, 440R.*
- Anand, R.R., Smith, R.E., Phang, C., Wildman, J.E., Robertson, I.D.M. and Munday, T.J., 1993b. Geochemical exploration in complex lateritic environments of the Yilgarn Craton, Western Australia. *CSIRO Exploration and Mining. Report, 442R.*
- Baumgartner, M.C. and Neuhoﬀ, L., 1998. The vertical distribution of indicator minerals within Kalahari cover overlying a kimberlite pipe. *Seventh International Kimberlite Conference, Cape Town, South Africa. Extended Abstracts, p.55-57.*
- Belperio, A.P. (Compiler), 1995. Chapter 11, Quaternary. *In: Drexel, J.F. and Preiss, W.V. (Eds), 1995. The Geology of South Australia. Vol. 2, The Phanerozoic. South Australia. Geological Survey. Bulletin, 54:218-280.*
- Benbow, M.C., Alley, N.F., Callen, R.A. and Greenwood, D.R., 1995a. Tertiary: Geological History and Palaeoclimate. *In: Drexel, J.F. and Preiss, W.V. (Eds), 1995. The Geology of South Australia. Vol. 2, The Phanerozoic. South Australia. Geological Survey. Bulletin, 54:208-217.*
- Benbow, M.C., Callen, R.A., Bourman, R.P. and Alley, N.F., 1995b. Deep weathering, Ferricrete and Silcrete. *In: Drexel, J.F. and Preiss, W.V. (Eds), 1995. The Geology of South Australia. Vol. 2, The Phanerozoic. South Australia. Geological Survey. Bulletin, 54:201-207.*
- Blissett, A.H., 1977. GAIRDNER map sheet. *South Australia. Geological Survey. Geological Atlas 1:250 000 Series, sheet SH 53-15.*
- Blissett, A.H., 1985. GAIRDNER, South Australia, map sheet SH 53-15, 1:250 000 Geological Atlas Series — Explanatory Notes. *South Australia. Geological Survey. ISBN 0 7243 7400 0.*
- Callen, R.A. and Benbow, M.C., 1995. The Deserts – playas, dunefields and watercourses. *In: Drexel, J.F. and Preiss, W.V. (Eds), 1995. The Geology of South Australia. Vol. 2, The Phanerozoic. South Australia. Geological Survey. Bulletin, 54:244-254.*
- Craig, M.A. (Compiler), 1996a. Wollubar Regolith-Landforms Schematic Diagram: 1:50,000 approximate scale map. *In: Lintern, M.J. and Gray, D.J., 1996. Progress statement for the Kalgoorlie Study Area – Enigma Prospect (Wollubar), Western Australia. Cooperative Research Centre for Landscape Evolution and Mineral Exploration. Report, 96R / CRC LEME – AMIRA Project 409.*
- Craig, M.A. (Compiler), 1996b. Steinway Regolith-Landforms Schematic Diagram: 1:50,000 approximate scale map. *In: Lintern, M.J. and Craig, M.A., 1996. Further geochemical studies of the soil at the Steinway gold prospect, Kalgoorlie, WA. Cooperative Research Centre for Landscape Evolution and Mineral Exploration. Report, 251R / CRC LEME – AMIRA Project 409.*
- Craig, M.A., 2001. ET Gold Prospect Regolith Landforms (1:10,000 scale) map. *Cooperative Research Centre for Landscape Evolution and Mineral Exploration, Perth/Canberra. [compiled within Geoscience Australia, Canberra and available through that agency].*
- Craig, M.A. and Wilford, J.R., 1997. Half Moon Lake Regolith-Landforms (1:100,000 scale) map. *Cooperative Research Centre for Landscape Evolution and Mineral Exploration, Perth/Canberra. [compiled within Geoscience Australia, Canberra and available through that agency].*
- Daly, S.J., 1981. The stratigraphy of the TARCOOLA 1:250 000 map sheet area. *South Australia. Department of Mines and Energy. Report Book, 81/5.*
- Daly, S.J., 1985. TARCOOLA map sheet. *South Australia. Geological Survey. Geological Atlas 1:250 000 Series, sheet SH 53-10.*
- Daly, S.J., 1986. Excursion Guide, TARCOOLA map sheet area. *South Australia. Department of Mines and Energy. Report Book, 86/42.*
- Daly, S.J. and Fanning, C.M., 1993. Chapter 3, Archaean. *In: Drexel, J.R., Preiss, W.V. and Parker, A.J., 1993. The Geology of South Australia. Vol. 1, The Precambrian. South Australia. Geological Survey. Bulletin, 54.*
- Daly, S.J. and van der Stelt, B., 1992. Archaean metabasic diamond drilling project (Northwest Gawler Craton Drilling Investigations 1991; Data Package Part B). *South Australia. Department of Mines and Energy. Confidential Envelope, 8541 (unpublished).*

- Davies, M.B., 2002a. Harris Greenstone Domain Bedrock Drilling, May–August 2001. *South Australia. Department of Primary Industries and Resources. Report Book*, 2002/11.
- Davies, M.B., 2002b. Harris ‘Greenstone’ Domain bedrock drilling Phase 2: June–August 2002. *South Australia. Department of Primary Industries and Resources. Report Book*, 2002/29.
- Drown, C., 2003. The Barns Gold Project – discovery in an emerging district. *South Australia. Department of Primary Industries and Resources. MESA Journal*, 28:4-9.
- Edgecombe, D., 1997. Challenger Gold Deposit. *South Australia. Department of Primary Industries and Resources. MESA Journal*, 4:8-11.
- Eggleton, R.A. (Ed.), 2001. *The Regolith Glossary: surficial geology, soils and landscapes*. Cooperative Research Centre for Landscape Evolution and Mineral Exploration. ISBN 0 7315 3343 7.
- Griffin, T. and McCaskill, M. (Eds), 1986. *Atlas of South Australia*. South Australian Government Printing Division and Wakefield Press on behalf of the South Australian Jubilee 150 Board, Adelaide. ISBN 0 7243 4688 0. pp. 50-51.
- Hall, G.E.M., 1999. ‘Near total’ acid digestions. *Explore*, 104: 15-18.
- Hibburt, J.E., 1995. Mulgathing Trough. In: Drexel, J.F. and Preiss, W.V. (Eds), 1995. *The Geology of South Australia. Vol. 2, The Phanerozoic. South Australia. Geological Survey. Bulletin*, 54, p 78.
- Hoatson, D.M., Direen, N.G., Whitaker, A.J., Lane, R.J.L., Daly, S.J., Schwarz, M.P. and Davies, M.B., 2002. Geophysical Interpretation of the Harris Greenstone Belt, Gawler Craton, South Australia. *Preliminary Edition Map 1:250,000 scale. Geoscience Australia. Canberra*.
- Hou, B., 2004. Palaeochannel studies related to the Harris Greenstone Belt, Gawler Craton, South Australia [Kingoonya Palaeochannel Project]. *Cooperative Research Centre for Landscape Evolution and Mineral Exploration. Open File Report*, 154 / *Primary Industries and Resources of South Australia. Office of Mineral and Energy Resources. Report Book*, 2004/01.
- Hou, B., Frakes, L. and Alley, N., 2000. Geoscientific signatures of Tertiary palaeochannels and their significance for mineral exploration in the Gawler Craton region. *South Australia. Department of Primary Industries and Resources. MESA Journal*, 19:36-39.
- Hou, B., Alley, N.F., Frakes, L.A., Gammon, P.R. and Clarke, J.D.A., 2003a. Facies and sequence stratigraphy of Eocene palaeovalley fills in the eastern Eucla Basin, South Australia. *Sedimentary Geology*, 163:111-130.
- Hou, B., Frakes, L.A., Alley, N.F. and Clarke, J.D.A., 2003b. Characteristics and evolution of the Tertiary palaeovalleys in the northwest Gawler Craton, South Australia. *Journal of Earth Science, Australia*, 50:215-230.
- Hou, B., Frakes, L.A., Alley, N.F. and Heithersay, P., 2003c. Evolution of beach placer shorelines and heavy-mineral deposition in the eastern Eucla Basin, South Australia. *Journal of Earth Science, Australia*, 50:955-966.
- Kelly, K.L. and Judd, D.R., 1976. *Color - Universal Language and Dictionary of Names*. National Bureau of Standards, United States Commerce Department, Washington, D.C.
- Krieg, G.W. (Compiler), 1995. Chapter 9, Mesozoic. In: Drexel, J.F. and Preiss, W.V. (Eds), 1995. *The Geology of South Australia. Vol. 2, The Phanerozoic. South Australia. Geological Survey. Bulletin*, 54:93-149.
- Lane, R.J.L., 2001a. Interpretation of Tempest Airborne Electromagnetic Data – Parts 1 to 4 (Lake Harris and Hopeful Hill strips). *Geoscience Australia. Unpublished Workshop PowerPoint Presentations, 30th November 2001*. In: ‘Lake Harris GIS Workshop Course, December 2001’, for Primary Industries and Resources of South Australia, Office of Mineral and Energy Resources, Geological Survey Branch, Gawler Craton Team. [4 pdf files, unpublished].
- Lane, R.J.L., 2001b. Lake Harris Drill Section [AEM Survey, conductivity section]. *Geoscience Australia. Unpublished communication, 14-12-2001*, 2 pages.
- Lintern, M.J., 1997. Calcrete sampling for gold exploration. *South Australia. Department of Primary Industries and Resources. MESA Journal*, 5:5-8.
- Lintern, M.J. and Butt, C.R.M., 1993. Pedogenic carbonate – an important sampling medium for gold exploration in semi-arid areas. *CSIRO. Division of Exploration. Geoscience Exploration Research News*, 7.
- Lintern, M.J., and Sheard, M.J., 1999. Regolith studies related to the Challenger Gold Deposit, Gawler Craton, South Australia. *Cooperative Research Centre for Landscape Evolution and Mineral Exploration. Open File Report*, 78 / *Primary Industries and Resources of South Australia. Office of Mineral and Energy Resources. Report Book*, 1998/10. ISBN v1: 0 643 06477 X v2: 0 643 06478 8 set: 0 643 06479 6.

- Lintern, M.J., Sheard, M.J. and Gouthas, G., 2000. Regolith studies related to the Birthday gold prospect, Gawler Craton, South Australia. *Cooperative Research Centre for Landscape Evolution and Mineral Exploration. Open File Report, 79 / Primary Industries and Resources of South Australia. Office of Mineral and Energy Resources. Report Book, 2000/00003. ISBN: 0 643 06480 X.*
- Lintern, M.J., Sheard, M.J. and Gouthas, G., 2002. Preliminary regolith studies at ET, Monsoon, Jumbuck, South Hilga and Golf Bore gold prospects, Gawler Craton, South Australia. *Cooperative Research Centre for Landscape Evolution and Mineral Exploration. Open File Report, 115 / CSIRO Exploration and Mining. Report, 864R / Primary Industries and Resources of South Australia. Office of Mineral and Energy Resources. Report Book, 2002_004. ISBN v1: 0 643 06783 3 v2: 0 643 06784 1 set: 0 643 06785 X.*
- Lintern, M.J., Tapley, I.T., Sheard, M.J., Craig, M.A., Gouthas, G. and Cornelius, A., 2003. Regolith studies at Edoldeh Tank (ET) gold prospect, Gawler Craton, South Australia. *Cooperative Research Centre for Landscape Environment and Mineral Exploration. Open File Report, 150 / CSIRO Exploration and Mining. Report, 1081F / Primary Industries and Resources of South Australia. Office of Mineral and Energy Resources. Report Book, 2003/4 ISBN v1: 0643 068481 v2: 0643 068503.*
- Marnham, J.R., Hall, G.J. and Langford, R.L., 2000. Regolith-Landform resources of the Cowaramup-Mentelle 1:50,000 sheet. *Western Australia. Department of Minerals and Energy. Geological Survey. Record, 2000/18. ISBN 0 7307 5661 0.*
- Mason, D.R. and Mason, J.E., 1998. A Petrographic study of Regolith Samples from the Challenger Project (Gawler Craton, South Australia). *Mason Geoscience Pty Ltd. Report, 2413. (For Mines and Energy, South Australia & CRC LEME).*
- McQueen, K.G., Hill, S.M. and Foster, K.A., 1999. The nature and distribution of regolith carbonate accumulations in southeastern Australia and their potential as a sampling medium in geochemical exploration. *Journal, Geochemical Exploration, 67:67-82.*
- Munsell Color, 1975. *Munsell Soil Color Charts.* Munsell Color, Baltimore, Maryland, United States of America.
- Parker, A.J., 1995. Chapter 2, Geological Framework. *In: Drexel, J.F. and Preiss, W.V. (Eds), 1995. The Geology of South Australia. Vol. 2, The Phanerozoic. South Australia. Geological Survey. Bulletin, 54:8-31.*
- Phillips, S.E. and Milnes, A.R., 1988. The Pleistocene terrestrial carbonate mantle on the southeastern margin of the St Vincent Basin, South Australia. *Journal of Earth Science, Australia, 25:405-428.*
- Pontual, S., Merry, N. and Gamson, P., 1997. *Regolith Logging. Spectral Analysis Guides for Mineral Exploration. G-Mex version 1.0 Volume 8.* AusSpec International Pty Ltd.
- R.A.S.C., 1983. 1:250 000 GAIRDNER Australia, Graphic Sheet SH 53-15. *Royal Australian Survey Corps. Joint Operations Graphic. DEF/ARMY/10844. December 1983, Canberra. Series 1501, Edition, 1.*
- Robertson, I.D.M. (Compiler), 1998. Field Guide : N.E. Goldfields Field Excursion. Regolith '98 Australian Regolith and Mineral Exploration. New Approaches to an Old Continent. Kalgoorlie, W. Aust., May 7-9, 1998. *Cooperative Research Centre for Landscape Evolution and Mineral Exploration. Open File Report, 80.*
- Robertson, I.D.M. and Butt, C.R.M., 1997. Atlas of Weathered Rocks. *Cooperative Research Centre for Landscape Evolution and Mineral Exploration. Open File Report, 1 / CSIRO Division of Exploration Geoscience. Report, 390, first revision.*
- Robertson, I.D.M., Dyson, M., Hudson, E.G., Crabb, J.F., Willing, M.J. and Hart, M.K.W., 1996a. A case-hardened, low contamination ring mill for multi-element geochemistry. *Journal of Geochemical Exploration, 57: 153-158.*
- Robertson, I.D.M., Koning, A.E., Anand, R.R. and Butt C.R.M. 1996b. Atlas of transported overburden. *CSIRO Exploration and Mining Restricted Report 296R. 122p. (Reissued as Open File Report 87, CRC LEME, Perth, 2001).*
- Schwarz, M., Morris, B., Sheard, M., Ferris, G., Daly, S. and Davies, M., 2002. Gawler Craton. *In: Heithersay, P.S., Drexel, J.F., Hibburt, J.E. and Thomas, C.A. (Eds), 2002. South Australian mineral explorers guide. Draft edition. Office of Minerals and Energy Resources. South Australian Department of Primary Industries and Resources, Adelaide, CD, ch. 4.*
- Sheard, M.J., 1990. Glendonites from the southern Eromanga Basin in South Australia: palaeoclimatic indicators for Cretaceous ice. *South Australia. Geological Survey. Quarterly Geological Notes, 114:17-23.*

- Sheard, M.J. and Bowman, G.M., 1996. Soils stratigraphy and engineering geology of near surface materials of the Adelaide Plains. *South Australia. Department of Mines and Energy. Report Book*, 94/9.
- Sheard, M.J. and Robertson, I.D.M., 2003. Lake Harris Regolith Landform Map. *South Australia. Geological Survey. Geological Atlas 1:10 000 series. SA_GEOLOGY/Geodetail. Preliminary digital map (27th June 2003). PIRSA Spatial Information, Adelaide, SA.*
- Taylor, D.H., 1997. Guidelines for Geological Survey regolith mapping. *Victoria. Department of Natural Resources. Geological Survey. Unpublished Report*, 1997/1.
- Taylor, D.H., 1999. Production of Geological Survey regolith maps. *Victoria. Department of Natural Resources. Geological Survey. Unpublished Report*, 1999/7.
- Taylor, D.H. and Joyce, E.B., 1997a. Ballarat 1:100,000 regolith-exploration map, 7622 Zone 54. *Victoria. Department of Natural Resources. Geological Survey. Edition 1, March 1997.*
- Taylor, D.H. and Joyce, E.B., 1997b. Ballarat 1:100,000 regolith-exploration map report. 7622 Zone 54 *Victoria. Department of Natural Resources. Geological Survey. Technical Record*, 1996/4.
- Taylor, G and Eggleton, R.A., 2001. *Regolith geology and geomorphology*. John Wiley & sons, Ltd, Chichester, 375 p.
- Wilford, J., Craig, M.A., Tapley, I.J. and Mauger, A.J., 1997. Regolith landform mapping and its implications for exploration over the Half Moon Lake region, Gawler Craton, South Australia. *Cooperative Research Centre for Landscape Evolution and Mineral Exploration, Perth/Canberra. Restricted Report*, 92R / *CSIRO Exploration and Mining. Report*, 542C.
- Worrall, L. and Clarke, J.D.A., 2004. The Effect of Middle to Late Tertiary Fluctuations of Sea Level in the Geochemical Evolution of the West Australian Regolith. *In: Fabel, D. (ed.). Abstracts of the 11th Australian and New Zealand Geomorphology Group Conference, Mt Buffalo, Victoria, February 15-20, 2004*, p80.

—oo0oo—